THE JOURNAL OF PHYSICAL CHEMISTRY B
A JOURNAL OF THE AMERICAN CHEMICAL SOCIETY

pubs.acs.org/JPCB

Article

Correlation-Based Predictions of Gas Solute Diffusivity in Ionic Liquid Solvents Based on Solvent-Accessible Surface Area

Feranmi V. Olowookere and C. Heath Turner*

Cite This: *J. Phys. Chem. B* 2024, 128, 9837−9846

Read Online

ACCESS | Metrics & More | Article Recommendations | Supporting Information

ABSTRACT: In our prior study [Olowookere, F. V.; Turner, C. H. *J. Phys. Chem. B* **2023**, *127*(42), 9144−9154], we introduced a new scaling relationship to predict gas solute diffusion at challenging conditions, focusing on CO_2 and SO_2 diffusion in multivalent ionic liquid (IL) solvents. This work extends our initial exploratory study into a much broader array of systems, encompassing additional solutes (N_2, CH_4, C_2H_6, C_3H_8, C_3H_8O, and H_2O) and a variety of different ionic liquid species ($[Bzmim_3]^{3+}$, $[Bzmim_4]^{4+}$, $[BMIM]^+$, $[EMIM]^+$, $[HMIM]^+$, $[NapO_2]^{2-}$, $[BzO_3]^{3-}$, $[BF_4]^-$, $[Tf_2N]^-$, and $[PF_6]^-$). Our study demonstrates a remarkably robust logarithmic correlation between solute diffusion and solvent accessible surface area (SA) across 20 different additional systems. We perform comprehensive analyses of the underlying molecular phenomena responsible for this correlation, including solute lifetime distributions, void space dynamics, and Voronoi tessellation, in order to elucidate a stronger mechanistic understanding of this behavior. Our findings highlight a direct link between the solvent accessible SA and the size of the void domains. Overall, our scaling approach provides an efficient and reliable approach for predicting diffusion from analyses of short simulations at higher temperatures.

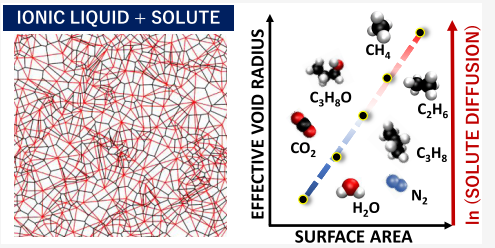

Downloaded via UNIV OF ALABAMA on December 11, 2024 at 15:18:56 (UTC).
See https://pubs.acs.org/sharingguidelines for options on how to legitimately share published articles.

1. INTRODUCTION

Transport processes are fundamental to improving gas separation and storage technologies.[1,2] While it can be challenging to experimentally trace diffusion events in certain situations and within complex materials, molecular dynamics (MD) simulation is a powerful tool for predicting gas diffusion behavior and understanding fundamental transport mechanisms.[3,4] For instance, the diffusion coefficient can be calculated by analyzing the mean square displacement (MSD) of gas molecules using the Einstein correlation.[5] However, complex fluid behavior (e.g., initial ballistic, intermediate sub diffusive, and ultimately long-term diffusive movements) in dense or viscous systems can require lengthy trajectories to accurately determine macroscopic diffusion coefficients.[6] Consequently, there is a strong need for methods which can predict gas diffusion behavior in these types of systems using shorter simulation trajectories.

In our previous study,[7] we explored various temperature scaling approaches to predict CO_2 and SO_2 diffusion coefficients in two multivalent ionic liquid (IL) solvents. We confirmed that gas diffusion does not scale with temperature in a straightforward manner due to the non-Arrhenius hopping behavior of gas molecules in the ILs, since the fluid structure and diffusion pathways are simultaneously affected by changes in temperature. Previous studies[8−10] have attempted to develop universal scaling relationships in soft/condensed matter which often rely on metrics (e.g., excess entropy) that are challenging to calculate. These approaches frequently result in exponential relationships that might require additional effort to determine the associated parameters. Moreover, while they work well for simple liquids, the interactions in ILs introduce further complexities. In contrast, we developed an efficient approach based on a strong logarithmic relationship between the gas diffusion coefficients and the solvent accessible surface areas (SAs) of the ILs as a function of temperature. This observed correlation was rationalized by Danckwerts' surface renewal theory[11] and the Vrentas−Duda free volume model.[12] According to the former, increased SA enhances surface renewal, which in turn increases molecular diffusivity

$$k_L = (D_{AB}s)^{0.5} \tag{1}$$

where k_L is the liquid-side mass transfer coefficient, s is the surface renewal frequency and D_{AB} is the molecular diffusivity of gas in the liquid. On the other hand, the Vrentas−Duda free volume model explains that diffusion is governed by the availability of free spaces in the liquid

$$D = D_0 \exp\left(-\frac{E}{RT}\right)\left(\frac{V_T}{V_1}\right)^{\alpha} \tag{2}$$

where D_0 is a pre-exponential factor at infinite temperature, E is activation energy for diffusion i.e., energy required for a

Received: July 18, 2024
Revised: September 16, 2024
Accepted: September 20, 2024
Published: September 27, 2024

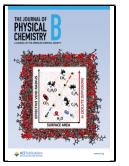

© 2024 American Chemical Society

https://doi.org/10.1021/acs.jpcb.4c04830
J. Phys. Chem. B 2024, 128, 9837−9846

solute molecule to "jump" between voids, R is universal gas constant, T is temperature, V_T and V_1 are the free volume fractions of the solvent at the reference and system temperatures, respectively, and α is a concentration-dependent diffusion parameter. Importantly, E is influenced by solute-IL interactions, as stronger interactions reduce the available free volume, making diffusion more challenging and increasing the energy required for solute movement.

In this study, we expand our analyses to include both multivalent and monovalent ILs, as well as larger solutes (ethane and propane) and polar solutes (propanol and water). These systems significantly broaden the scope of intermolecular interactions encountered, which should provide more evidence for the wider applicability of our scaling approach to other solute/solvent systems. We also investigate the factors underlying this correlation by analyzing the shapes and diameters of the void domains responsible for facilitating gas solute diffusion. Our findings show a direct linear relationship between the SA and the average radius of void domains across varying temperatures. Overall, the observed scaling behavior provides an efficient approach for predicting gas diffusion in viscous IL solvents based on short, high-temperature simulations.

2. METHODS AND COMPUTATIONAL DETAILS

Table 1 lists the composition of IL ion pairs and solutes studied in the present study. Gas solubilities in the ILs

Table 1. Composition of Ion Pairs and Solutes (x = Number of Solute Molecules, m = Number of Cation Molecules, n = Number of Anion Molecules) across the 20 Different Systems Studied

solute (x)	cation (m)	anion (n)	x	m	n
N_2	$[BMIM]^+$	$[BF_4]^-$	6	5000	5000
N_2	$[BMIM]^+$	$[Tf_2N]^-$	5	5000	5000
N_2	$[Bzmim_4]^{4+}$	$[NapO_2]^{2-}$	18	216	432
N_2	$[Bzmim_4]^{3+}$	$[NapO_2]^{2-}$	16	432	648
H_2O	$[BMIM]^+$	$[PF_6]^-$	12	5000	5000
H_2O	$[HMIM]^+$	$[PF_6]^-$	14	5000	5000
CO_2	$[BMIM]^+$	$[BF_4]^-$	20	500	500
CO_2	$[EMIM]^+$	$[Tf_2N]^-$	10	2000	2000
CO_2	$[HMIM]^+$	$[PF_6]^-$	25	500	500
CO_2	$[BMIM]^+$	$[Tf_2N]^-$	29	500	500
CH_4	$[BMIM]^+$	$[BF_4]^-$	4	2000	2000
CH_4	$[BMIM]^+$	$[Tf_2N]^-$	14	5000	5000
CH_4	$[EMIM]^+$	$[Tf_2N]^-$	8	1000	1000
CH_4	$[Bzmim_4]^{3+}$	$[BzO_3]^{3-}$	19	216	216
CH_4	$[Bzmim_3]^{4+}$	$[BzO_3]^{3-}$	80	648	864
C_3H_8O	$[BMIM]^+$	$[BF_4]^-$	8	5000	5000
C_3H_8	$[EMIM]^+$	$[Tf_2N]^-$	11	500	500
C_3H_8	$[BMIM]^+$	$[Tf_2N]^-$	18	500	500
C_2H_6	$[BMIM]^+$	$[BF_4]^-$	6	2000	2000
C_2H_6	$[EMIM]^+$	$[Tf_2N]^-$	7	5000	5000

corresponding to 300 K and 1 bar were sourced from experimental data[7,13−25] to determine the number of solute molecules in each system. Larger systems were used for low-solubility cases, e.g., N_2 in $[BMIM]^+[BF4]^-$, to ensure statistical reliability. Figure 1 shows the chemical structures of the ions and solutes. The OPLS-AA force field parameters for the monovalent ILs were obtained from Doherty et al.,[26] including a charge scaling value of 0.8 to account for polarization and charge transfer effects. For the multivalent ILs, parameters were sourced from Liu et al.,[25] with partial charges estimated using Charge Model 5 (CM5)[27] at the B3LYP/6-311+g(d,p) level and scaled by a factor of 1.2, consistent with previous work.[24,25,28] Parameters for C_2H_6, C_3H_8, and C_3H_8O were derived from LigParGen,[29] while CO_2, CH_4 and N_2 parameters were modeled using the TraPPE force field by Potoff and Siepmann,[30,31] and H_2O was modeled with the SPC/E model.[32] The force field parameters for the ILs and solutes are presented in the Supporting Information.

The MD simulations were conducted using Gromacs 2022.4[33] and visualization was performed with Visual Molecular Dynamics (VMD).[34] Initial configurations for the simulations were built using the PACKMOL package.[35] Following our previous protocol[7,24] simulations were run for 10 ns with a time step of 1 fs at 1 bar in the isothermal−isobaric (NPT) ensemble to equilibrate the systems after energy minimization via the steepest-descent algorithm. Periodic boundary conditions were implemented in all three dimensions, and hydrogen bond lengths were constrained using the LINCS method.[36] The Lennard-Jones potential (for van der Waals (vdW) interactions) and electrostatics were calculated with a 1.2 nm cutoff, while the particle mesh Ewald (PME) method[37] with a 0.12 nm Fourier spacing was used for long-range electrostatics. The Lorentz−Berthelot mixing rules were used to calculate unlike pair interactions, while the Nose-Hoover thermostat[38] and Parrinello−Rahman barostat[39] maintained temperature and pressure, with time constants of 0.5 and 1 ps, respectively. Production phases varied from hundreds of nanoseconds to several microseconds, depending on convergence behavior in the different systems at different temperatures, all conducted at 1 bar. It is important to mention that many of these simulations were conducted at temperatures above the decomposition range of the ILs. However, these systems at elevated temperatures are intended to serve as theoretical replicas to explore phase space, similar to parallel tempering MD techniques which are often conducted at temperatures that exceed the underlying stability limits of the molecules being simulated.

The diffusion coefficient D_i for a solute i was determined by averaging the MSDs over time using the Einstein correlation[5]

$$D_i = \frac{1}{6N}\lim_{t\to\infty}\frac{\mathrm{d}}{\mathrm{d}t}\langle |\boldsymbol{r}_i(t) - \boldsymbol{r}_i(0)|^2\rangle \tag{3}$$

where N is the number of particles, $\boldsymbol{r}_i(t)$ and $\boldsymbol{r}_i(0)$ are the positions of the i-th solute at times t and 0, respectively. Further, we calculated the reduced diffusion coefficient D^* by normalizing D_i at a given temperature with respect to D_i at 300 K, which was then used to evaluate the scaling relationship in this study.

Our in-house code performed SA analyses by determining accessible surfaces of solvent molecules based on their diameters defined by the Lennard-Jones parameters of the OPLS-AA force field, using a spherical probe particle with a radius of 0.075 nm (see Figure S1) and following the method of Gelb and Gubbins.[40] To ensure reliable average SA values, 50−100 different snapshots were extracted from the MD trajectories and analyzed.

Following Gehrke et al.'s methodology,[41] we mapped voids within the systems through Voronoi tessellation using the TRAVIS package.[42] Figure S2 provides a visual summary of the void-related calculations discussed in this work. First, we aligned void spheres within atom spaces by adjusting their

https://doi.org/10.1021/acs.jpcb.4c04830
J. Phys. Chem. B 2024, 128, 9837−9846

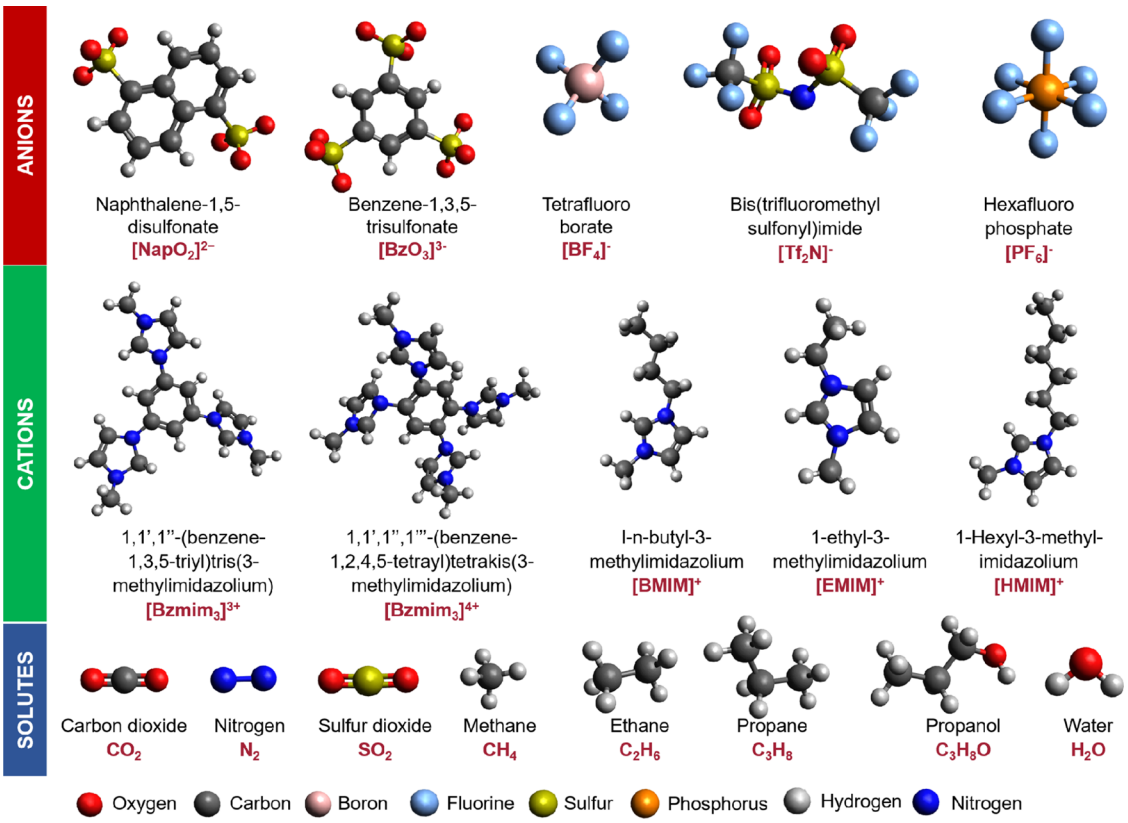

Figure 1. Chemical structures of anions, cations, and solutes composing the systems simulated in this study.

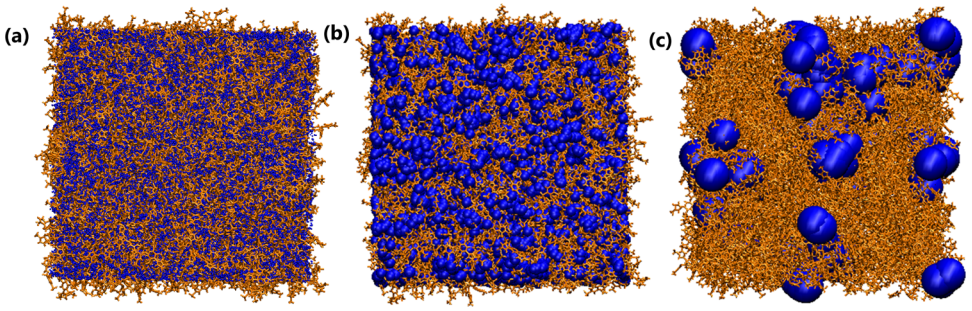

Figure 2. Snapshots of the CH_4-$[Bzmim_3]^{4+}[BzO_3]^{3-}$ system visualizing void spheres with different radii (a) 40 pm, (b) 110 pm, (c) 210 pm in van der Waals (vdW) representation in blue, while the ionic liquid molecules are represented in orange cpk-model.

center and radius. The center was incrementally shifted along a vector starting from the nearest atom to a Voronoi vertex, and this vector was updated as the sphere touched more atoms. At the same time, the radius was increased until the sphere touched four atoms, ensuring the void sphere fits ideally into the void space. Finally, we calculated the exact center and radius by solving the equation

$$r^2 = (x_i - x_k)^2 + (y_i - y_k)^2 + (z_i - z_k)^2 \quad (4)$$

for each of the four atoms with coordinates (x_i, y_i, z_i), where (x_k, y_k, z_k) are the coordinates of the void sphere's center and r is its radius.

Another Voronoi tessellation is then performed in which these void spheres are treated as pseudo atoms and added to the simulation cell. The Voronoi cells corresponding to void spheres are merged to form one or more void domains. To characterize the void network in detail, we calculate the isoperimetric ratio $R_{V/A}$ for the Voronoi cell volume V and surface area A using the formula

$$R_{V/A} = 6\sqrt{\pi}\frac{V}{A^{1.5}} \quad (5)$$

where $R_{V/A} = 1$ for an ideal sphere and decreases as the shape deviates from a sphere. Therefore, a void domain with a high $R_{V/A}$ value suggests that the voids are nearly perfect, isolated spheres. In contrast, interconnected voids with narrow channels have a large surface area relative to their volume, resulting in a lower $R_{V/A}$ value.

Next, we introduce a threshold radius within the IL structure and ignore all void spheres smaller than this threshold. We then repeat the Voronoi tessellation without the omitted void spheres. By gradually increasing the threshold radius stepwise and recalculating the $R_{V/A}$ values, smaller voids are excluded, causing the channels connecting the voids to collapse and leaving only the larger spherical voids. If a probe size between

https://doi.org/10.1021/acs.jpcb.4c04830
J. Phys. Chem. B 2024, 128, 9837−9846

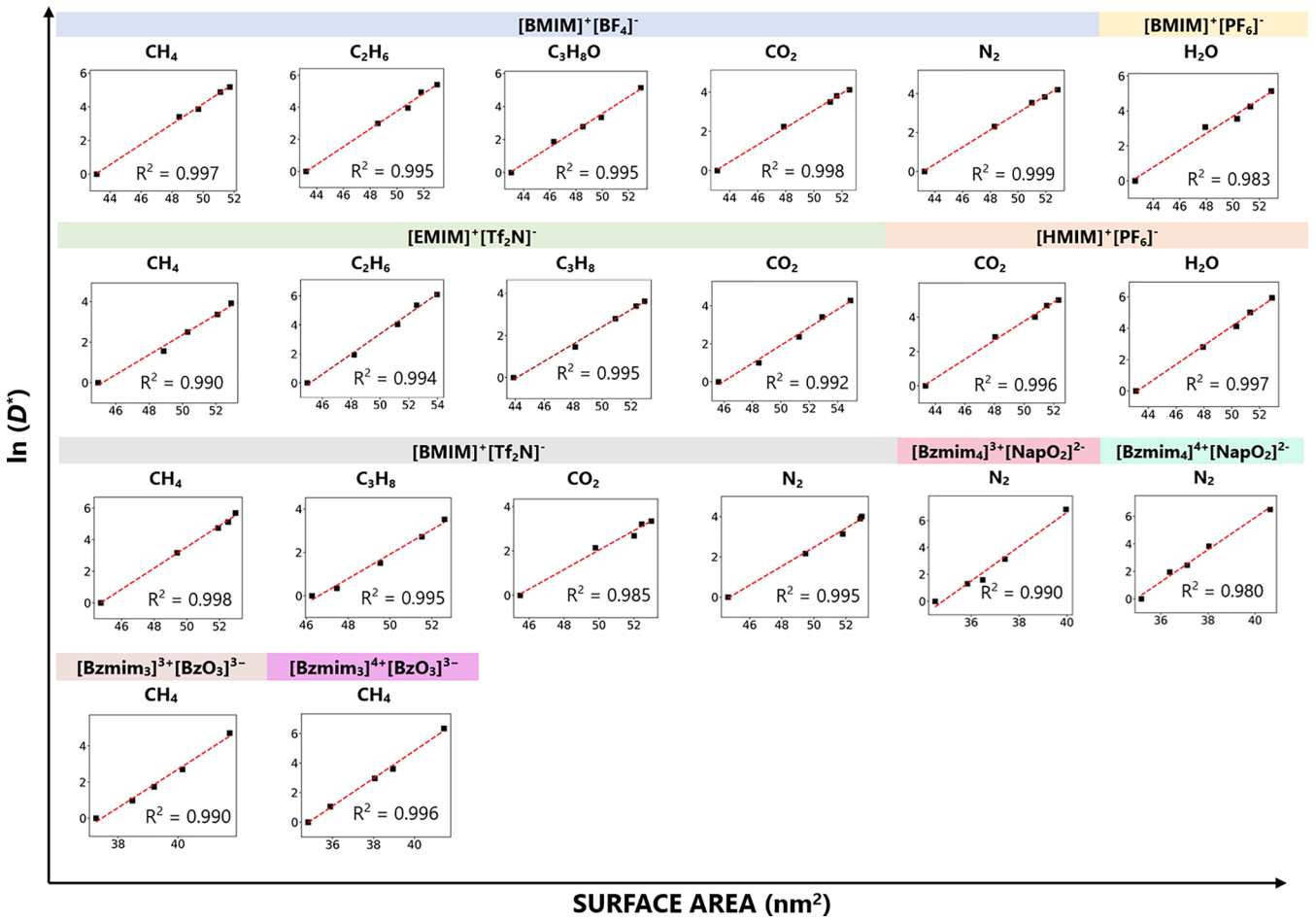

Figure 3. ln D^* as a function of the SA for the systems under study, calculated using a probe size of r = 0.075 nm, as well as R^2 of the scaling relationship across the 20 different systems studied.

two voids is smaller than the threshold, those voids are no longer considered connected, leading to an increase in the average $R_{V/A}$ values (see Figure S2). This increase indicates the decomposition of the void network. For example, as shown in Figure 2, increasing the probe size transitions the void network from interconnected (e.g., 40 pm) to more isolated void spaces (e.g., 210 pm). It should be noted that the voids are shown as ideal spheres.

Similar to Koza et al.'s approach,[43] we also measured percolation within the IL structure by identifying clusters of adjacent voids. First, we extracted coordinates of void domains via the previously mentioned Voronoi tessellation with different threshold radii. Here, the minimum distance between two void sphere centers is set as 50 pm to ensure that the spheres do not significantly overlap. We then divided the simulation box into uniform slices of thickness along the z-direction (z = 0 to $z = L$, where L represents the box length), with each slice having a thickness equal to the void sphere size. For instance, for a 90 pm threshold radius, the slice thickness is 90 pm. Each slice was then transformed into a two-dimensional square lattice along the other two coordinate dimensions (see Figure S3). We classified a lattice site as a void if the center of a void sphere was located within that site. Nearest neighboring lattice sites (including diagonal ones) classified as voids were clustered using a depth-first search algorithm.[44] We also extended this search across the z-direction to account for neighboring void sites in adjacent layers. Finally, we identified the sizes of these percolation networks and computed their occurrence using different threshold radii and corresponding to different system temperatures.

We also calculated the lifetime of a given solute molecule within a void space over a 350 ns duration. The solute is considered to remain in a void space if its net radial displacement $d_n \leq 0.5$ nm from its original location. The algorithm starts with a reference displacement ($d_n = 0$) at $t = 0$, updates this reference when d_n exceeds 0.5 nm, and repeats the process for each solute molecule. The average solute lifetimes in the IL voids ($\tau_{sol\text{-}void}$) were determined using kernel density estimation (KDE)[45] by tracking 10 randomly selected solute molecules. Sensitivity analyses were also conducted for other thresholds ($d_n \leq 0.1$, 1.0 nm).

3. RESULTS AND DISCUSSION

In this section, we evaluate the ln D^* versus SA scaling relationship across 20 systems over a temperature range of 300−800 K. The MSD plots are shown in the Supporting Information (Figures S12−S31), and the ln D^* versus SA plots are shown in Figure 3. The diffusion coefficient and SA both increase with temperature, with similar SA ranges for ILs across different solutes due to minimal structural perturbation by the solutes. Even after several microseconds of simulation, the displacement of CH_4 in $[Bzmim_4]^{3+}[BzO_3]^{3-}$ and $[Bzmim_4]^{4+}[BzO_3]^{3-}$ was still very low (d < 0.6 nm) at temperatures of 300−400 K. Therefore, we collected data at

https://doi.org/10.1021/acs.jpcb.4c04830
J. Phys. Chem. B 2024, 128, 9837−9846

higher temperatures (500−1000 K) to analyze these systems (see Figures S28 and S29). The solute diffusion coefficients in the monovalent ILs at 300 K are in excellent agreement with experimental data[13,46,47] and previous simulations,[48−50] all within the same order of magnitude (10^{-10} m^2/s). While the multivalent ILs have been experimentally synthesized,[51] and some of the physical properties have been evaluated, the diffusion coefficients are not currently available.

In Figure 3, we see that the linear fit of the scaling relationship has an $R^2 \geq 0.98$ for all systems; the lowest values correspond to N_2 in $[Bzmim_4]^{4+}[NapO_2]^{2-}$ (R^2 = 0.980) and H_2O in $[BMIM]^+[PF_6]^-$ (R^2 = 0.983). Thus, it is possible to reliably extrapolate the diffusion coefficient from high to low temperatures, with a high degree of confidence. We can also verify that this method is relatively robust, based on the diversity of solvent and solute molecules tested so far. It should be noted that at high solute concentrations, the diffusion coefficient could be influenced by solute−solute collisions and the occupation of void spaces, which may affect surface area and void connectivity, potentially leading to solvent expansion. Crowding effects can also change diffusion pathways. Therefore, the scaling relation may not hold under these conditions. However, these scenarios are less relevant for our work, as high solute concentrations typically imply very high gas phase partial pressures in IL solvents.

By comparing eq 2 and the ln D^* relationship in Figure 3, the SA is analogous to free volume in the theoretical model. Both emphasize that diffusion increases with more available free space, though the mathematical forms differ. This could arise from the unique structural properties of ILs and their interaction with solutes, which might not be fully captured by the simpler assumptions in the Vrentas-Duda model.

This study validates the broader applicability of our method (beyond our initial case studies[7]) and motivates further investigation to understand the factors behind the strong correlation. Thus, we performed a more rigorous evaluation of four selected systems, each with very different interactions: CH_4 in $[Bzmim_4]^{4+}[BzO_3]^{3-}$, N_2 in $[Bzmim_4]^{3+}[NapO_2]^{2-}$, CO_2 in $[BMIM]^+[BF_4]^-$, and CO_2 in $[HMIM]^+[PF_6]^-$. The consistent results across these ILs suggest that our findings should be applicable to the other IL systems in this study and potentially to other solvents.

Solute diffusion in these systems is generally ascribed to a transport mechanism involving solute molecules hopping between neighboring voids within the solvent.[52−54] Void spaces within the fluid accommodate the solute species, and connections or windows between these regions provide a percolating network to allow for solute diffusion through the fluid. Figure S3 shows a static two-dimensional void structure along the z-direction corresponding to different slices within the $[Bzmim_4]^{4+}[BzO_3]^{3-}$ system, suggesting a heterogeneous distribution. Figure S4a quantifies the probability of finding different numbers of neighboring vacant sites within each unique void region (i.e., cluster). As the size of a cluster increases, its occurrence decreases sharply, and the probability also naturally decreases with increasing threshold radius. When smaller threshold radii (e.g., 90 pm) are tested, voids are theoretically more connected, enhancing percolation, whereas larger radii tend to merge voids into larger, more disconnected clusters. At higher temperatures (Figure S4b), there is a general growth of void cluster size, corresponding to enhanced solute hopping and increased diffusion through the IL fluid.

We analyzed the hopping of solute molecule between void spaces in the IL over a 350 ns duration, as shown in Figure 4

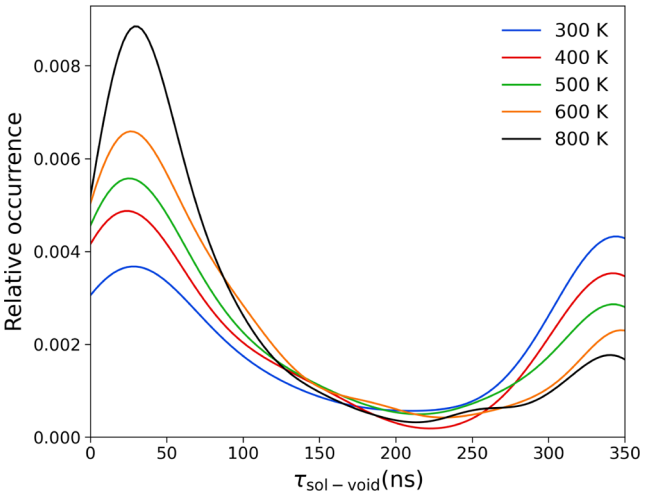

Figure 4. Temperature-dependent distribution of $\tau_{sol\text{-}void}$ of CH_4 in the $[Bzmim_3]^{4+}[BzO_3]^{3-}$ system (within a 350 ns duration).

(representative displacement plots of solute molecules can be found in Figure S5). The $\tau_{sol\text{-}void}$ distribution shows two peaks: an initial peak around 40 ns and a second peak around 340 ns. The height of the first peak increases with temperature (relative to the second peak), suggesting an acceleration in the void-to-void hoping frequency. On the other hand, the height of the second peak reduces with temperature, implying that prolonged entrapment in stable pockets (i.e., large $\tau_{sol\text{-}void}$ values) is more common at lower temperatures due to insufficient kinetic energy to overcome diffusion barriers. Krishnan et al.'s study[55] on hydrogen diffusion in clathrate hydrates is consistent with the behavior observed in our IL systems (i.e., increasing temperature enhances intercage hopping). We also tested the sensitivity of both peaks to variations in the net radial displacement d_n used for calculating average solute lifetime (Figure S6). As d_n increases, the peak around 40 ns reduces, while the peak around 340 ns become more pronounced, suggesting that the higher threshold makes solutes less likely to escape from one pocket to another.

Next, we analyzed the void network using the Voronoi tessellation approach described earlier in Section 2. Figure S7 shows the $R_{V/A}$ distributions of void domains (formed by combined Voronoi cells of the void spheres), while Figure S8 provides a visual representation of the void spaces within the CH_4-$[Bzmim_4]^{4+}[BzO_3]^{3-}$ and CO_2-$[BMIM]^+[BF_4]^-$ systems at 300 and 800 K. At 300 K, most void domains have an $R_{V/A}$ around 0.8, indicating they are nearly spherical ($R_{V/A}$ = 1). For $[Bzmim_4]^{4+}[BzO_3]^{3-}$ and $[Bzmim_4]^{3+}[NapO_2]^{2-}$, there is a shoulder peak at around 0.6. As temperature increases, the monovalent ILs ($[BMIM]^+[BF_4]^-$ and $[HMIM]^+[PF_6]^-$) show a narrowing distribution which shifts closer to $R_{V/A}$ = 1, while the distributions corresponding to the multivalent ILs ($[Bzmim_4]^{4+}[BzO_3]^{3-}$ and $[Bzmim_4]^{3+}[NapO_2]^{2-}$) are much more stagnant. This is likely due to the simpler coordination environments and lower viscosities of the monovalent ILs.[56,57]

To characterize the size of void domains, we adopt the definition of Gehrke et al.[41] by defining an effective void radius $r_{eff} = \left(\frac{3V}{4\pi}\right)^{1/3}$; this radius corresponds to the same volume as a

https://doi.org/10.1021/acs.jpcb.4c04830
J. Phys. Chem. B 2024, 128, 9837−9846

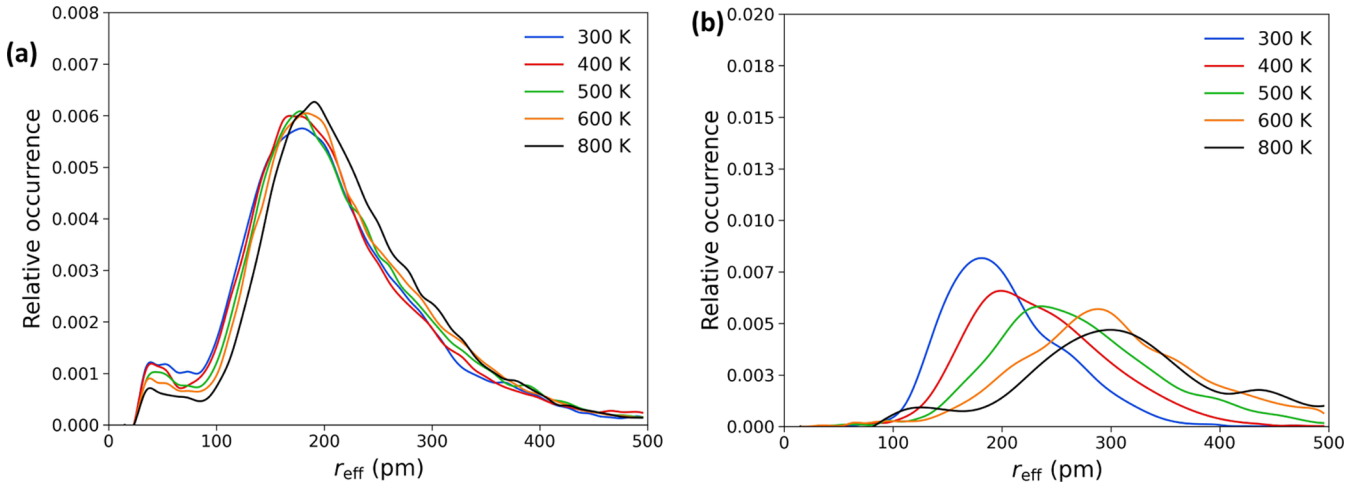

Figure 5. Distribution of effective void radii r_{eff} in (a) CH_4-$[Bzmim_3]^{4+}[BzO_3]^{3-}$ and (b) CO_2–$[BMIM]^{+}[BF_4]^{-}$ systems from a Voronoi-based void analysis of the systems.

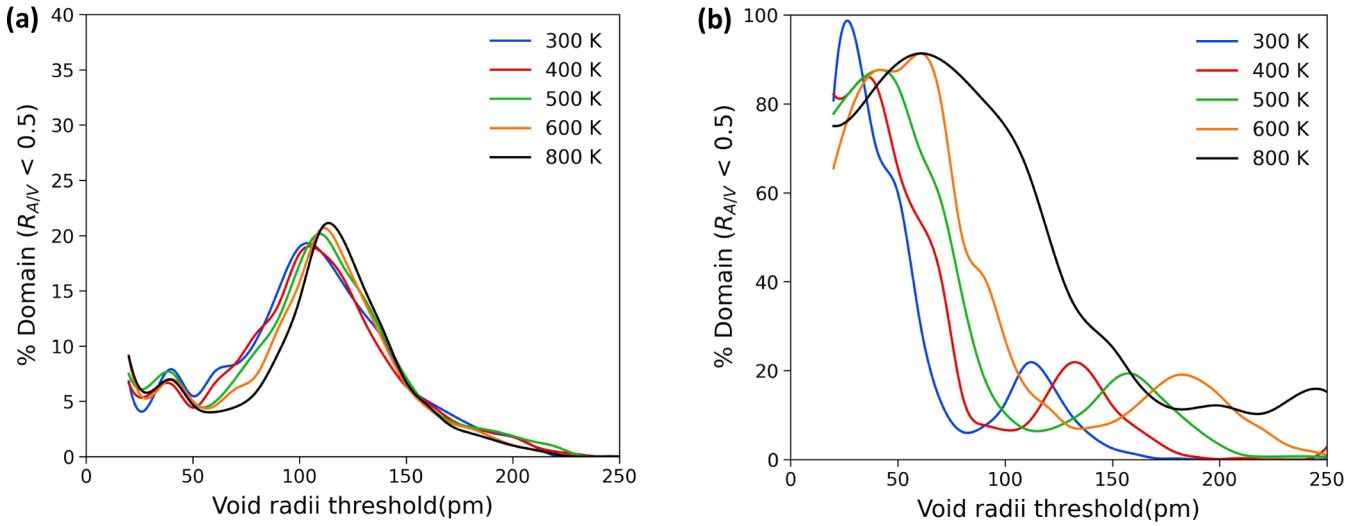

Figure 6. Fraction of the void domains with $R_{V/A}$ < 0.5 for different threshold radii in (a) CH_4-$[Bzmim_3]_4^{+}[BzO_3]_3^{-}$, (b) CO_2-$[BMIM]^{+}[BF_4]^{-}$.

void domain with a spherical shape. Our initial tests in Figure S9 show that setting the criteria for a spherical shape to $R_{V/A}$ > 0.4, 0.5, and 0.6 results in similar distribution curves. However, choosing a highly restrictive criterion (e.g., $R_{V/A}$ > 0.8) could result in ignoring small void domain sizes, such as the shoulder peak around 50 pm. Thus, a criterion of $R_{V/A}$ > 0.5 is chosen here (consistent with Gehrke et al. and Brehm et al.[41,58]) to distinguish between relatively spherical versus nonspherical domains.

We present the r_{eff} distribution for CH_4-$[Bzmim_3]^{4+}[BzO_3]^{3-}$ and CO_2-$[BMIM]^{+}[BF_4]^{-}$ in Figure 5 and N_2-$[Bzmim_4]^{3+}[NapO_2]^{2-}$ and CO_2-$[HMIM]^{+}[PF_6]^{-}$ in Figure S10. For CH_4-$[Bzmim_3]^{4+}[BzO_3]^{3-}$ and $[Bzmim_4]^{3+}[NapO_2]^{2-}$, there is a peak around 180 pm at 300 K. This peak indicates the most common void domain size at this temperature. Although the overall distribution remains relatively consistent across all temperatures, the peak shifts slightly and broadens toward larger radii at higher temperatures. A secondary peak (of lower occurrence) around 50 pm is present at all temperatures but becomes less pronounced with increasing temperature.

For CO_2-$[BMIM]^{+}[BF_4]^{-}$ and CO_2-$[HMIM]^{+}[PF_6]^{-}$, the peak occurs around 190 pm at 300 K. As temperature increases from 300 to 800 K, the peak shifts significantly toward larger radii (around 300 pm at 800 K). The peak occurrence decreases, and the distribution broadens. This shift to larger r_{eff} at higher temperatures suggests that the void spaces are expanding, which also corresponds to increased diffusion rates.

Further, we analyzed the decomposition of the void domains described in Section 2. Figure 6 shows the percentage of domains with an $R_{V/A}$ < 0.5 when different threshold radii are used. As previously mentioned, $R_{V/A}$ = 1 for an ideal sphere and decreases as the shape deviates more from a spherical shape. These regions ($R_{V/A}$ < 0.5) are interpreted to correspond to the void pathways connecting the more spherical void regions in the fluid. Therefore, a high fraction of void domains with $R_{V/A}$ < 0.5 suggests the presence of many interconnected voids, while a low fraction suggests that these voids would generally be more isolated. Even if the void network is highly connected at a specific threshold radius, these spaces are very small. Most solutes would be larger than these radii. However, due to the soft nature of the system, molecules can still squeeze through these spaces. When the

https://doi.org/10.1021/acs.jpcb.4c04830
J. Phys. Chem. B 2024, 128, 9837−9846

void network consists mainly of isolated spheres with fewer connections, solute transport becomes significantly hindered.

In $[Bzmim_3]^{4+}[BzO_3]^{3-}$ (Figure 6a), we observe a small peak around 40 pm showing ∼8% of the domains are connected. At threshold radii ranging from 20 and 50 pm, the percentage of connected voids is low across all temperatures. This is likely due to the complex coordination environment and dense nature of the IL fluid, which obstructs the connection of very small void spaces. On the other hand, we observe a higher peak around 100 pm at 300 K with ∼20% of the domains having $R_{V/A}$ < 0.5, indicating moderate connectivity between the IL void spaces. Generally, one would expect an increase in $R_{V/A}$ values with larger thresholds. However, the lower peak around 40 pm suggests the presence of very small void spots distributed throughout the system. These voids can either be spherical and located within clusters of closely packed molecules or take the form of thread-like connections between larger networks. Increasing the threshold from 50 to 110 pm excludes these small voids, thereby reducing the number of spherical domains and enhancing the presence of network-like domains. Therefore, this peak around 100 pm suggests the most probable threshold radius for void connectivity, even though the void spaces are still relatively unconnected (∼20%). In other words, on average 80% of the void domains remain isolated, which impedes the transport of the CH_4 molecules. As the threshold radius increases from 100 to 170 pm, the percentage of domains with $R_{V/A}$ < 0.5 declines sharply, signifying a higher prevalence of isolated void spheres. Beyond 170 pm, there are no domains with $R_{V/A}$ < 0.5, suggesting that the network becomes completely disconnected into separate void spaces. With rising temperatures, the peak around 100 pm becomes more pronounced, indicating an increase in the number of connected voids. Additionally, this peak shifts slightly to the right, implying that it can accommodate larger solute molecules, making it easier for CH_4 molecules to move through the channels between the void spaces in the fluid.

For the $[BMIM]^+[BF_4]^-$ system (Figure 6b), the percentage of domains with $R_{V/A}$ < 0.5 around 50 pm is about 80% at 300 K, indicating a highly connected void network at that small scale, facilitating CO_2 transport through the IL. At around 110 pm, there is still some connectivity (20% of domains with $R_{V/A}$ < 0.5) at 300 K, similar to the $[Bzmim_3]^{4+}[BzO_3]^{3-}$ system. Gehrke et al.[41] also observed similar trends in the diffusion analyses of CO_2 in ethylammonium nitrate.

Above 150 pm, we observe complete decomposition of the void network (0% of the domains with $R_{V/A}$ < 0.5). Between 300 and 800 K, the connectivity increases from around 80 to 95% using a 50 pm void threshold. The shoulder peak shifts from 110 pm at 300 K to about 220 pm at 800 K, indicating larger void spaces which are occasionally connected (20%). This shift with respect to the temperature is more noticeable in the $[BMIM]^+[BF_4]^-$ (Figure 6b) compared to $[Bzmim_3]^{4+}[BzO_3]^{3-}$ (Figure 6a). The former exhibits a higher percentage (60−100%) of connected networks between 10 and 50 pm, whereas the latter shows 5−10%. This could explain the difference in the order of magnitude of displacement of CO_2 in $[BMIM]^+[BF_4]^-$ and CH_4 in $[Bzmim_3]^{4+}[BzO_3]^{3-}$; the MSD in $[BMIM]^+[BF_4]^-$ at 300 K is ∼400 nm^2 after 250 ns (Figure S12), whereas in $[Bzmim_3]^{4+}[BzO_3]^{3-}$ the MSD is ∼0.2 nm^2 (Figure S29) even at 500 K. Similar trends in the decomposition of the void network are observed in the $[Bzmim_4]^{3+}[NapO_2]^{2-}$ and $[HMIM]^+[PF_6]^-$ systems (see Figure S11).

Overall, increasing temperature facilitates void connectivity, characterized by voids in a network-like structure. For $[Bzmim_3]^{4+}[BzO_3]^{3-}$ and $[Bzmim_4]^{3+}[NapO_2]^{2-}$, there is an optimal connection between voids of sizes 110 pm (∼20%), whereas for $[BMIM]^+[BF_4]^-$ and $[HMIM]^+[PF_6]^-$, the voids are well connected (∼80%) when 50 pm void sizes are used, and there are occasional connections between void sizes around 100 pm (∼20%) at 300 K. The connectivity between the voids in these ILs facilitates the diffusion of molecules through the liquid and contributes to the accessible areas (i.e., solvent surface areas) through which they move.

Although the three-dimensional void network is of paramount importance to characterizing the solute diffusion behavior, we have found that this network can be dimensionally reduced to an equivalent void SA, which can be used as a surrogate for analyzing the solute transport within the different IL solvents and at different temperatures. To corroborate this, we observe a positive linear correlation in Figure 7 between the

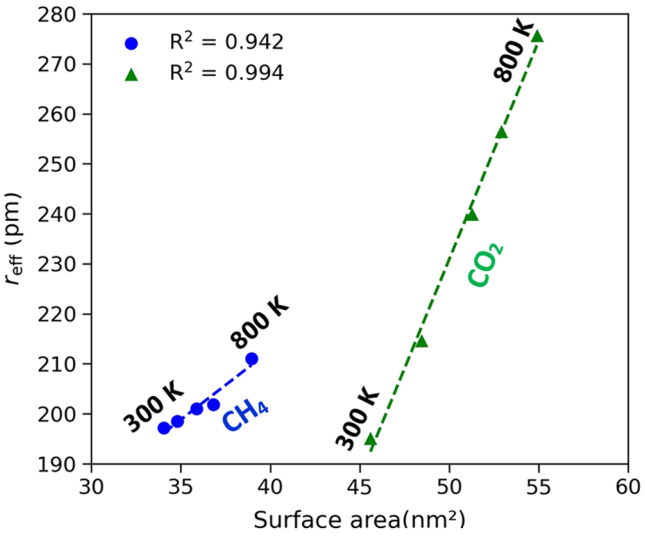

Figure 7. $\bar{r}_{eff}$ versus solvent accessible SA for CH_4-$[Bzmim_3]^{4+}[BzO_3]^{3-}$ (blue spheres) and CO_2-$[BMIM]^+[BF_4]^-$ (green triangles) systems.

average effective void radius ($\bar{r}_{eff}$) and solvent SA, where $\bar{r}_{eff}$ was calculated from Figure 5 as the weighted average of the effective void radii based on relative occurrences. The data points for the two IL systems are distinct. The CO_2-$[BMIM]^+[BF_4]^-$ system shows a stronger correlation (R^2 = 0.994) than the CH_4-$[Bzmim_3]^{4+}[BzO_3]^{3-}$ system with an R^2 of 0.942. This is likely because CO_2-$[BMIM]^+[BF_4]^-$ has a more uniform distribution of voids or a more well-developed network structure for solute movement. In contrast, CH_4-$[Bzmim_3]^{4+}[BzO_3]^{3-}$ may have more variability in void sizes or less connectivity, as described in Figures 5 and 6. Furthermore, if both ln D^* and $\bar{r}_{eff}$ scale linearly with SA, ln D^* can be inferred to scale linearly with $\bar{r}_{eff}$. However, there is an advantage of using SA for this scaling relationship due to the higher computational effort required for calculating $\bar{r}_{eff}$.

The isoperimetric ratio in eq 5 and effective void radius can be combined to establish a relationship between r_{eff} and void SA

https://doi.org/10.1021/acs.jpcb.4c04830
J. Phys. Chem. B 2024, 128, 9837−9846

$$r_{\text{eff}} = \frac{R_{V/A}^{0.33}}{2\pi^{0.5}} A^{0.5} \quad (6)$$

The above equation suggests a square root relationship between r_{eff} and A. However, due to slight variations in $R_{V/A}$ (as shown in Figure S7), the relationship may approximate a linear form over the range of SA values, making the correlation $r_{\text{eff}} \propto A^{0.5}$ appear linear, especially when averaged across the system. The slope from eq 6 highlights how void geometry influences the relationship between the void domain size and void SA. A steeper slope, such as in the CO_2-$[BMIM]^+[BF4]^-$ system (Figure 7), indicates that for a given increase in SA, r_{eff} increases more significantly, implying more spherical and potentially more connected voids.

In summary, the strong logarithmic correlation between diffusion coefficient and SA can be rationalized by larger $\overline{r}_{\text{eff}}$ at higher temperatures facilitating molecule movement through the IL network and reducing resistance through diffusion barriers. Higher temperatures increase molecular motion, leading to larger and better-connected voids, which in turn increases the solvent accessible SA. The relationship between $\overline{r}_{\text{eff}}$ and SA may explain the ln D^* versus SA relationship, providing a comparison of diffusion behaviors and void connectivity across different ILs and temperatures, which influence accessible SA.

4. CONCLUSIONS

In this study, we investigated the relationship between gas solute diffusivity and solvent accessible SA in a range of IL solvents, encompassing both multivalent and monovalent ILs, as well as larger solutes (ethane and propane) and polar solutes (propanol and water). Our results revealed a robust logarithmic correlation between ln D^* and SA, with $R^2 \geq 0.98$ for all studied systems. By characterizing the void domains within the ILs via Voronoi tessellation analyses, we determined the effective void radii and found that higher temperatures increase void size and connectivity, corresponding to enhanced diffusion. Furthermore, we found a positive linear correlation between the effective void radii and the solvent accessible SA, rationalizing the phenomenological ln D^* and SA relationship by the increased molecular movement through the IL network at higher temperatures.

Overall, our findings confirm that the solvent accessible SA is a reliable predictor of gas solute diffusivity in IL solvents, allowing for reliable extrapolation of diffusion coefficients from high-temperature simulations to lower temperatures. This simple and efficient scaling approach reduces the computational effort required for lengthy MD simulations, accelerating gas diffusion predictions in ILs, which could benefit other computational studies involving gas separation and storage. In the future, we are interested in exploring the applicability limits of the scaling relation, particularly in high solute concentration scenarios and in other conventional solvent systems.

■ ASSOCIATED CONTENT

Data Availability Statement

The data sets generated during and/or analyzed during the current study are available from the corresponding author on reasonable request.

Supporting Information

The Supporting Information is available free of charge at https://pubs.acs.org/doi/10.1021/acs.jpcb.4c04830.

Snapshot of SA analysis, schematic illustrating void-related calculations, void lattice representation, occurrence of void clusters with varying threshold radii and at different temperatures, displacement plots, $R_{V/A}$ distributions, snapshots of void spaces, r_{eff} distribution based on different criteria, additional plots for the fraction of the void domains with an $R_{V/A} < 0.5$ for different threshold radii, MSDs versus time at various temperatures (PDF)

Force field parameters for the anions, cations, and solutes (PDF)

■ AUTHOR INFORMATION

Corresponding Author

C. Heath Turner − *Department of Chemical and Biological Engineering, The University of Alabama, Tuscaloosa, Alabama 35487-0203, United States;* orcid.org/0000-0002-5707-9480; Phone: 205-348-1733; Email: hturner@eng.ua.edu

Author

Feranmi V. Olowookere − *Department of Chemical and Biological Engineering, The University of Alabama, Tuscaloosa, Alabama 35487-0203, United States*

Complete contact information is available at: https://pubs.acs.org/10.1021/acs.jpcb.4c04830

Notes

The authors declare no competing financial interest.

■ ACKNOWLEDGMENTS

This work is supported by the National Science Foundation (Award #: 2132133 and 2029387). We are grateful to the Alabama Supercomputer Authority for computational support.

■ REFERENCES

(1) Fu, Y.; Yang, Z.; Mahurin, S. M.; Dai, S.; Jiang, D.-e. Ionic liquids for carbon capture. *MRS Bull.* **2022**, *47* (4), 395−404.

(2) Bukowski, B. C.; Keil, F. J.; Ravikovitch, P. I.; Sastre, G.; Snurr, R. Q.; Coppens, M.-O. Connecting theory and simulation with experiment for the study of diffusion in nanoporous solids. *Adsorption* **2021**, *27* (5), 683−760.

(3) Aghaie, M.; Rezaei, N.; Zendehboudi, S. New insights into bulk and interface properties of [Bmim][Ac]/[Bmim][BF4] ionic liquid/CO2 systems—Molecular dynamics simulation approach. *J. Mol. Liq.* **2020**, *317*, No. 113497.

(4) Reddy, T. D. N.; Mallik, B. S. Ionic dynamics of hydroxylammonium ionic liquids: a classical molecular dynamics simulation study. *J. Phys. Chem. B* **2020**, *124* (24), 4960−4974.

(5) Cappelezzo, M.; Capellari, C.; Pezzin, S.; Coelho, L. Stokes-Einstein relation for pure simple fluids. *J. Chem. Phys.* **2007**, *126* (22), No. 224516.

(6) Song, S.; Park, S. J.; Kim, M.; Kim, J. S.; Sung, B. J.; Lee, S.; Kim, J.-H.; Sung, J. Transport dynamics of complex fluids. *Proc. Natl. Acad. Sci. U.S.A.* **2019**, *116* (26), 12733−12742.

(7) Olowookere, F. V.; Turner, C. H. Predicting Gaseous Solute Diffusion in Viscous Multivalent Ionic Liquid Solvents. *J. Phys. Chem. B* **2023**, *127* (42), 9144−9154.

(8) Dzugutov, M. addendum: A universal scaling law for atomic diffusion in condensed matter. *Nature* **2001**, *411* (6838), 720.

(9) Mittal, J.; Errington, J. R.; Truskett, T. M. Does confining the hard-sphere fluid between hard walls change its average properties? *J. Chem. Phys.* **2007**, *126* (24), No. 244708.

(10) Mittal, J.; Errington, J. R.; Truskett, T. M. Relationships between self-diffusivity, packing fraction, and excess entropy in simple

bulk and confined fluids. *J. Phys. Chem. B* **2007**, *111* (34), 10054−10063.
(11) Danckwerts, P. V. Significance of liquid-film coefficients in gas absorption. *Ind. Eng. Chem.* **1951**, *43* (6), 1460−1467.
(12) Vrentas, J. S.; Duda, J.; Ling, H. C.; Hou, A. C. Free-volume theories for self-diffusion in polymer−solvent systems. II. Predictive capabilities. *J. Polym. Sci., Polym. Phys. Ed.* **1985**, *23* (2), 289−304.
(13) Shiflett, M. B.; Yokozeki, A. Solubilities and diffusivities of carbon dioxide in ionic liquids:[bmim][PF6] and [bmim][BF4]. *Ind. Eng. Chem. Res.* **2005**, *44* (12), 4453−4464.
(14) Jacquemin, J.; Gomes, M. F. C.; Husson, P.; Majer, V. Solubility of carbon dioxide, ethane, methane, oxygen, nitrogen, hydrogen, argon, and carbon monoxide in 1-butyl-3-methylimidazolium tetrafluoroborate between temperatures 283 and 343 K and at pressures close to atmospheric. *J. Chem. Thermodyn.* **2006**, *38* (4), 490−502.
(15) Hong, G.; Jacquemin, J.; Deetlefs, M.; Hardacre, C.; Husson, P.; Gomes, M. C. Solubility of carbon dioxide and ethane in three ionic liquids based on the bis{(trifluoromethyl) sulfonyl}imide anion. *Fluid Phase Equilib.* **2007**, *257* (1), 27−34.
(16) Chen, Y.; Mutelet, F.; Jaubert, J.-N. Solubility of carbon dioxide, nitrous oxide and methane in ionic liquids at pressures close to atmospheric. *Fluid Phase Equilib.* **2014**, *372*, 26−33.
(17) Liu, X.; Afzal, W.; Prausnitz, J. M. Solubilities of Small Hydrocarbons in Tetrabutylphosphonium Bis (2,4,4-trimethylpentyl) Phosphinate and in 1-Ethyl-3-methylimidazolium Bis (trifluoromethylsulfonyl) imide. *Ind. Eng. Chem. Res.* **2013**, *52* (42), 14975−14978.
(18) Akbari, F.; ALmutairi, F. D.; Alavianmehr, M. M. Solubility of gases in ionic liquids using PHTC equation of state. *J. Mol. Liq.* **2019**, *276*, 553−561.
(19) Lee, B.-C.; Outcalt, S. L. Solubilities of gases in the ionic liquid 1-n-butyl-3-methylimidazolium bis (trifluoromethylsulfonyl) imide. *J. Chem. Eng. Data* **2006**, *51* (3), 892−897.
(20) Tagiuri, A.; Sumon, K. Z.; Henni, A. Solubility of carbon dioxide in three [Tf2N] ionic liquids. *Fluid Phase Equilib.* **2014**, *380*, 39−47.
(21) Ramdin, M.; Balaji, S. P.; Vicent-Luna, J. M.; Gutiérrez-Sevillano, J. J.; Calero, S.; De Loos, T. W.; Vlugt, T. J. Solubility of the precombustion gases CO2, CH4, CO, H2, N2, and H2S in the ionic liquid [bmim][Tf2N] from Monte Carlo simulations. *J. Phys. Chem. C* **2014**, *118* (41), 23599−23604.
(22) Crosthwaite, J. M.; Aki, S. N.; Maginn, E. J.; Brennecke, J. F. Liquid phase behavior of imidazolium-based ionic liquids with alcohols. *J. Phys. Chem. B* **2004**, *108* (16), 5113−5119.
(23) Freire, M. G.; Santos, L. M.; Fernandes, A. M.; Coutinho, J. A.; Marrucho, I. M. An overview of the mutual solubilities of water−imidazolium-based ionic liquids systems. *Fluid Phase Equilib.* **2007**, *261* (1−2), 449−454.
(24) Liu, X.; Bara, J. E.; Turner, C. H. Understanding gas solubility of pure component and binary mixtures within multivalent ionic liquids from molecular simulations. *J. Phys. Chem. B* **2021**, *125* (29), 8165−8174.
(25) Liu, X.; O'Harra, K. E.; Bara, J. E.; Turner, C. H. Molecular insight into the anion effect and free volume effect of CO 2 solubility in multivalent ionic liquids. *Phys. Chem. Chem. Phys.* **2020**, *22* (36), 20618−20633.
(26) Doherty, B.; Zhong, X.; Gathiaka, S.; Li, B.; Acevedo, O. Revisiting OPLS force field parameters for ionic liquid simulations. *J. Chem. Theory Comput.* **2017**, *13* (12), 6131−6145.
(27) Marenich, A. V.; Jerome, S. V.; Cramer, C. J.; Truhlar, D. G. Charge model 5: An extension of Hirshfeld population analysis for the accurate description of molecular interactions in gaseous and condensed phases. *J. Chem. Theory Comput.* **2012**, *8* (2), 527−541.
(28) Barbosa, G. D.; Liu, X.; O'Harra, K. E.; Bara, J. E.; Turner, C. H. Charge scaling parameter evaluation for multivalent ionic liquids with fixed point charge force fields. *J. Ionic Liq.* **2022**, *2* (1), No. 100020.
(29) Dodda, L. S.; Cabeza de Vaca, I.; Tirado-Rives, J.; Jorgensen, W. L. LigParGen web server: an automatic OPLS-AA parameter generator for organic ligands. *Nucleic Acids Res.* **2017**, *45* (W1), W331−W336.
(30) Potoff, J. J.; Siepmann, J. I. Vapor−liquid equilibria of mixtures containing alkanes, carbon dioxide, and nitrogen. *AIChE J.* **2001**, *47* (7), 1676−1682.
(31) Chen, B.; Siepmann, J. I. Transferable potentials for phase equilibria. 3. Explicit-hydrogen description of normal alkanes. *J. Phys. Chem. B* **1999**, *103* (25), 5370−5379.
(32) Berendsen, H.-J.-C.; Grigera, J.-R.; Straatsma, T. P. The missing term in effective pair potentials. *J. Phys. Chem. A* **1987**, *91* (24), 6269−6271.
(33) Abraham, M. J.; Murtola, T.; Schulz, R.; Páll, S.; Smith, J. C.; Hess, B.; Lindahl, E. GROMACS: High performance molecular simulations through multi-level parallelism from laptops to supercomputers. *SoftwareX* **2015**, *1−2*, 19−25.
(34) Humphrey, W.; Dalke, A.; Schulten, K. VMD: visual molecular dynamics. *J. Mol. Graphics* **1996**, *14* (1), 33−38.
(35) Martínez, L.; Andrade, R.; Birgin, E. G.; Martínez, J. M. PACKMOL: A package for building initial configurations for molecular dynamics simulations. *J. Comput. Chem.* **2009**, *30* (13), 2157−2164.
(36) Hess, B.; Bekker, H.; Berendsen, H. J.; Fraaije, J. G. LINCS: a linear constraint solver for molecular simulations. *J. Comput. Chem.* **1997**, *18* (12), 1463−1472.
(37) Darden, T.; York, D.; Pedersen, L. Particle mesh Ewald: An N·log (N) method for Ewald sums in large systems. *J. Chem. Phys.* **1993**, *98* (12), 10089−10092.
(38) Hoover, W. G. Canonical dynamics: Equilibrium phase-space distributions. *Phys. Rev. A* **1985**, *31* (3), 1695.
(39) Parrinello, M.; Rahman, A. Crystal structure and pair potentials: A molecular-dynamics study. *Phys. Rev. Lett.* **1980**, *45* (14), 1196.
(40) Gelb, L. D.; Gubbins, K. E. Pore size distributions in porous glasses: a computer simulation study. *Langmuir* **1999**, *15* (2), 305−308.
(41) Gehrke, S.; Macchieraldo, R.; Kirchner, B. Understanding the fluidity of condensed phase systems in terms of voids—novel algorithm, implementation and application. *Phys. Chem. Chem. Phys.* **2019**, *21* (9), 4988−4997.
(42) Brehm, M.; Thomas, M.; Gehrke, S.; Kirchner, B. TRAVIS—A free analyzer for trajectories from molecular simulation. *J. Chem. Phys.* **2020**, *152* (16), No. 164105.
(43) Koza, Z.; Kondrat, G.; Suszczyński, K. Percolation of overlapping squares or cubes on a lattice. *J. Stat. Mech.: Theory Exp.* **2014**, *2014* (11), No. P11005.
(44) Tarjan, R. Depth-first search and linear graph algorithms. *SIAM J. Comput.* **1972**, *1* (2), 146−160.
(45) Botev, Z. I.; Grotowski, J. F.; Kroese, D. P. Kernel density estimation via diffusion. *Ann. Stat.* **2010**, *38*, 2916−2957.
(46) Friedrich, M. F.; Kokolakis, S.; Lucas, M.; Claus, P. Measuring Diffusion and Solubility of Slightly Soluble Gases in [C n MIM][NTf2] Ionic Liquids. *J. Chem. Eng. Data* **2016**, *61* (4), 1616−1624.
(47) Camper, D.; Becker, C.; Koval, C.; Noble, R. Diffusion and solubility measurements in room temperature ionic liquids. *Ind. Eng. Chem. Res.* **2006**, *45* (1), 445−450.
(48) Budhathoki, S.; Shah, J. K.; Maginn, E. J. Molecular Simulation Study of the Solubility, Diffusivity and Permselectivity of Pure and Binary Mixtures of CO2 and CH4 in the Ionic Liquid 1-n-Butyl-3-methylimidazolium bis (trifluoromethylsulfonyl) imide. *Ind. Eng. Chem. Res.* **2015**, *54* (35), 8821−8828.
(49) Méndez-Morales, T.; Carrete, J.; Cabeza, O.; Gallego, L. J.; Varela, L. M. Molecular dynamics simulation of the structure and dynamics of water−1-alkyl-3-methylimidazolium ionic liquid mixtures. *J. Phys. Chem. B* **2011**, *115* (21), 6995−7008.
(50) Sharma, A.; Ghorai, P. K. Effect of water on structure and dynamics of [BMIM][PF6] ionic liquid: An all-atom molecular

https://doi.org/10.1021/acs.jpcb.4c04830
J. Phys. Chem. B 2024, 128, 9837−9846

dynamics simulation investigation. *J. Chem. Phys.* **2016**, *144* (11), No. 114505.
(51) O'Harra, K. E.; DeVriese, E. M.; Turflinger, E. M.; Noll, D. M.; Bara, J. E. Design and gas separation performance of imidazolium Poly (ILs) containing multivalent imidazolium fillers and crosslinking agents. *Polymers* **2021**, *13* (9), 1388.
(52) Gaudin, T.; Ma, H. The macroscopic viscosity approximation: A first-principle relationship between molecular diffusion and viscosity. *AIP Adv.* **2020**, *10* (3), No. 035321.
(53) Xi, L.; Shah, M.; Trout, B. L. Hopping of water in a glassy polymer studied via transition path sampling and likelihood maximization. *J. Phys. Chem. B* **2013**, *117* (13), 3634−3647.
(54) Lim, S. Y.; Tsotsis, T. T.; Sahimi, M. Molecular simulation of diffusion and sorption of gases in an amorphous polymer. *J. Chem. Phys.* **2003**, *119* (1), 496−504.
(55) Krishnan, Y.; Ghaani, M. R.; Desmedt, A.; English, N. J. Hydrogen inter-cage hopping and cage occupancies inside hydrogen hydrate: Molecular-dynamics analysis. *Appl. Sci.* **2021**, *11* (1), 282.
(56) Song, D.; Chen, J. Densities and viscosities for ionic liquids mixtures containing [eOHmim][BF4],[bmim][BF4] and [bpy]-[BF4]. *J. Chem. Thermodyn.* **2014**, *77*, 137−143.
(57) Tomida, D.; Kenmochi, S.; Qiao, K.; Bao, Q.; Yokoyama, C. Viscosity of ionic liquid mixtures of 1-alkyl-3-methylimidazolium hexafluorophosphate+ CO2. *Fluid Phase Equilib.* **2011**, *307* (2), 185−189.
(58) Brehm, M.; Weber, H.; Thomas, M.; Hollóczki, O.; Kirchner, B. Domain Analysis in Nanostructured Liquids: A Post-Molecular Dynamics Study at the Example of Ionic Liquids. *ChemPhysChem* **2015**, *16* (15), 3271−3277.

https://doi.org/10.1021/acs.jpcb.4c04830
J. Phys. Chem. B 2024, 128, 9837−9846

Supporting Information

Correlation-Based Predictions of Gas Solute Diffusivity in Ionic Liquid Solvents Based on Solvent-Accessible Surface Area

Feranmi V. Olowookere and C. Heath Turner*

Department of Chemical and Biological Engineering, The University of Alabama, Tuscaloosa, AL 35487-0203,

United States

Snapshot of SA analysis, schematic illustrating void-related calculations, void lattice representation, occurrence of void clusters with varying threshold radii and at different temperatures, displacement plots, $R_{V/A}$ distributions, snapshots of void spaces, r_{eff} distribution based on different criteria, additional plots for the fraction of the void domains with an $R_{V/A} < 0.5$ for different threshold radii, MSDs versus time at various temperatures

*****Corresponding author contact:

C. Heath Turner

E-mail address: hturner@eng.ua.edu

Phone number: 205-348-1733

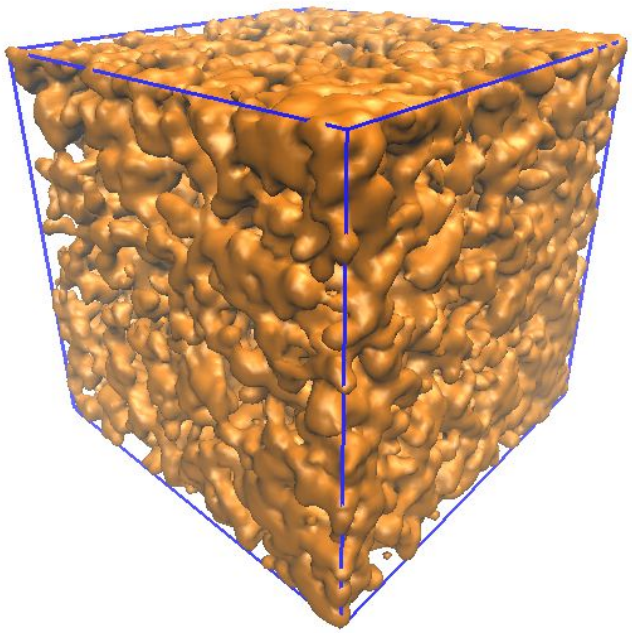

Figure S1. Snapshot of the solvent accessible SA analysis in the $[Bzmim_4]^{4+}[BzO_3]^{3-}$ IL (without CH_4 molecules present), calculated with a probe size of 0.075 nm and visualized using a density isovalue of 2.0.

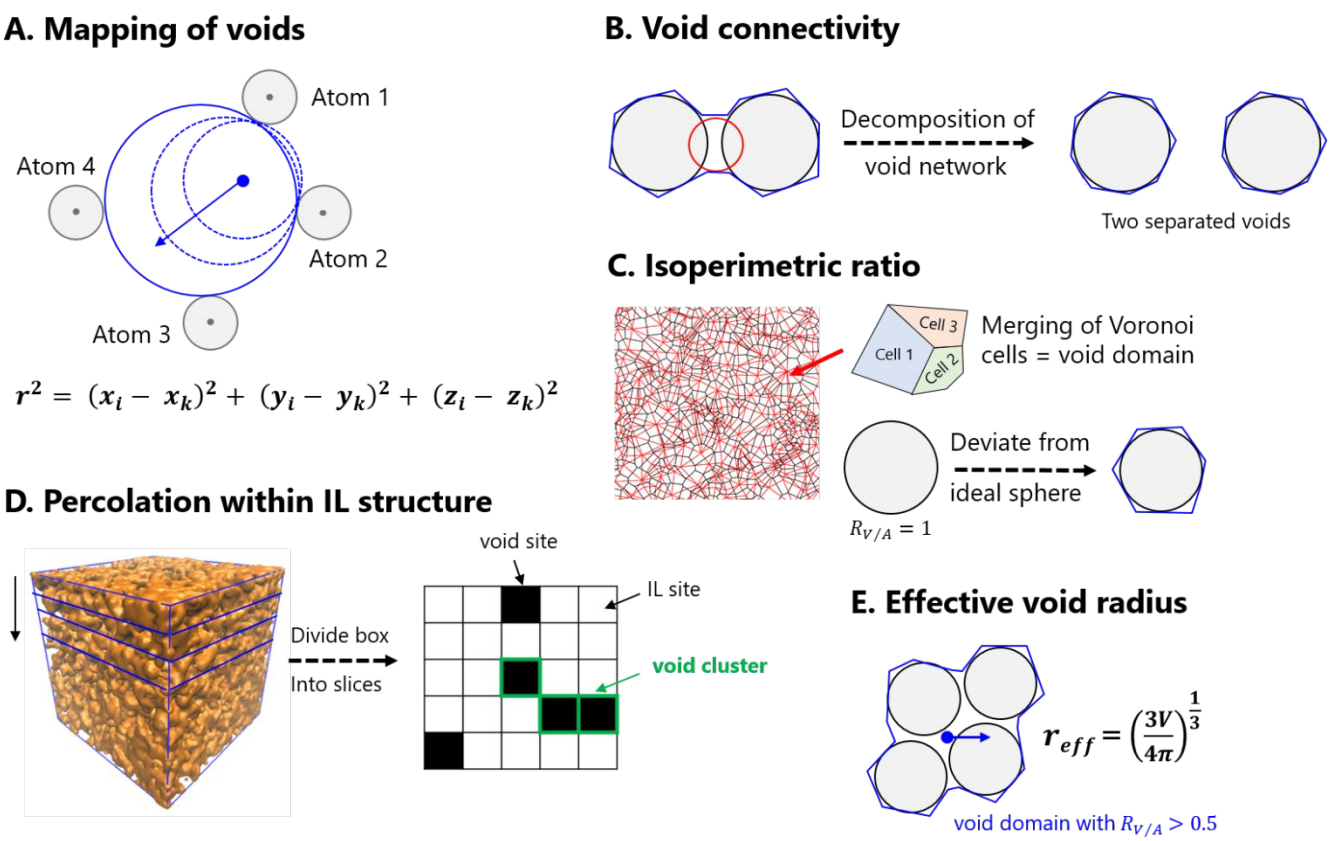

Figure S2. Schematic illustrations of void-related calculations: A. Void mapping via Voronoi tessellation, adjusting void centers and radii; B. Void connectivity, showing how ignoring a void connection (red) collapses the channel thereby leading to an increase in $R_{V/A}$ values; C. Isoperimetric ratio calculation, where $R_{V/A}$ = 1 represents an ideal sphere; D. Percolation quantified by clustering adjacent neighboring void lattice sites; and E. Effective void radius calculated as the radius of a sphere with the same volume as the void domain.

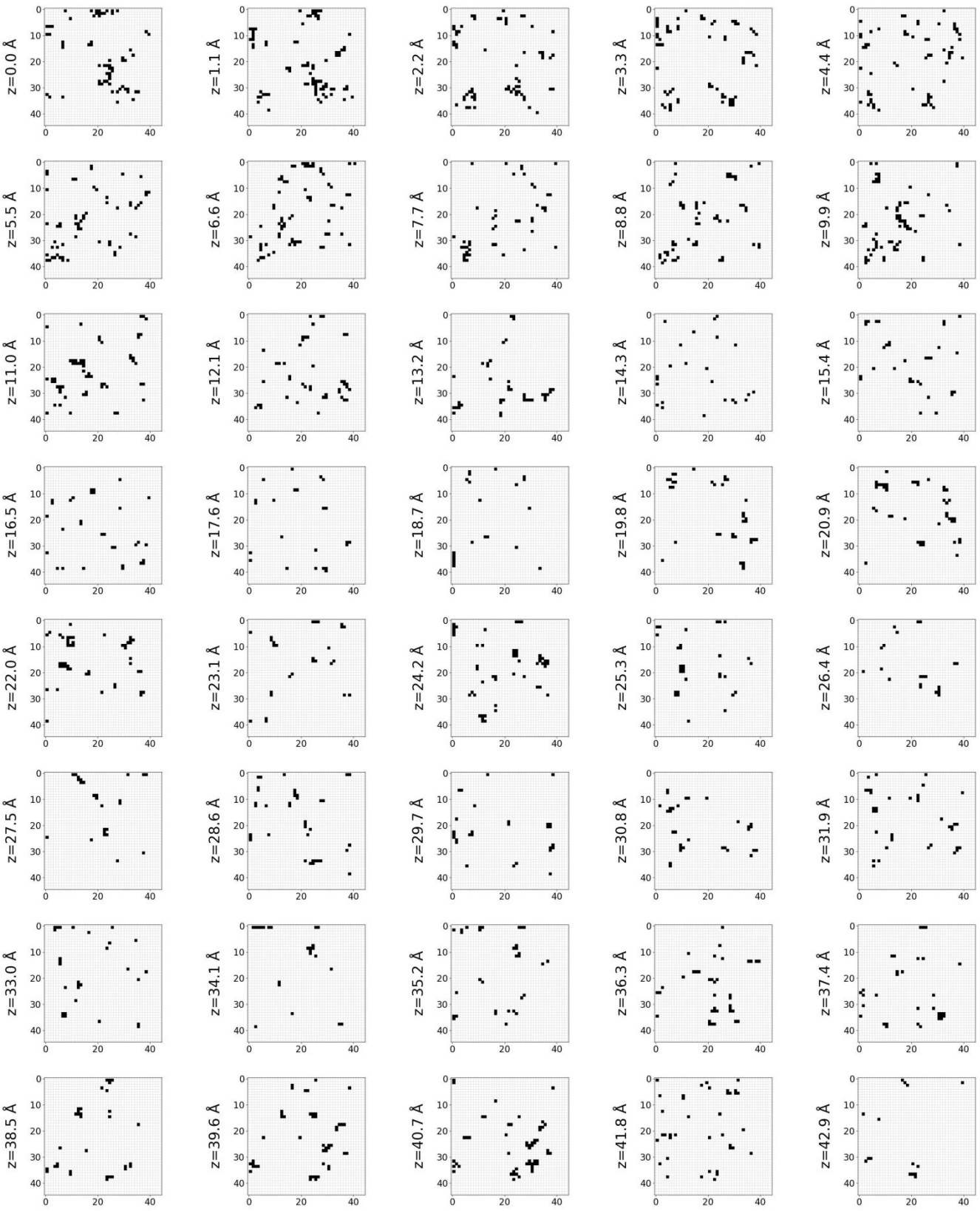

Figure S3. Two-dimensional lattice representation corresponding to different slices along the z-dimension (z=0.0 Å to z=42.9 Å) of the $[Bzmim_4]^{4+}[BzO_3]^{3-}$ system (without CH_4 molecules present). The lattice spacing corresponds to 1.1 Å, and the configuration corresponds to the system at t = 50 ns at a temperature of 300 K. The void spaces are represented by black squares while the IL molecules are represented by white squares. The minimum distance between two void sphere centers is 50 pm.

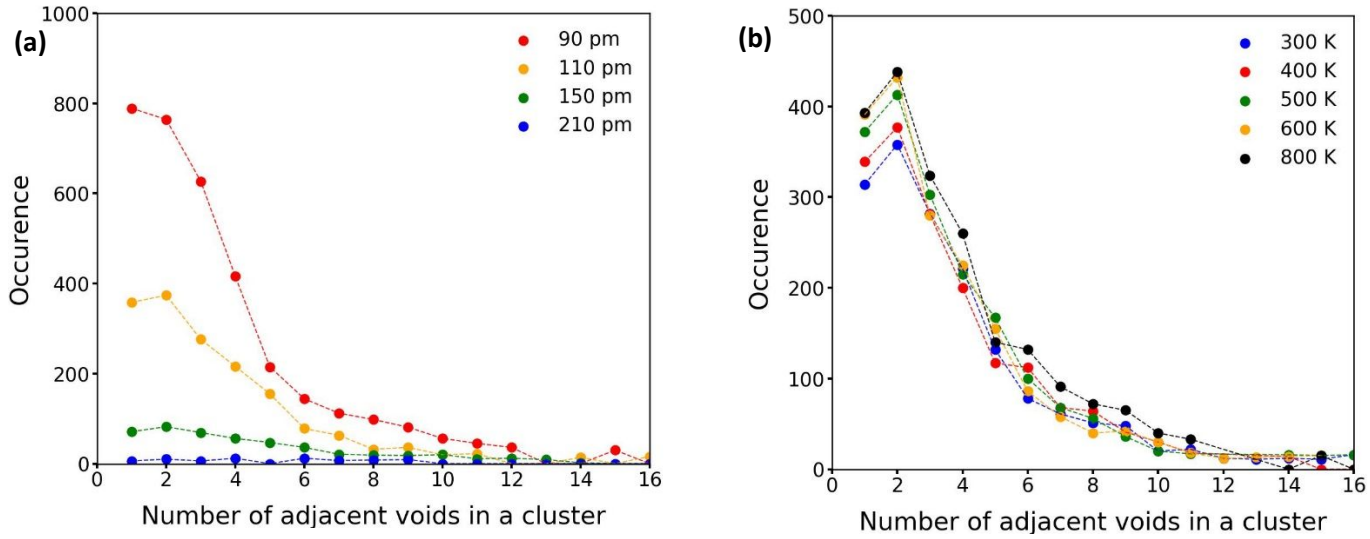

Figure S4. Occurrence of the void clusters (a) with varying threshold radii (at 300 K) and (b) at various temperatures (with a 90 pm threshold radius).

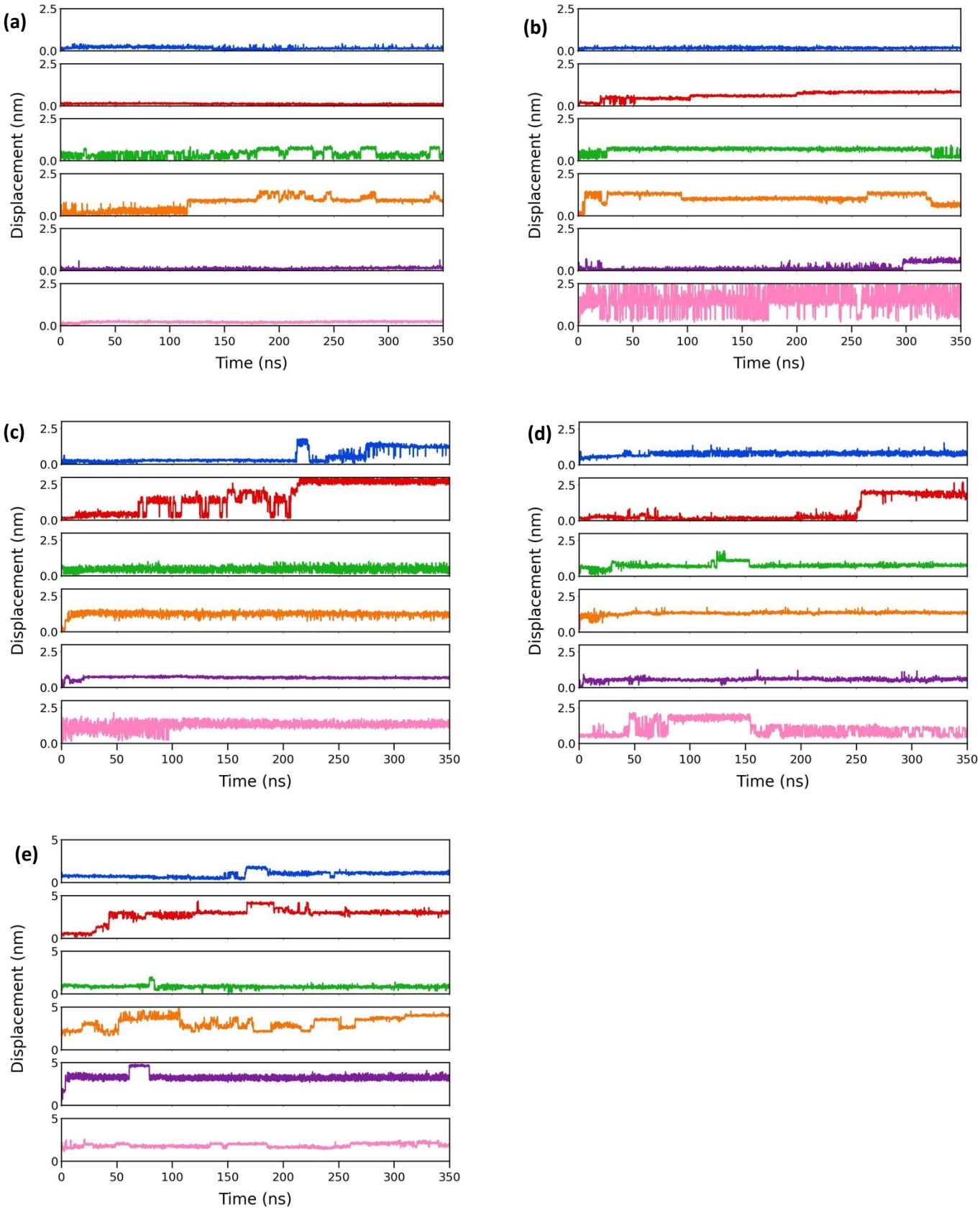

Figure S5. Relative distance of CH_4 molecules from their initial positions as a function of time at (a) 300 K, (b) 400 K, (c) 500 K, (d) 600 K, and (e) 800 K in the $[Bzmim_4]^{4+}[BzO_3]^{3-}$ solvent. Five randomly CH_4 chosen molecules (each corresponding to a different color) are displayed for visualization purposes.

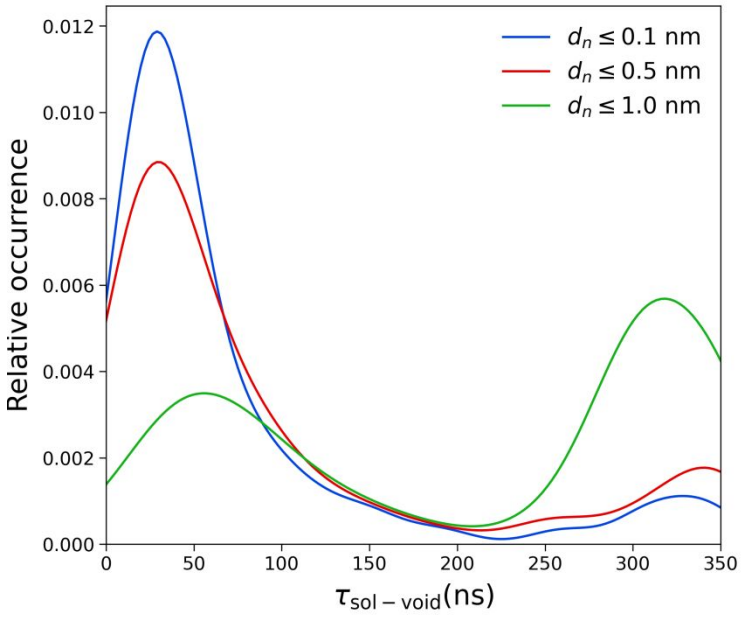

Figure S6. $\tau_{sol\text{-}void}$ distribution of CH_4 in the $[Bzmim_3]^{4+}[BzO_3]^{3-}$ system if the net radial displacement criterion is varied ($d_n \leq 0.1$, 0.5, 1.0 nm) at 800 K.

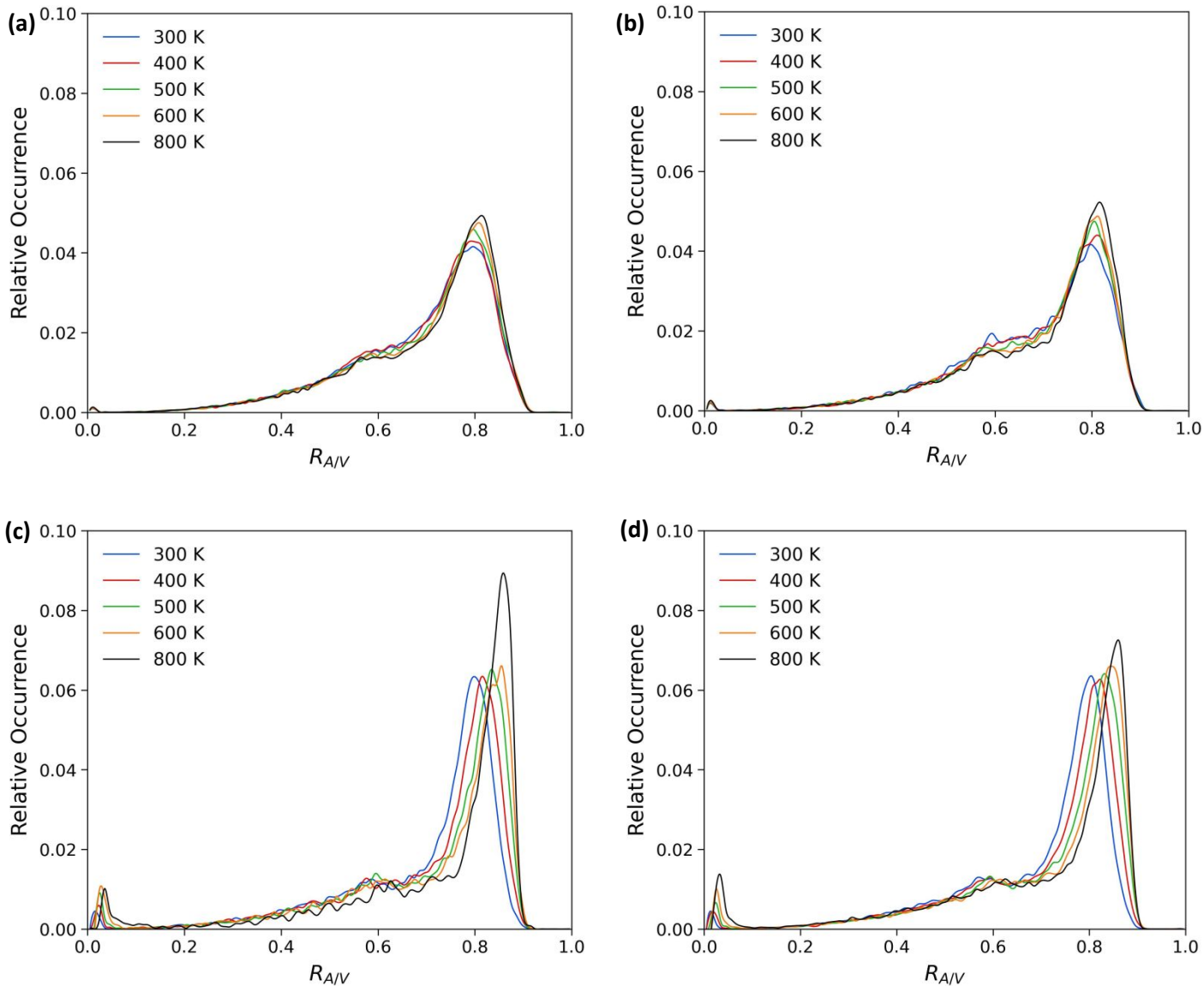

Figure S7. Relative occurrence of $R_{V/A}$ values of the void domains formed from the combined Voronoi cells of the void spheres in selected systems: (a) CH_4-$[Bzmim_4]^{4+}[BzO_3]^{3-}$, (b) N_2-$[Bzmim_4]^{3+}[NapO_2]^{2-}$, (c) CO_2-$[BMIM]^+[BF_4]^-$, (d) CO_2-$[HMIM]^+[PF_6]^-$.

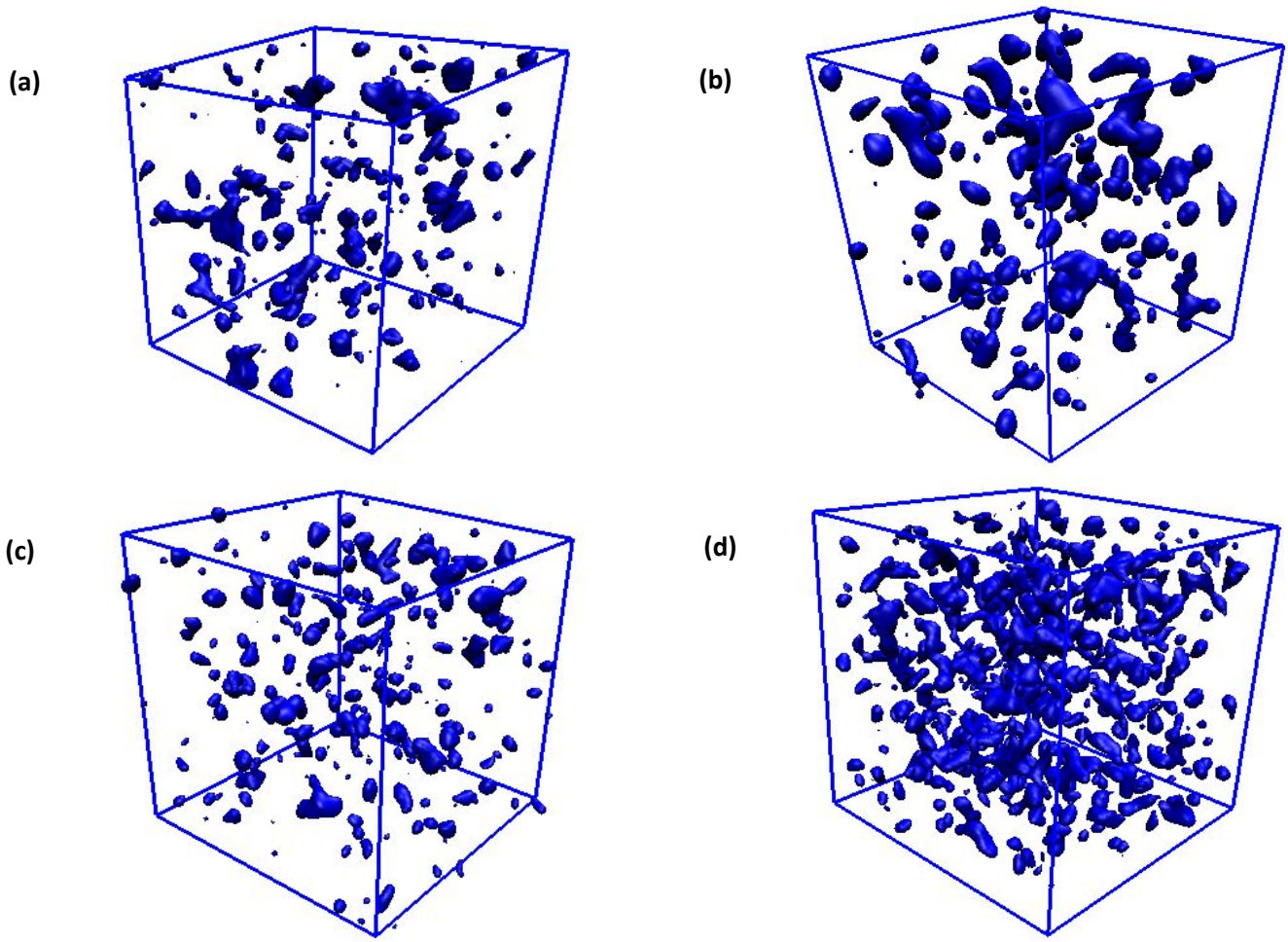

Figure S8. Visual snapshots of void spaces within the (a) CH_4-$[Bzmim_4]^{4+}[BzO_3]^{3-}$ and (b) CO_2-$[BMIM]^+[BF_4]^-$ system at 300 K, (c) CH_4-$[Bzmim_4]^{4+}[BzO_3]^{3-}$ and (d) CO_2-$[BMIM]^+[BF_4]^-$ system at 800 K visualized using a density isovalue of 3.5. The void spaces are illustrated for the IL systems without the solute molecules present.

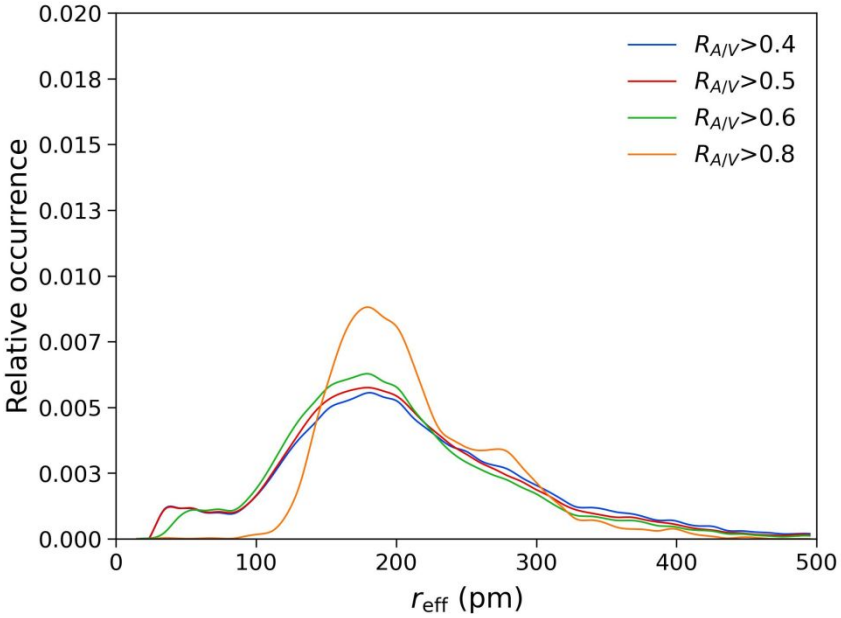

Figure S9. Distribution of effective void radii r_{eff} in CH_4-$[Bzmim_3]^{4+}[BzO_3]^{3-}$ at 300 K based on different criteria ($R_{V/A}$ > 0.4, 0.5, 0.6, or 0.8) used to categorize a void domain as having a spherical shape.

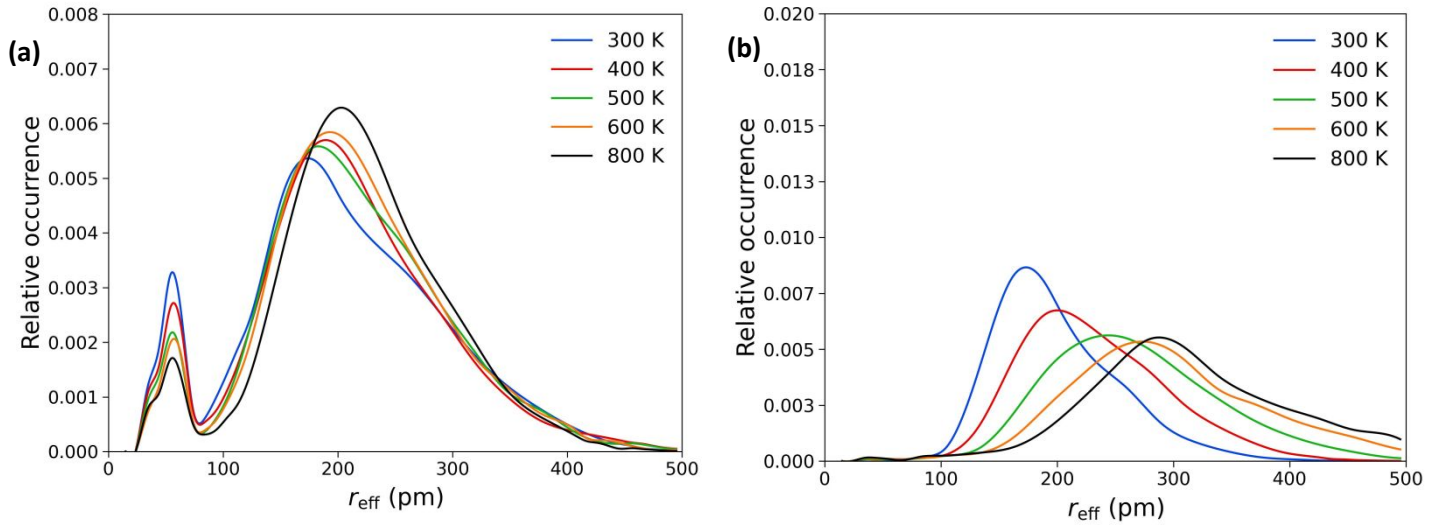

Figure S10. Distribution of effective void radii r_{eff} in (a) N_2-$[Bzmim_4]^{3+}[NapO_2]^{2-}$ and (b) CO_2-$[HMIM]^+[PF_6]^-$ systems.

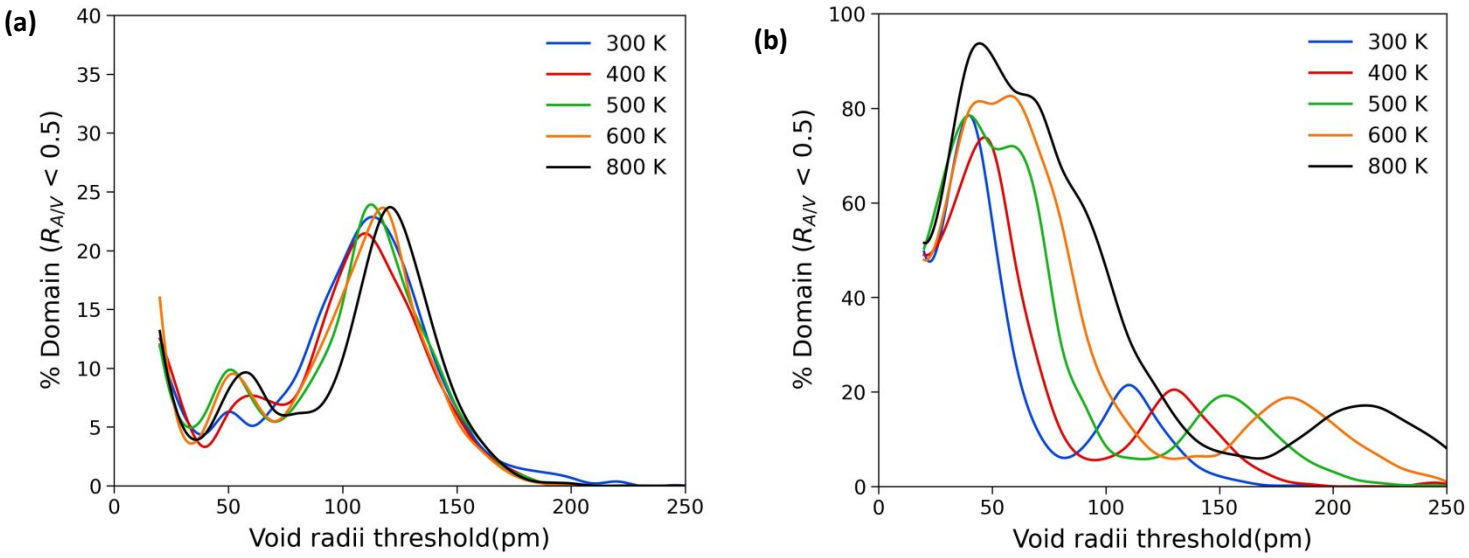

Figure S11. Fraction of the void domains with an $R_{V/A}$ < 0.5 for different threshold radii in (a) N_2-$[Bzmim_4]^{3+}[NapO_2]^{2-}$ and (b) CO_2-$[HMIM]^+[PF_6]^-$ systems.

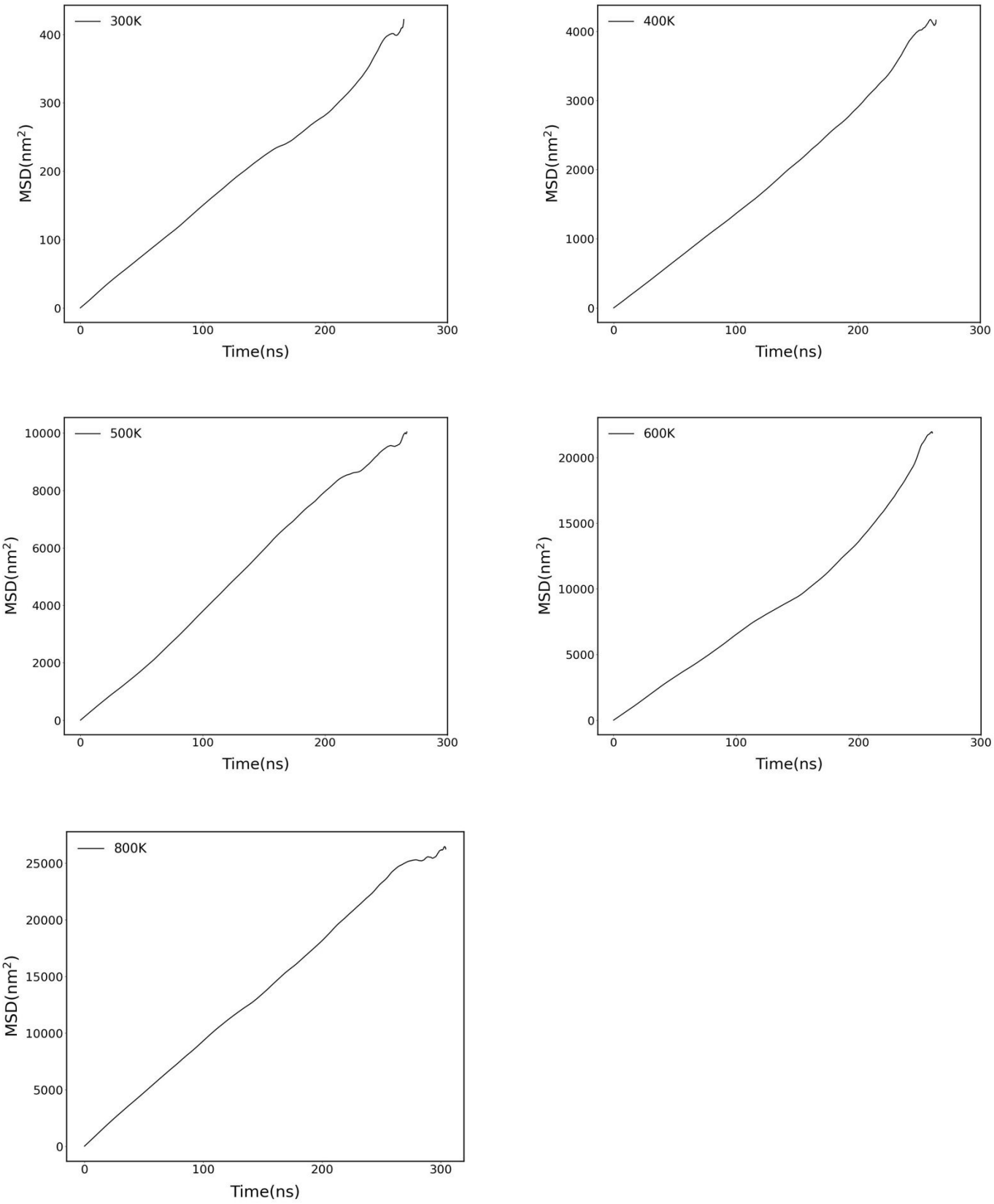

Figure S12. Mean squared displacement of CO_2 in $[BMIM]^+[BF_4]^-$, corresponding to different temperatures.

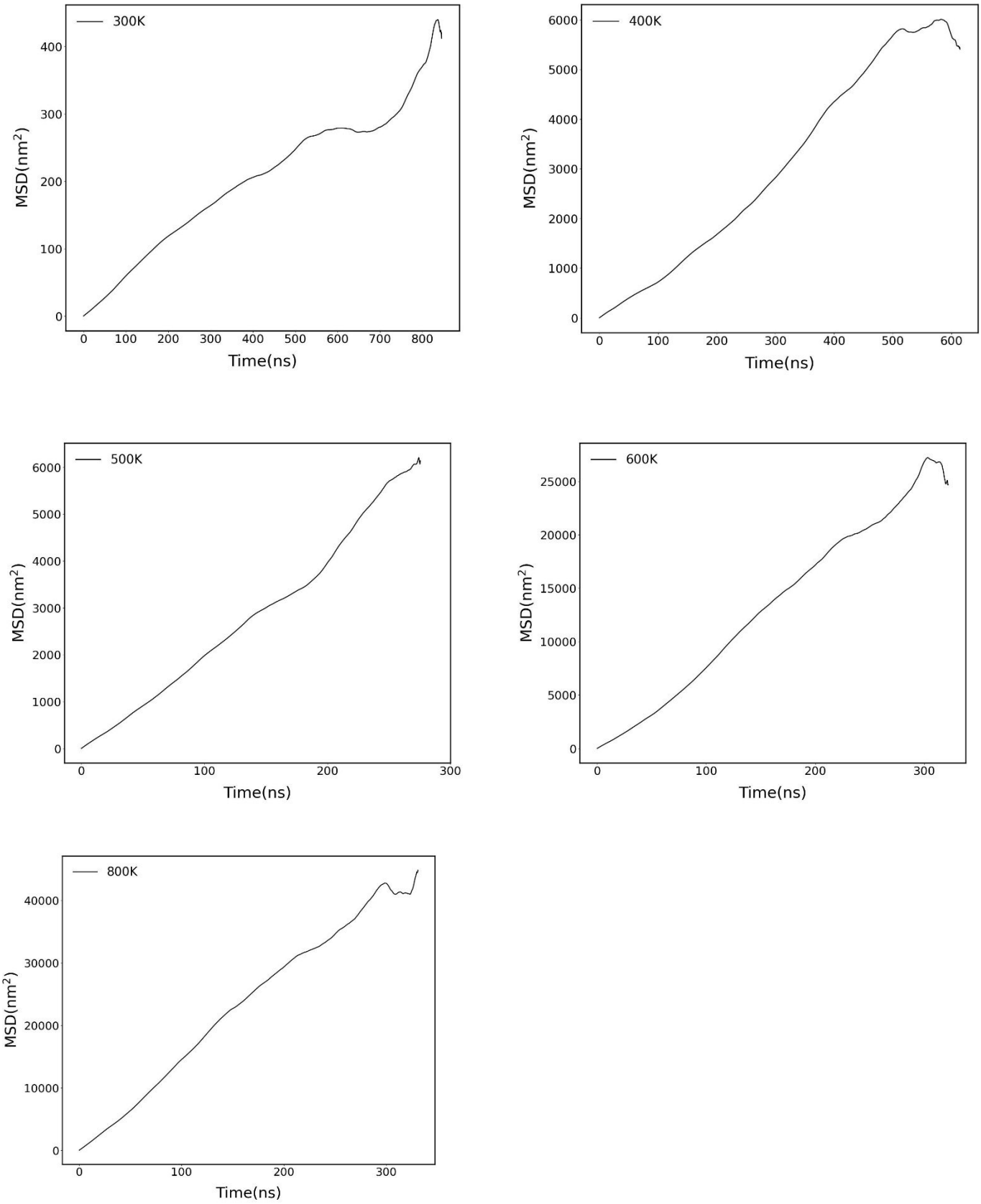

Figure S13. Mean squared displacement of CH_4 in $[BMIM]^+[BF_4]^-$, corresponding to different temperatures.

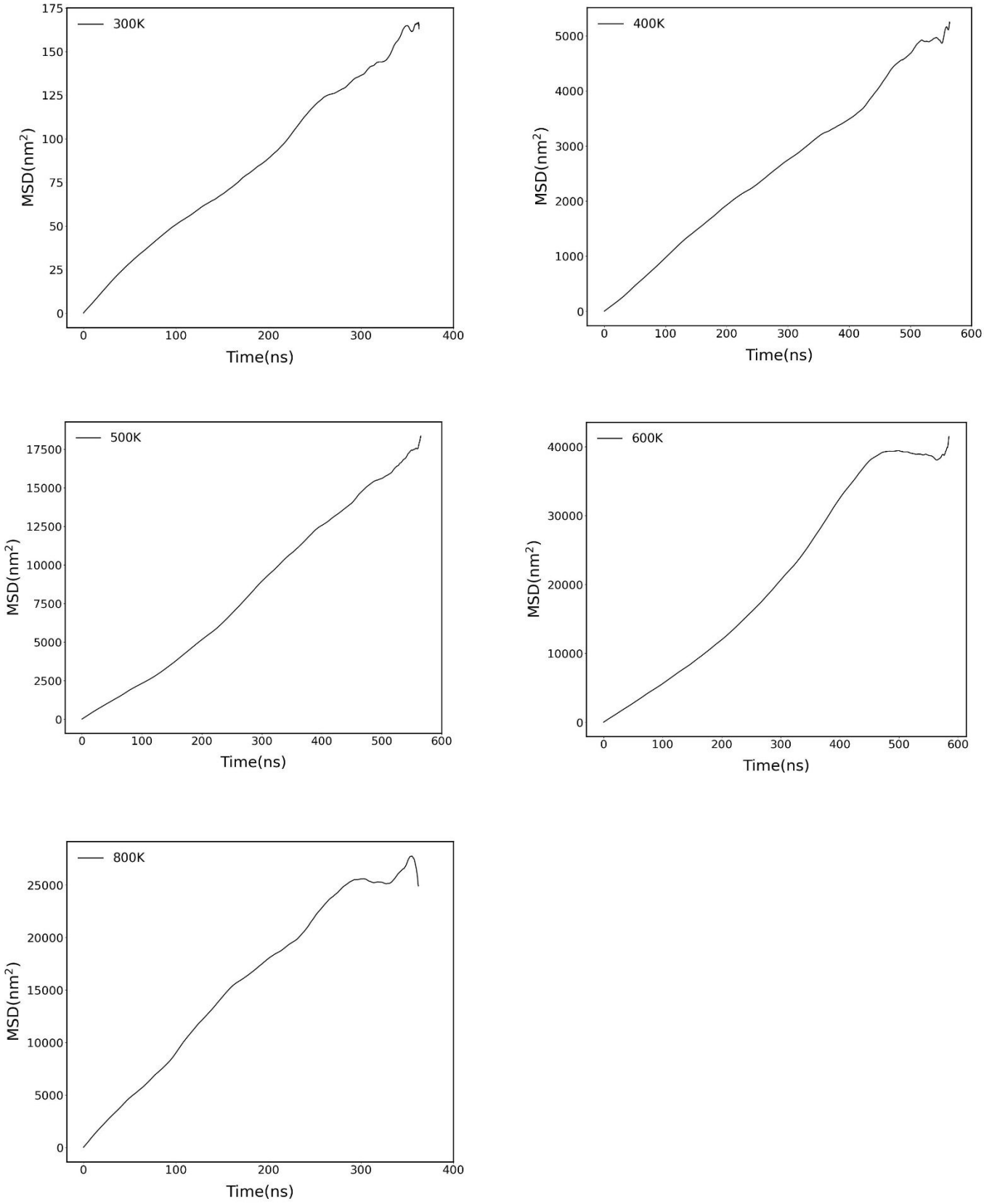

Figure S14. Mean squared displacement of C_2H_6 in $[BMIM]^+[BF_4]^-$, corresponding to different temperatures.

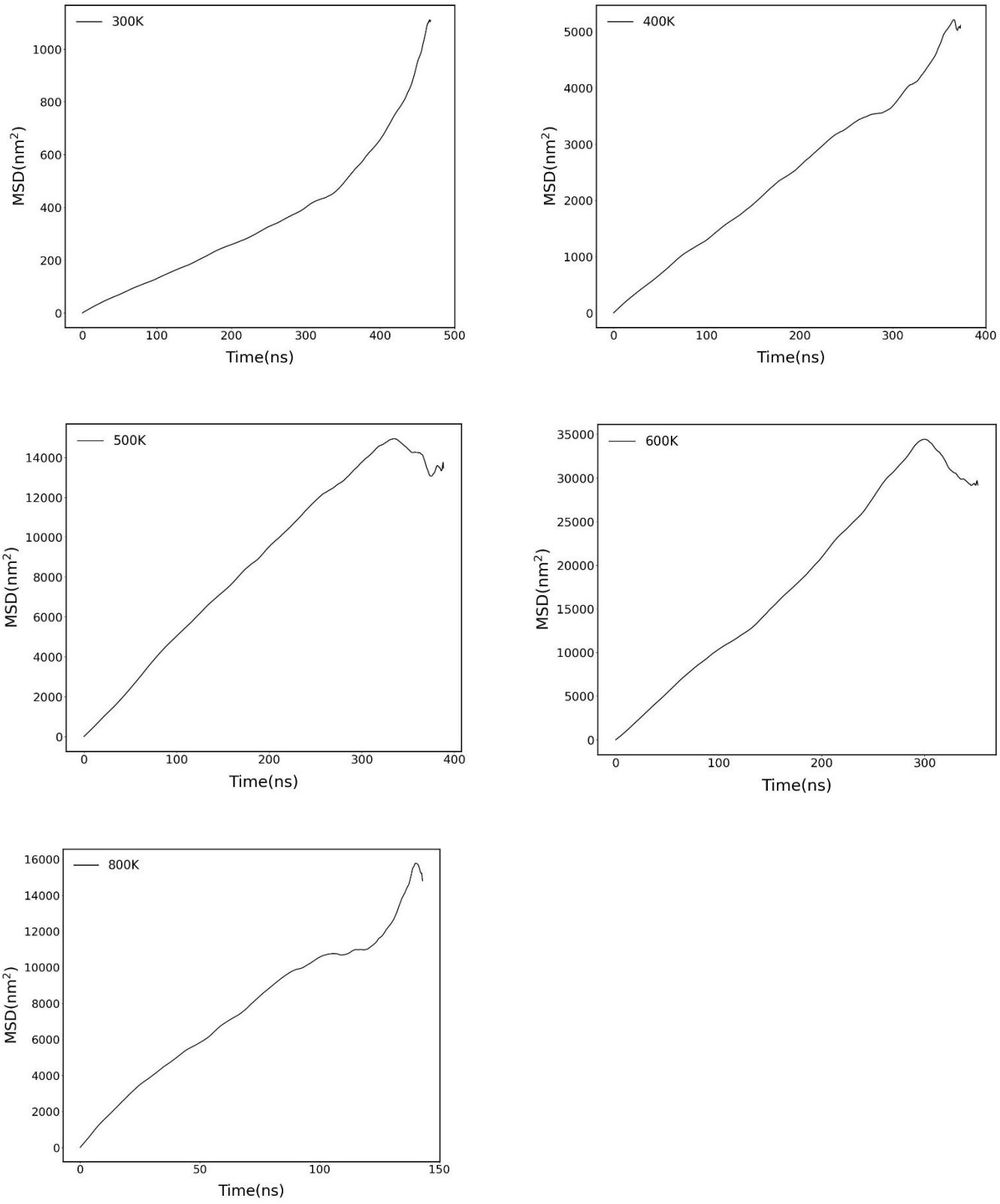

Figure S15. Mean squared displacement of N_2 in $[BMIM]^+[BF_4]^-$, corresponding to different temperatures.

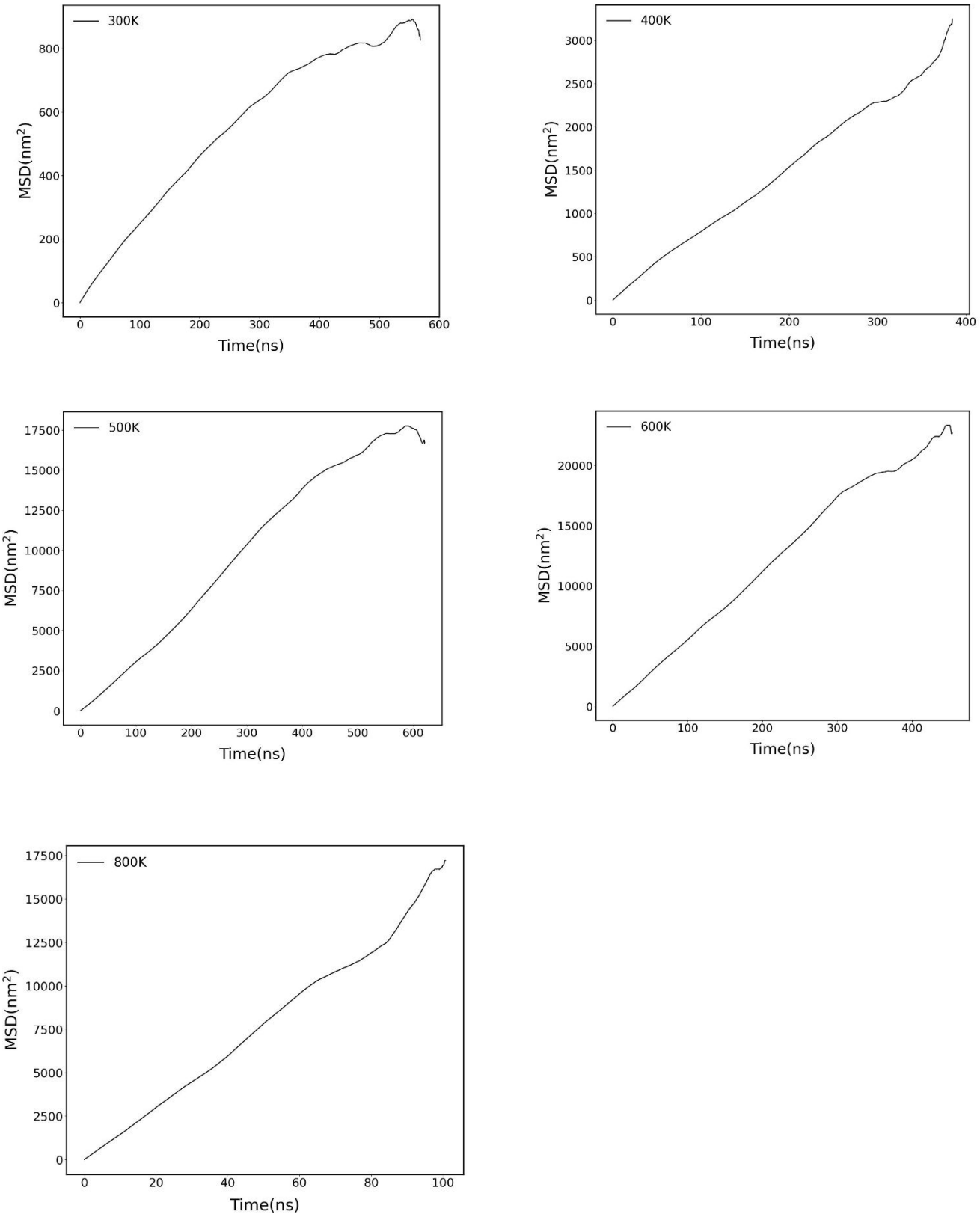

Figure S16. Mean squared displacement of CO_2 in $[EMIM]^+[Tf_2N]^-$, corresponding to different temperatures.

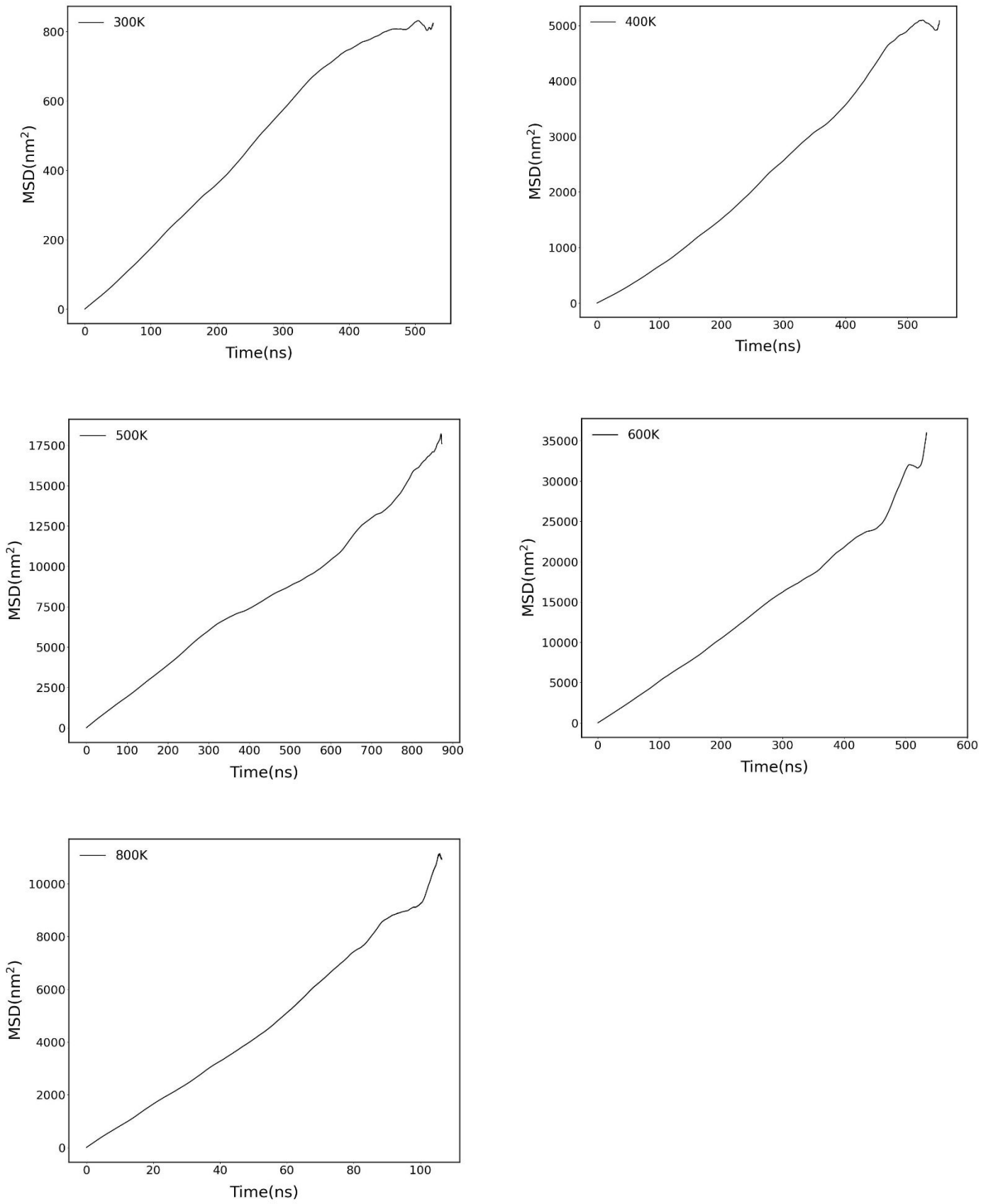

Figure S17. Mean squared displacement of CH_4 in $[EMIM]^+[Tf_2N]^-$, corresponding to different temperatures.

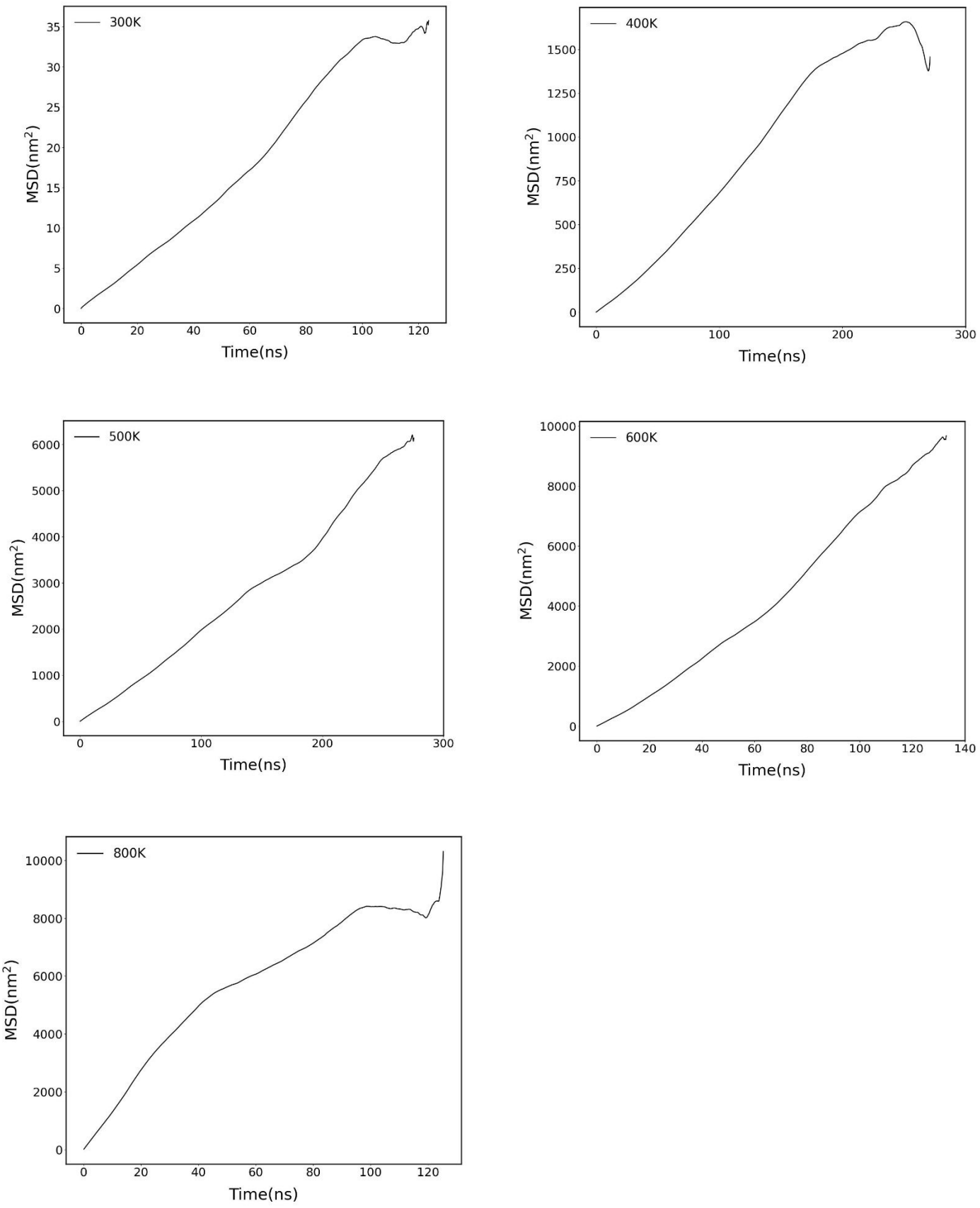

Figure S18. Mean squared displacement of C_2H_6 in $[EMIM]^+[Tf_2N]^-$, corresponding to different temperatures.

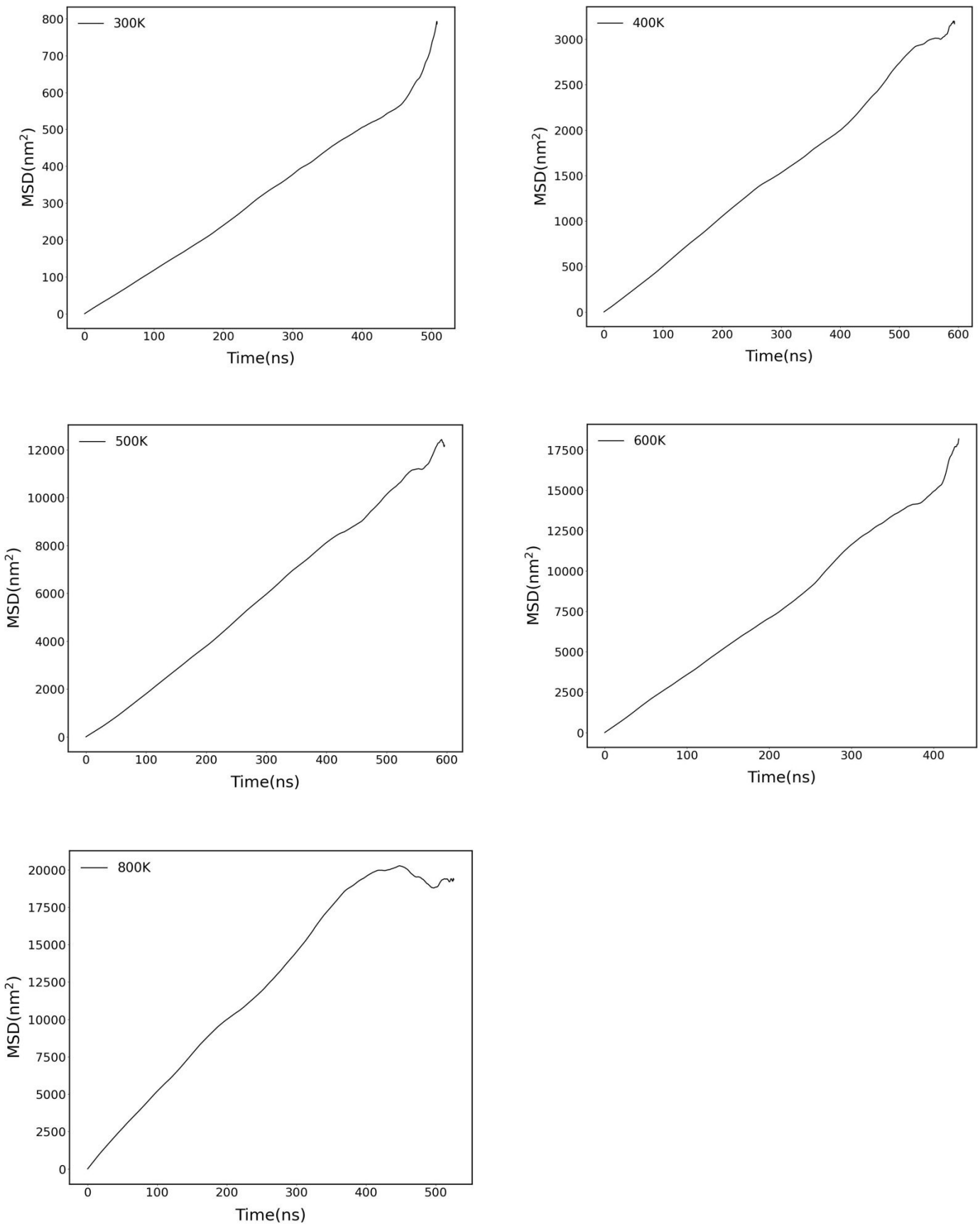

Figure S19. Mean squared displacement of C_3H_8 in $[EMIM]^+[Tf_2N]^-$, corresponding to different temperatures.

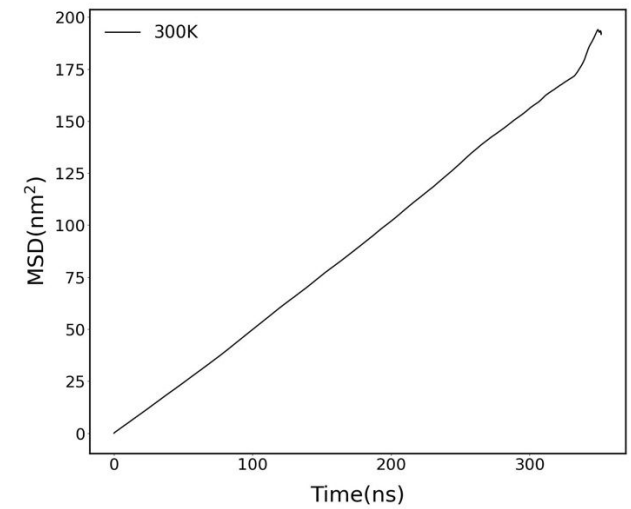

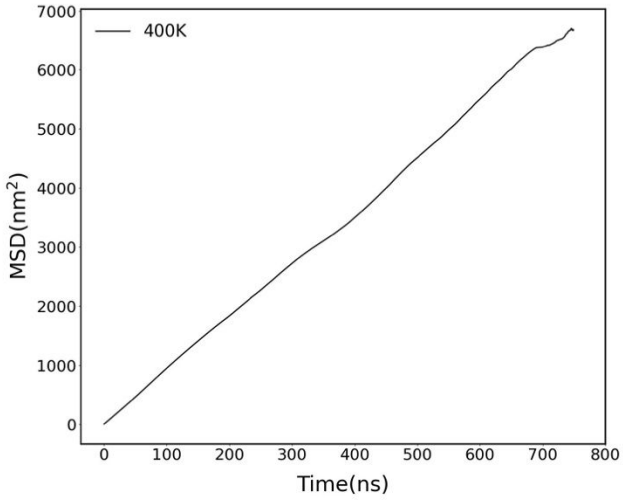

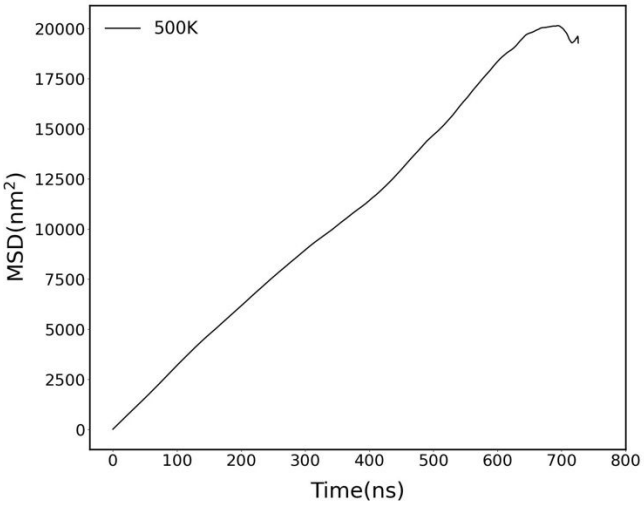

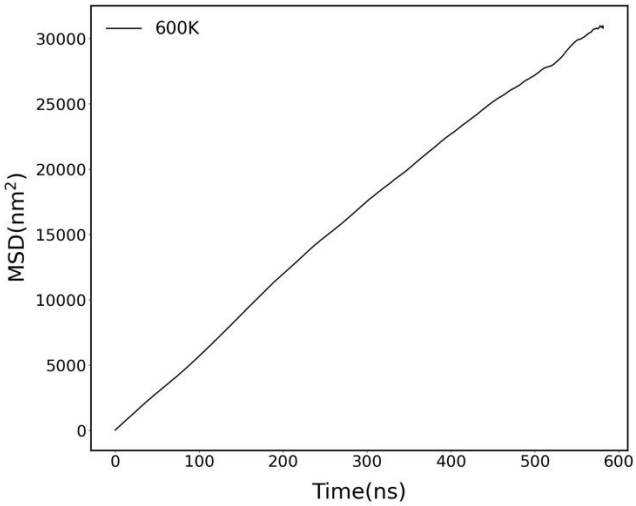

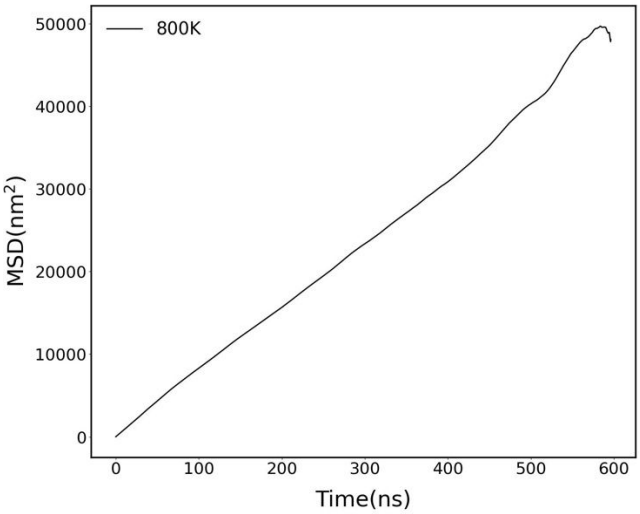

Figure S20. Mean squared displacement of CO_2 in $[HMIM]^+[PF_6]^-$, corresponding to different temperatures.

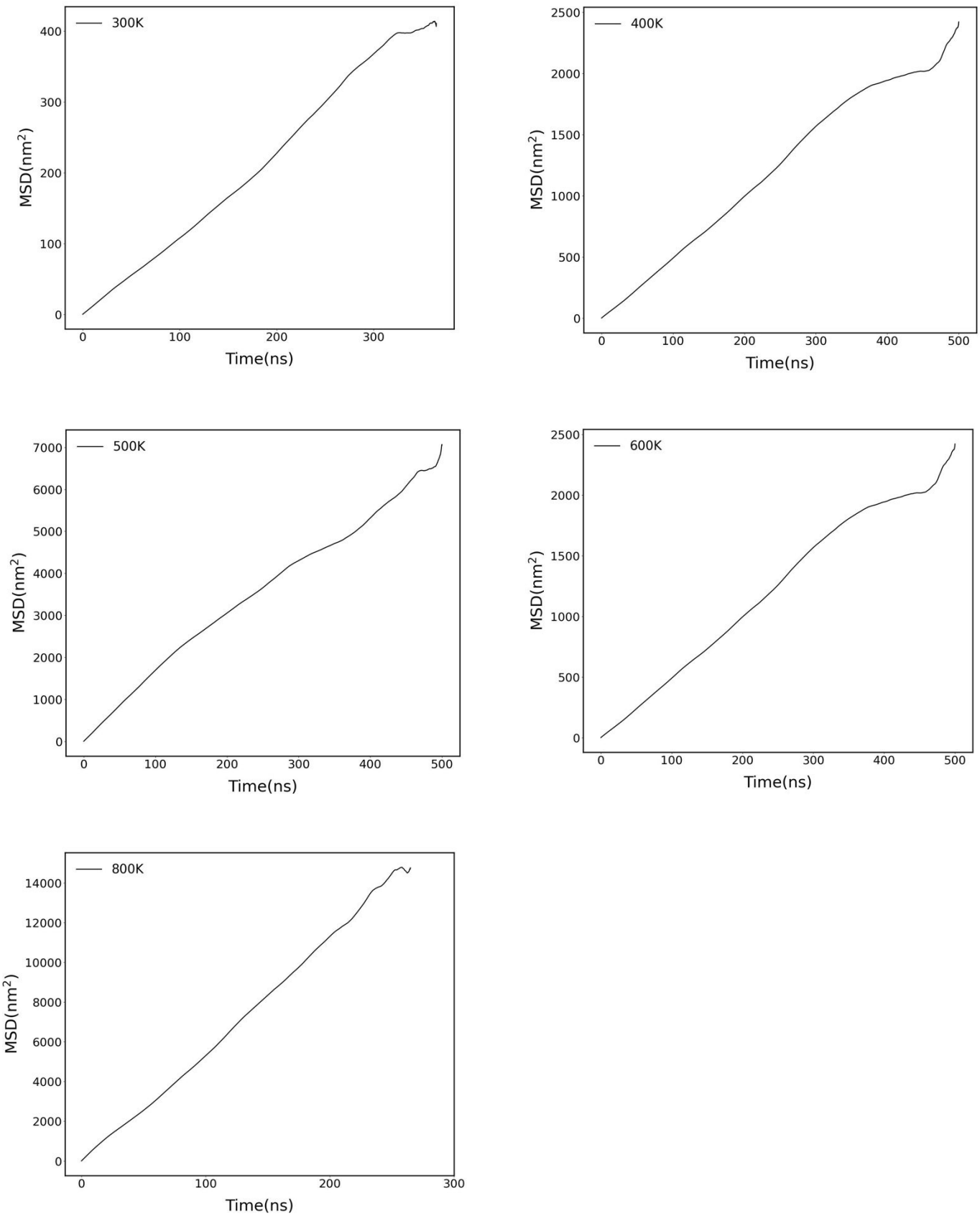

Figure S21. Mean squared displacement of C_3H_8 in $[BMIM]^+[Tf_2N]^-$, corresponding to different temperatures.

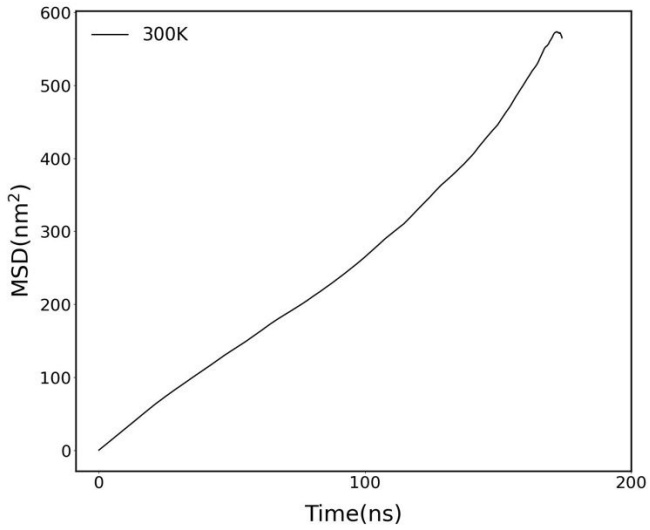

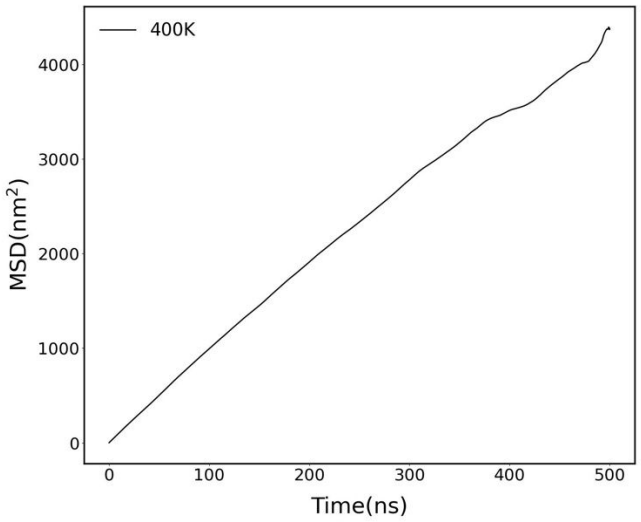

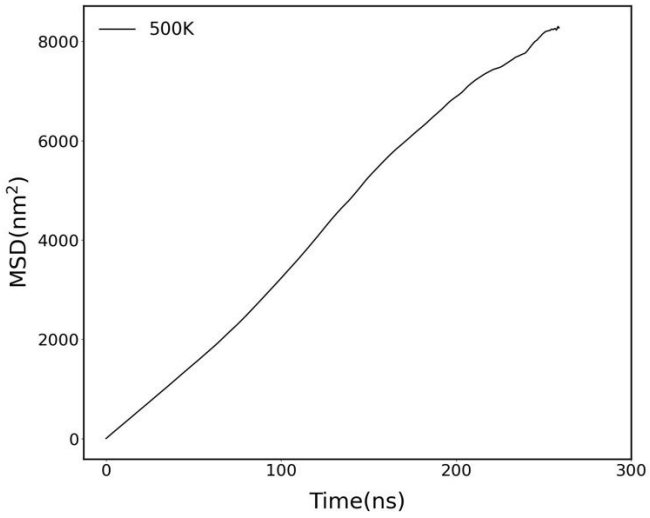

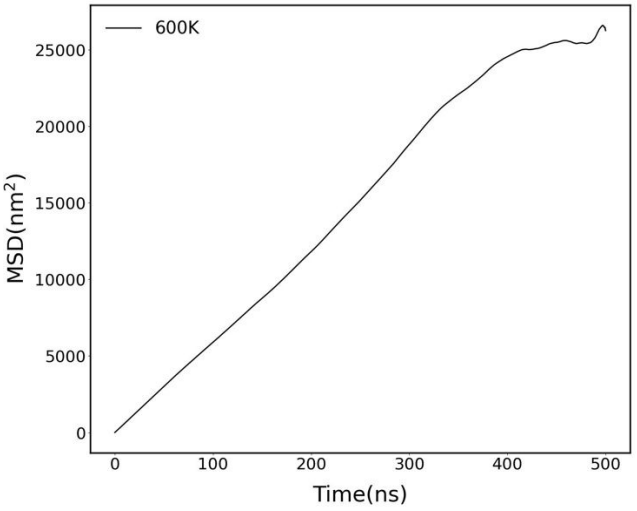

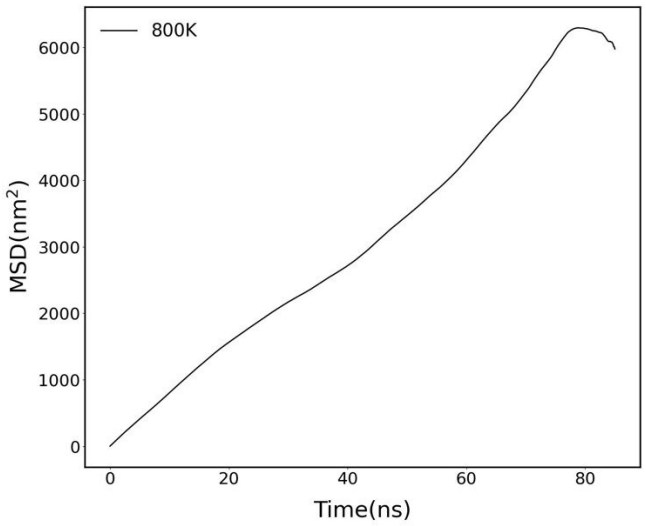

Figure S22. Mean squared displacement of CO_2 in $[BMIM]^+[Tf_2N]^-$, corresponding to different temperatures.

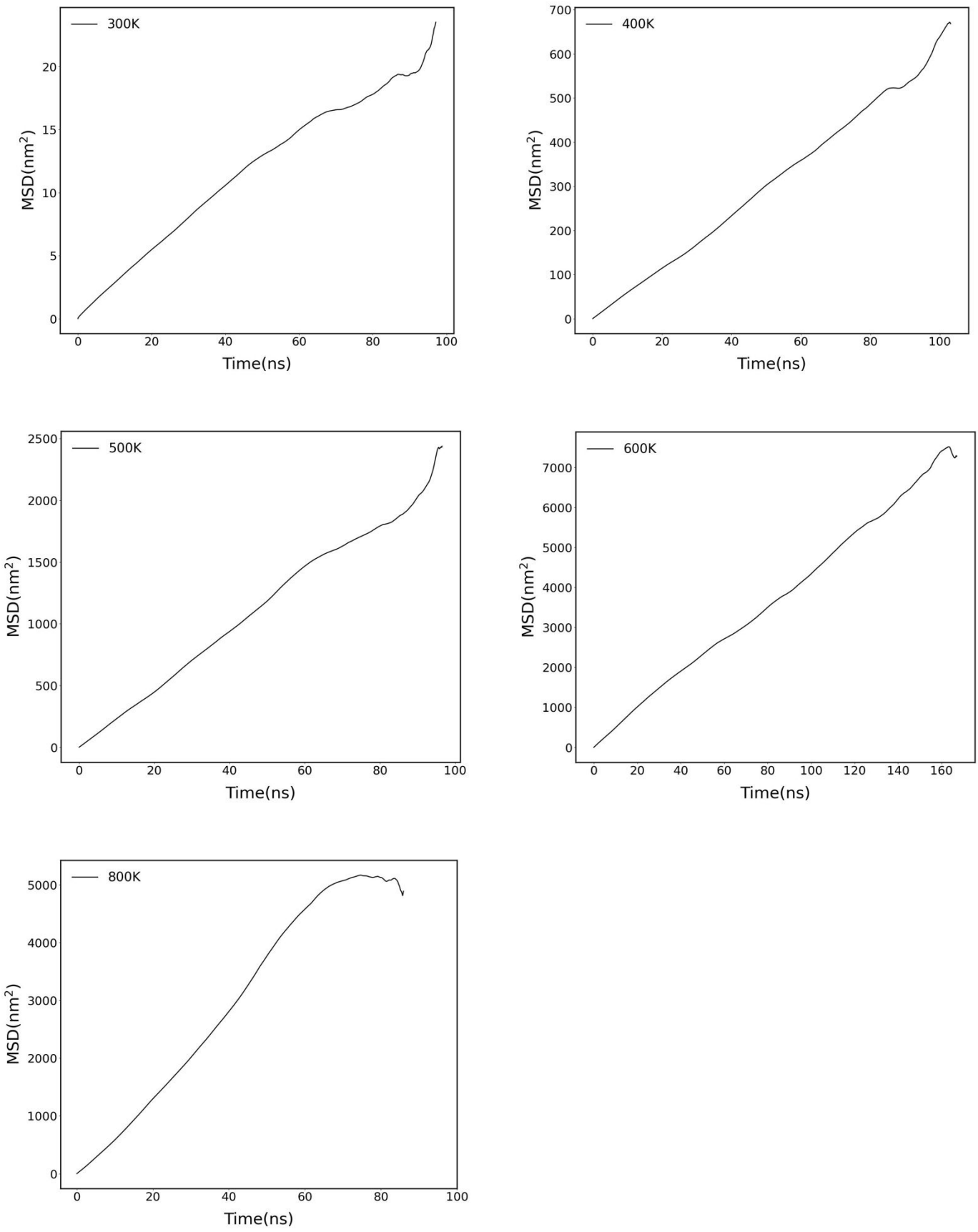

Figure S23. Mean squared displacement of CH_4 in $[BMIM]^+[Tf_2N]^-$, corresponding to different temperatures.

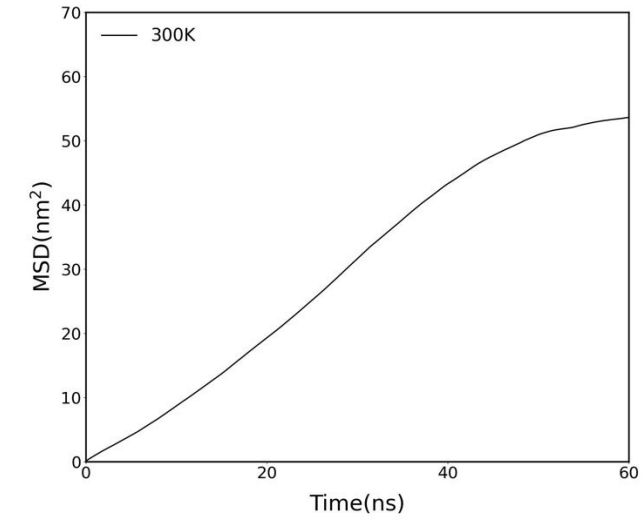

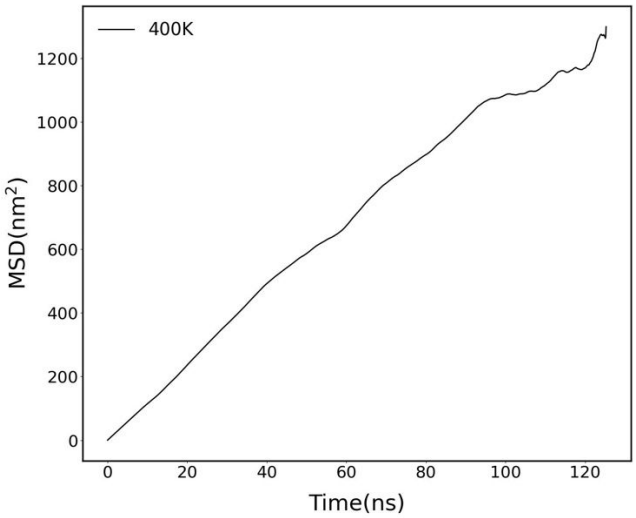

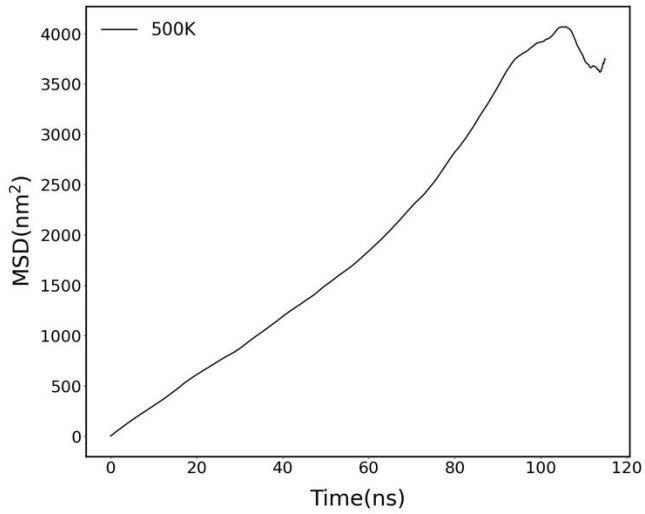

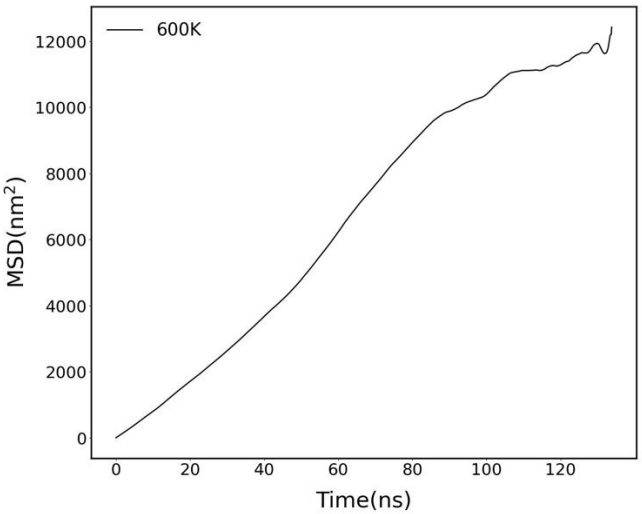

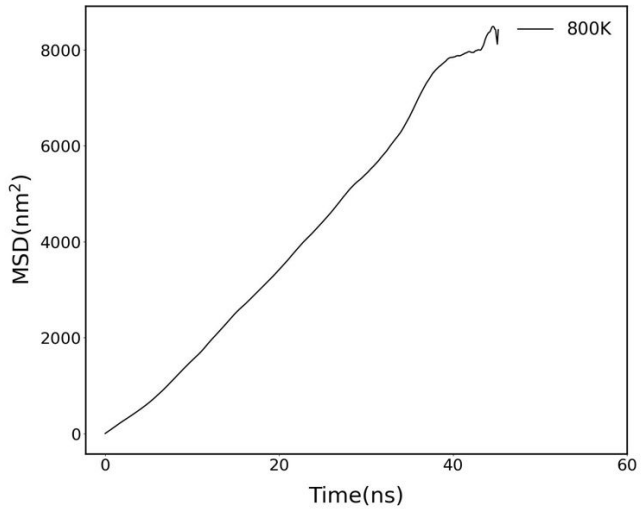

Figure S24. Mean squared displacement of N_2 in $[BMIM]^+[Tf_2N]^-$, corresponding to different temperatures.

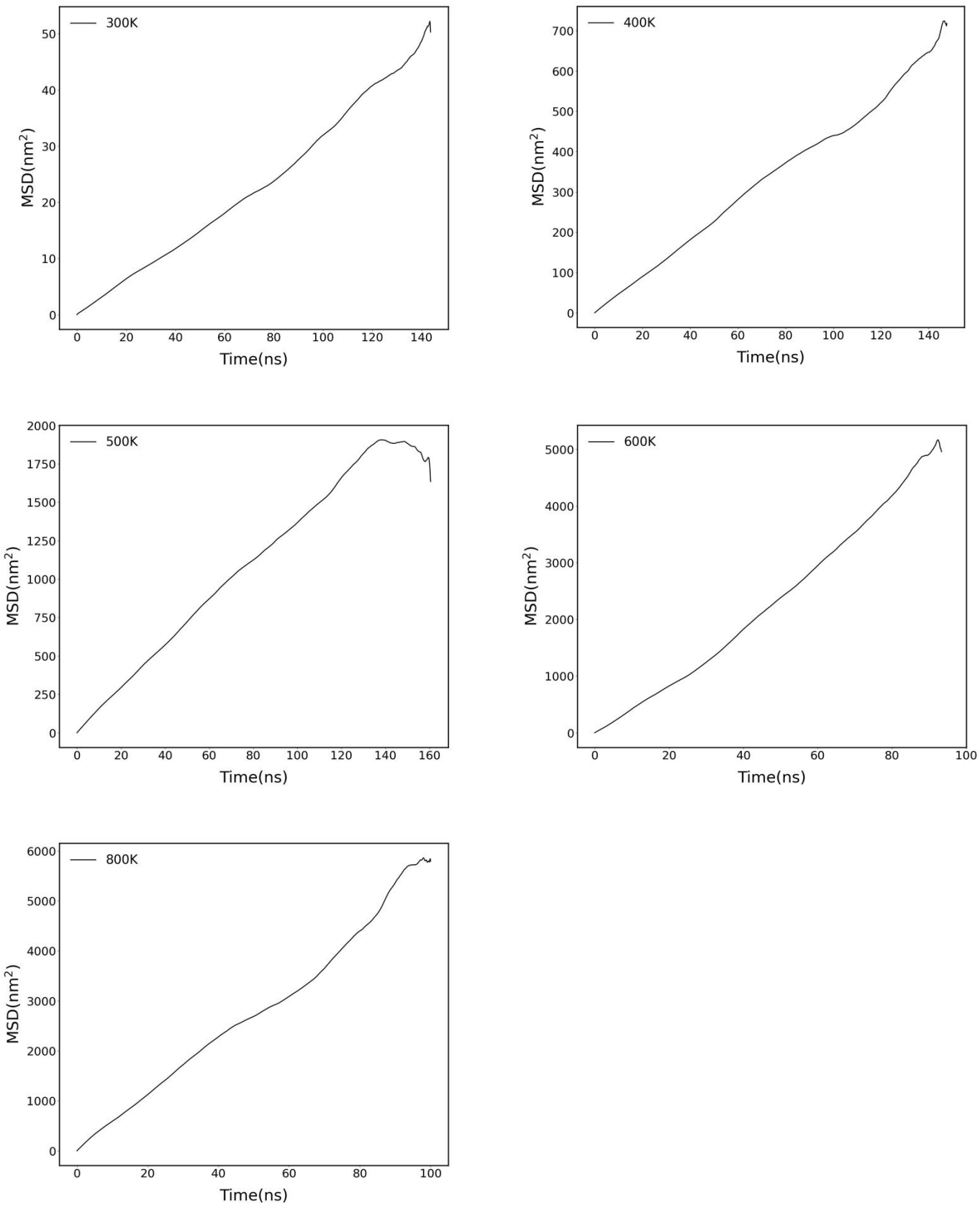

Figure S25. Mean squared displacement of C_3H_8O in $[BMIM]^+[BF_4]^-$, corresponding to different temperatures.

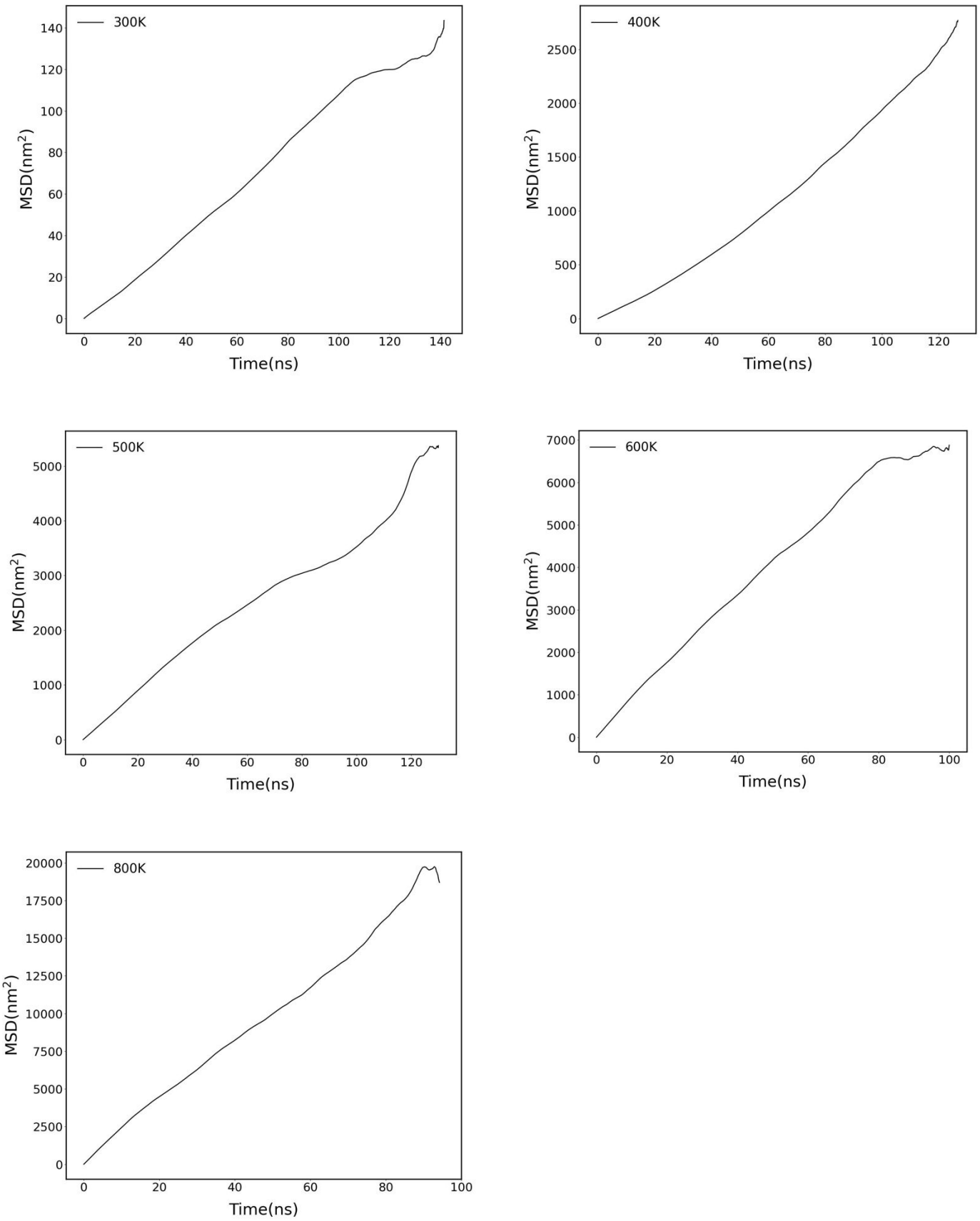

Figure S26. Mean squared displacement of H_2O in $[BMIM]^+[PF_6]^-$, corresponding to different temperatures.

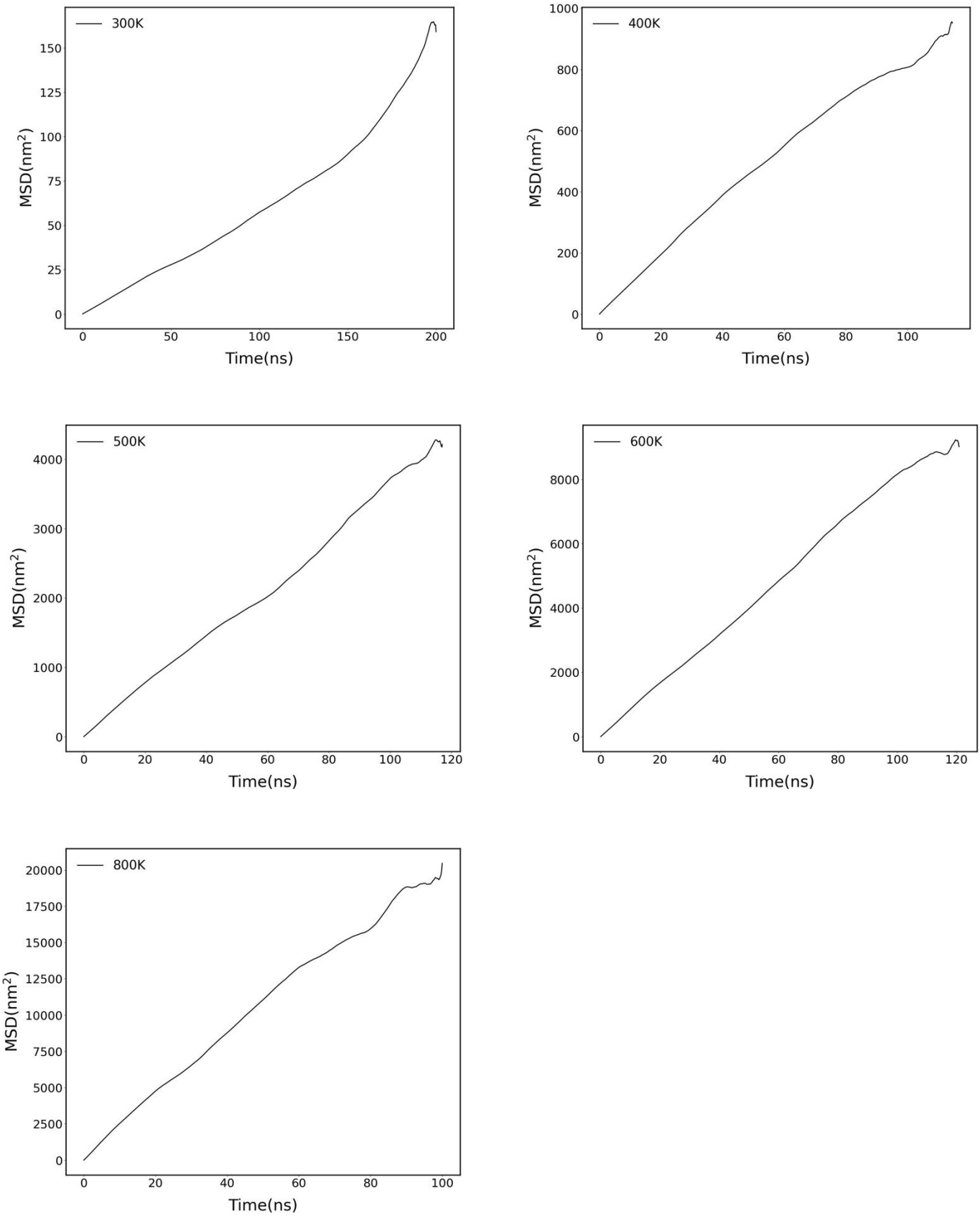

Figure S27. Mean squared displacement of H_2O in $[HMIM]^+[PF_6]^-$, corresponding to different temperatures.

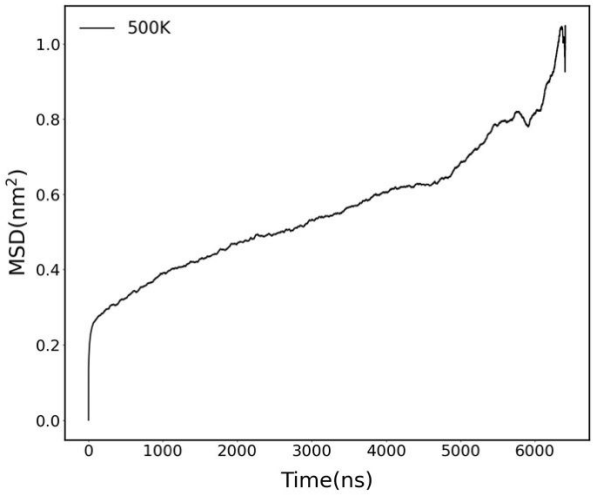

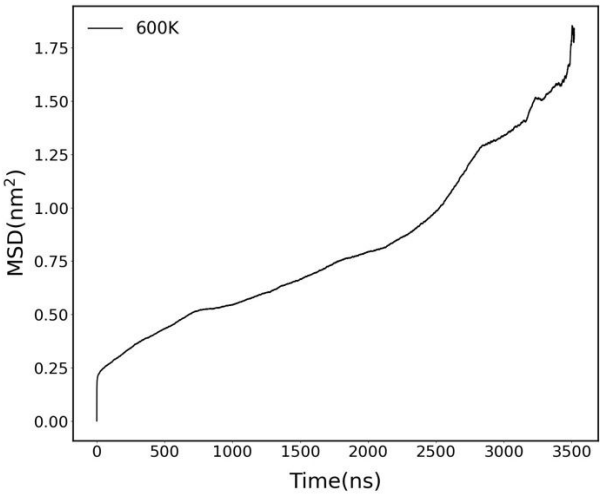

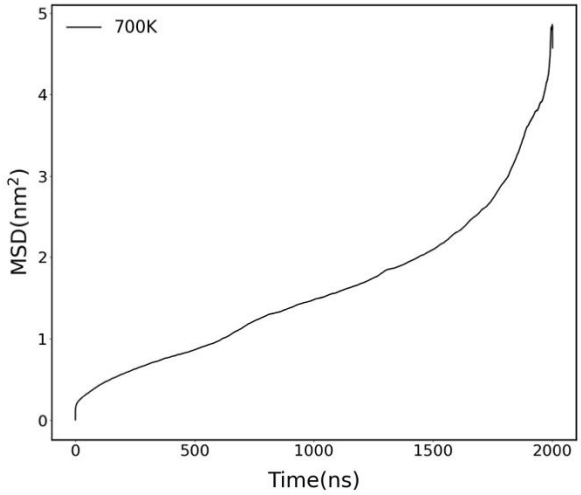

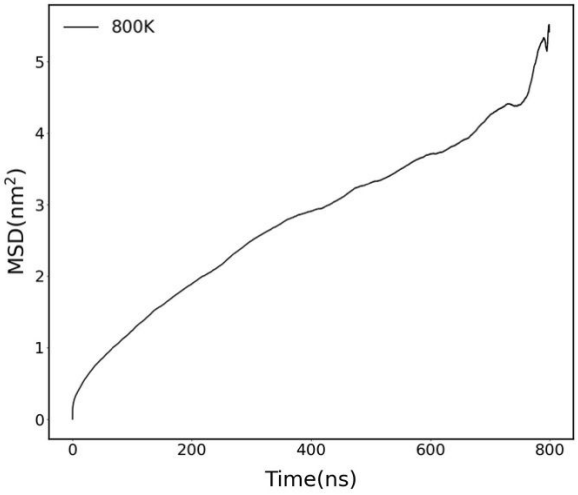

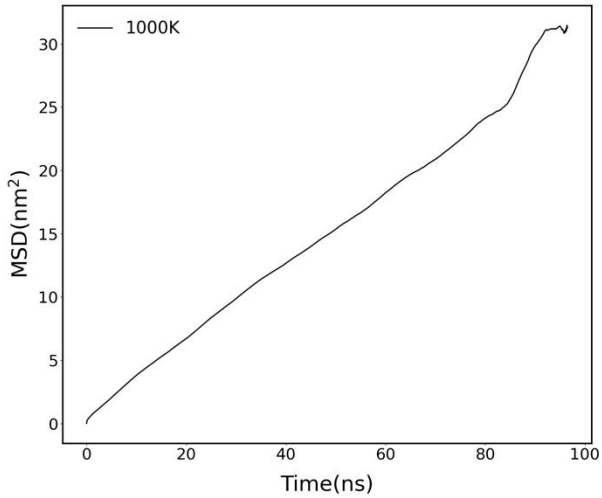

Figure S28. Mean squared displacement of CH_4 in $[Bzmim_3]^{3+}[BzO_3]^{3-}$, corresponding to different temperatures.

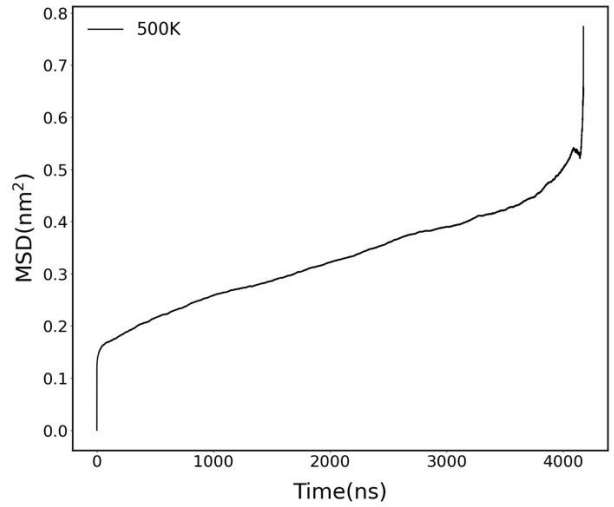

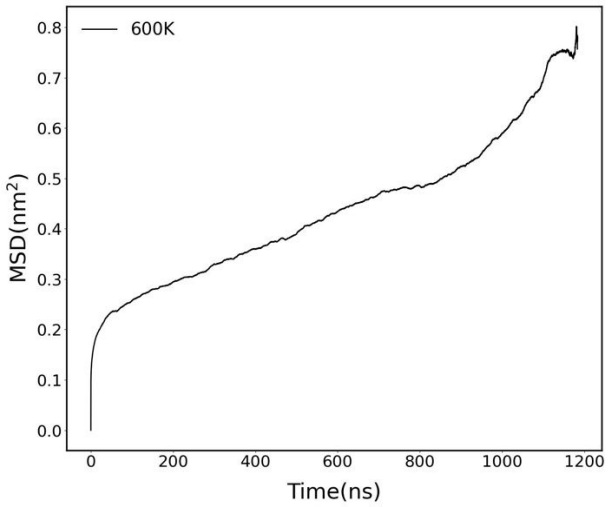

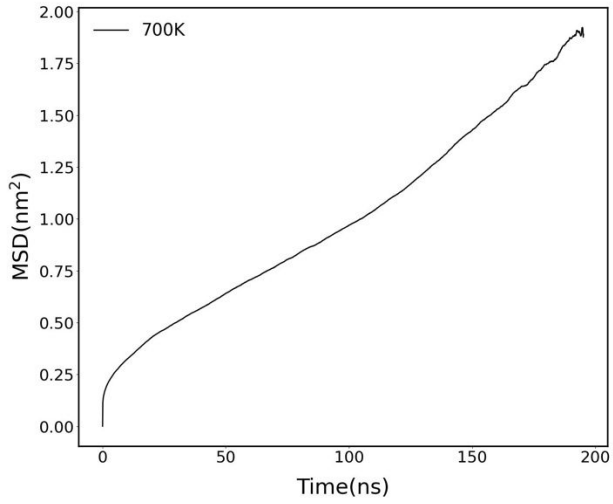

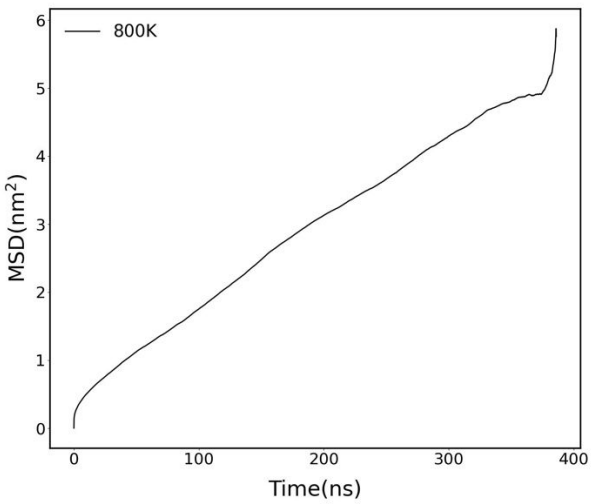

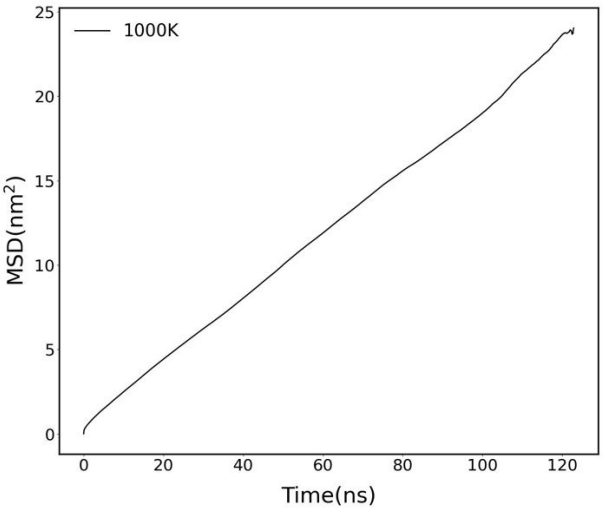

Figure S29. Mean squared displacement of CH_4 in $[Bzmim_3]^{4+}[BzO_3]^{3-}$, corresponding to different temperatures.

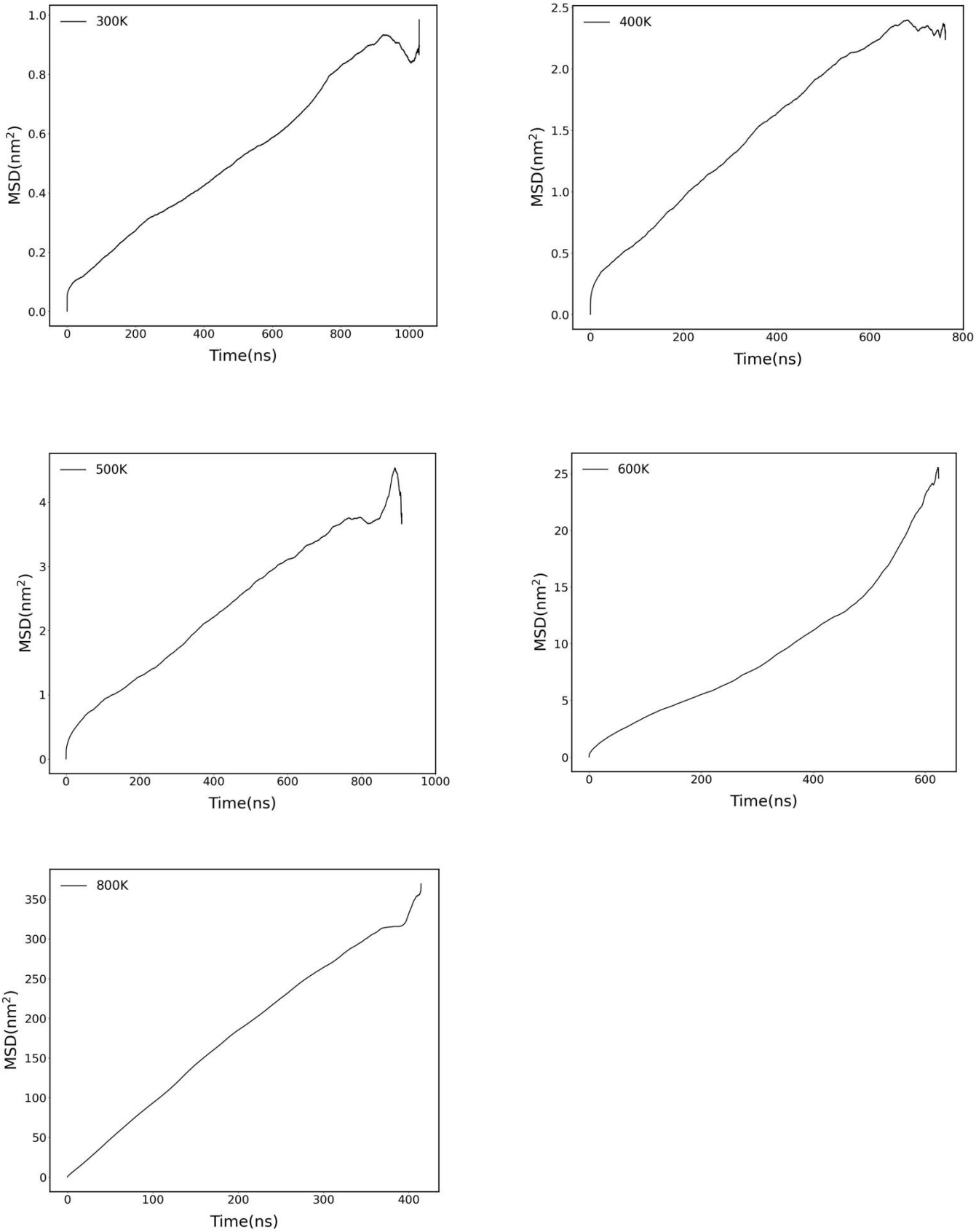

Figure S30. Mean squared displacement of N_2 in $[Bzmim_4]^{3+}[NapO_2]^{2-}$, corresponding to different temperatures.

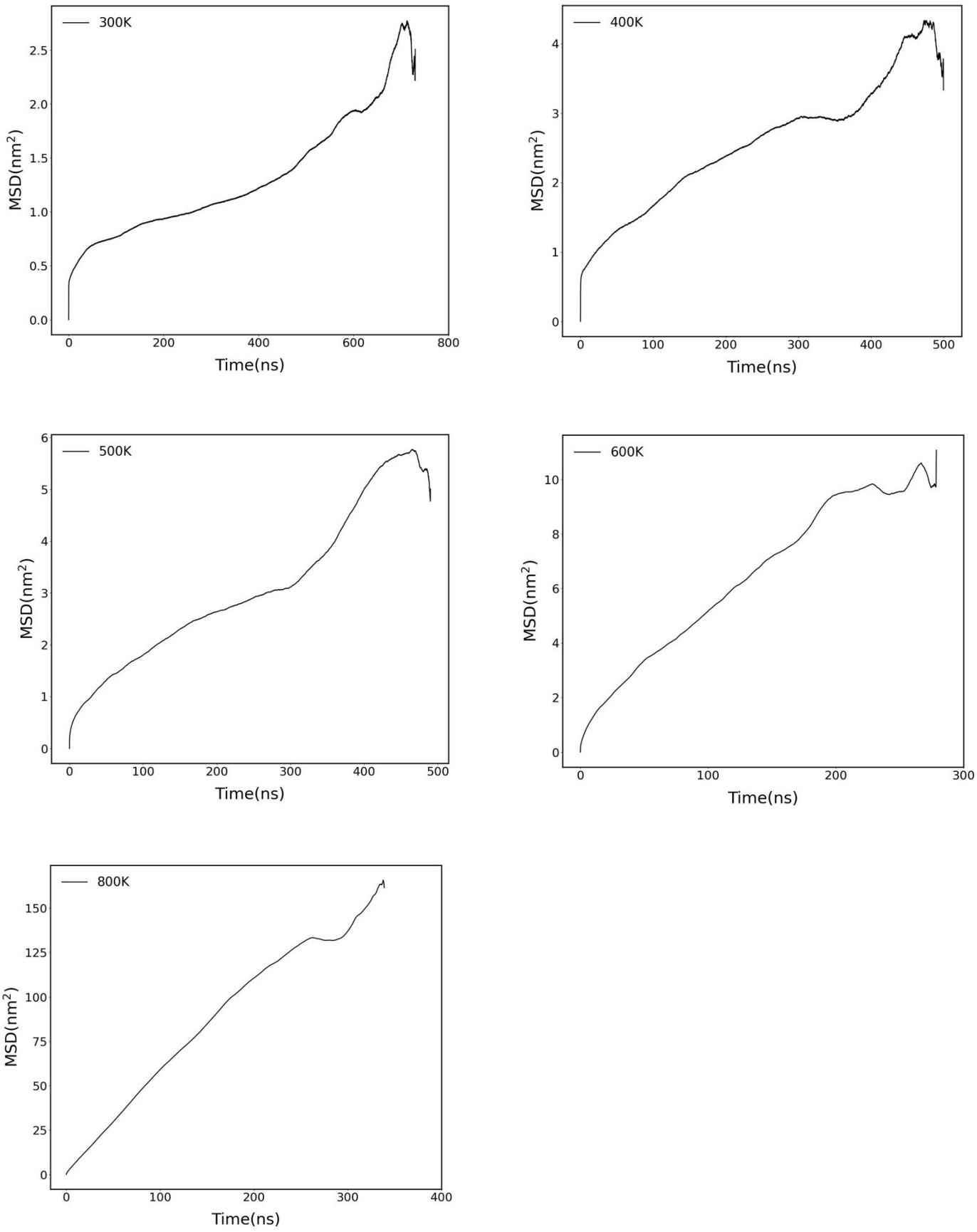

Figure S31. Mean squared displacement of N_2 in $[Bzmim_4]^{4+}[NapO_2]^{2-}$, corresponding to different temperatures.

Supporting Information

Correlation-Based Predictions of Gas Solute Diffusivity in Ionic Liquid Solvents Based on Solvent-Accessible Surface Area

Feranmi V. Olowookere and C. Heath Turner*

Department of Chemical and Biological Engineering, The University of Alabama, Tuscaloosa, AL 35487-0203, United States

Force field parameters for the anions, cations, and solutes

*Corresponding author contact:

C. Heath Turner

E-mail address: hturner@eng.ua.edu

Phone number: 205-348-1733

Topology file for cation C2 [$Bzmim_3$]$^{3+}$

Bonded parameters

```
[ moleculetype ]
; Name               nrexcl
C2                   3
[ atoms ]
;   nr       type  resnr residue  atom   cgnr     charge       mass
     1   opls_1000      1     C2   C000      1    0.14401     12.0110
     2   opls_1001      1     C2   C001      1    -0.06141    12.0110
     3   opls_1002      1     C2   C002      1    0.14304     12.0110
     4   opls_1003      1     C2   N003      1    -0.25873    14.0070
     5   opls_1004      1     C2   C004      1    0.25668     12.0110
     6   opls_1005      1     C2   N005      1    -0.25000    14.0070
     7   opls_1006      1     C2   C006      1    0.08644     12.0110
     8   opls_1007      1     C2   C007      1    0.06224     12.0110
     9   opls_1008      1     C2   C008      1    -0.08339    12.0110
    10   opls_1009      1     C2   C009      1    -0.06110    12.0110
    11   opls_1010      1     C2   C00A      1    0.14351     12.0110
    12   opls_1011      1     C2   C00B      1    -0.06164    12.0110
    13   opls_1012      1     C2   N00C      1    -0.25853    14.0070
    14   opls_1013      1     C2   C00D      1    0.06222     12.0110
    15   opls_1014      1     C2   C00E      1    0.08662     12.0110
    16   opls_1015      1     C2   N00F      1    -0.24992    14.0070
    17   opls_1016      1     C2   C00G      1    0.25688     12.0110
    18   opls_1017      1     C2   C00H      1    -0.08335    12.0110
    19   opls_1018      1     C2   N00I      1    -0.25802    14.0070
    20   opls_1019      1     C2   C00J      1    0.25564     12.0110
    21   opls_1020      1     C2   N00K      1    -0.24985    14.0070
    22   opls_1021      1     C2   C00M      1    0.08706     12.0110
    23   opls_1022      1     C2   C00N      1    0.06360     12.0110
    24   opls_1023      1     C2   C00O      1    -0.08339    12.0110
    25   opls_1024      1     C2   H00P      1    0.16637      1.0080
    26   opls_1025      1     C2   H00Q      1    0.21356      1.0080
    27   opls_1026      1     C2   H00R      1    0.21036      1.0080
    28   opls_1027      1     C2   H00S      1    0.19093      1.0080
    29   opls_1028      1     C2   H00T      1    0.16963      1.0080
    30   opls_1029      1     C2   H00U      1    0.17601      1.0080
    31   opls_1030      1     C2   H00V      1    0.17620      1.0080
    32   opls_1031      1     C2   H00W      1    0.16703      1.0080
    33   opls_1032      1     C2   H00X      2    0.16596      1.0080
    34   opls_1033      1     C2   H00Y      2    0.19098      1.0080
    35   opls_1034      1     C2   H00Z      2    0.21047      1.0080
    36   opls_1035      1     C2   H010      2    0.21392      1.0080
    37   opls_1036      1     C2   H011      2    0.17624      1.0080
    38   opls_1037      1     C2   H012      2    0.17602      1.0080
    39   opls_1038      1     C2   H013      2    0.16964      1.0080
    40   opls_1039      1     C2   H014      2    0.21267      1.0080
    41   opls_1040      1     C2   H015      2    0.21079      1.0080
    42   opls_1041      1     C2   H016      2    0.19276      1.0080
    43   opls_1042      1     C2   H017      2    0.16937      1.0080
    44   opls_1043      1     C2   H018      2    0.17620      1.0080
    45   opls_1044      1     C2   H019      2    0.17627      1.0080
[ bonds ]
    2     1     1      0.1400 392459.200
    3     2     1      0.1400 392459.200
    4     3     1      0.1440 322168.000
    5     4     1      0.1343 399153.600
    6     5     1      0.1343 399153.600
    7     6     1      0.1381 357313.600
    8     4     1      0.1381 357313.600
    9     6     1      0.1475 282001.600
   10     3     1      0.1400 392459.200
   11    10     1      0.1400 392459.200
   12     1     1      0.1400 392459.200
   13    11     1      0.1440 322168.000
   14    13     1      0.1381 357313.600
   15    14     1      0.1375 428441.600
   16    15     1      0.1381 357313.600
   17    13     1      0.1343 399153.600
   18    16     1      0.1475 282001.600
   19     1     1      0.1440 322168.000
   20    19     1      0.1475 282001.600
   21    20     1      0.1510 234304.000
   22    21     1      0.1450 334720.000
```

```
   23    19     1      0.1381 357313.600
   24    21     1      0.1471 307105.600
   25     2     1      0.1080 307105.600
   26     5     1      0.1080 307105.600
   27     7     1      0.1080 307105.600
   28     8     1      0.1080 307105.600
   29     9     1      0.1090 284512.000
   30     9     1      0.1090 284512.000
   31     9     1      0.1090 284512.000
   32    10     1      0.1080 307105.600
   33    12     1      0.1080 307105.600
   34    14     1      0.1080 307105.600
   35    15     1      0.1080 307105.600
   36    17     1      0.1080 307105.600
   37    18     1      0.1090 284512.000
   38    18     1      0.1090 284512.000
   39    18     1      0.1090 284512.000
   40    20     1      0.1088 284512.000
   41    22     1      0.1080 307105.600
   42    23     1      0.1080 307105.600
   43    24     1      0.1090 284512.000
   44    24     1      0.1090 284512.000
   45    24     1      0.1090 284512.000
    8     7     1      0.1375 428441.600
   12    11     1      0.1400 392459.200
   17    16     1      0.1343 399153.600
   23    22     1      0.1433 357313.600

[ angles ]
;  ai    aj    ak funct            c0            c1            c2            c3
    1     2     3     1    120.000    527.184
    2     3     4     1    108.700    585.760
    3     4     5     1    125.200    585.760
    4     5     6     1    120.000    585.760
    5     6     7     1    109.800    585.760
    3     4     8     1    125.200    585.760
    5     6     9     1    112.400    527.184
    2     3    10     1    120.000    527.184
    3    10    11     1    120.000    527.184
    2     1    12     1    120.000    527.184
   10    11    13     1    108.700    585.760
   11    13    14     1    125.200    585.760
   13    14    15     1    120.000    585.760
   14    15    16     1    120.000    585.760
   11    13    17     1    125.200    585.760
   15    16    18     1    112.400    527.184
    2     1    19     1    108.700    585.760
    1    19    20     1    112.400    527.184
   19    20    21     1    109.430    358.401
   20    21    22     1    114.000    460.240
    1    19    23     1    125.200    585.760
   20    21    24     1    113.000    418.400
    1     2    25     1    120.000    292.880
    4     5    26     1    120.000    292.880
    6     7    27     1    121.600    292.880
    4     8    28     1    121.600    292.880
    6     9    29     1    109.500    292.880
    6     9    30     1    109.500    292.880
    6     9    31     1    109.500    292.880
    3    10    32     1    120.000    292.880
    1    12    33     1    120.000    292.880
   13    14    34     1    121.600    292.880
   14    15    35     1    130.700    292.880
   13    17    36     1    120.000    292.880
   16    18    37     1    109.500    292.880
   16    18    38     1    109.500    292.880
   16    18    39     1    109.500    292.880
   19    20    40     1    109.500    292.880
   21    22    41     1    118.760    505.678
   19    23    42     1    121.600    292.880
   21    24    43     1    109.500    292.880
   21    24    44     1    109.500    292.880
   21    24    45     1    109.500    292.880
   15    14    34     1    130.700    292.880
   19    23    22     1    121.600    585.760
    7     8    28     1    130.700    292.880
    8     7    27     1    130.700    292.880
```

```
   29     9    30     1    107.800    276.144
   14    13    17     1    109.800    585.760
    7     6     9     1    112.400    527.184
    3     2    25     1    120.000    292.880
   21    20    40     1    114.300    292.880
   30     9    31     1    107.800    276.144
   11    12    33     1    120.000    292.880
   29     9    31     1    107.800    276.144
   11    10    32     1    120.000    292.880
   17    16    18     1    112.400    527.184
   44    24    45     1    107.800    276.144
    6     7     8     1    120.000    585.760
    4     3    10     1    108.700    585.760
   21    22    23     1    119.700    711.280
    5     4     8     1    109.800    585.760
   23    22    41     1    126.900    292.880
   16    17    36     1    120.000    292.880
   22    21    24     1    114.000    460.240
   22    23    42     1    130.700    292.880
   10    11    12     1    120.000    527.184
   13    17    16     1    120.000    585.760
   12     1    19     1    108.700    585.760
    6     5    26     1    120.000    292.880
   37    18    38     1    107.800    276.144
    4     8     7     1    120.000    585.760
   12    11    13     1    108.700    585.760
   15    16    17     1    109.800    585.760
   43    24    45     1    107.800    276.144
   43    24    44     1    107.800    276.144
   16    15    35     1    121.600    292.880
   37    18    39     1    107.800    276.144
   38    18    39     1    107.800    276.144
    1    12    11     1    120.000    527.184
   20    19    23     1    112.400    527.184

[ dihedrals ]
; IMPROPER DIHEDRAL ANGLES
;  ai    aj    ak    al funct            c0            c1            c2            c3            c4            c5
    10     3     2     4     4        180.000     10.460     2
    33    12     1    11     4        180.000     10.460     2
    32    10     3    11     4        180.000     10.460     2
    25     2     1     3     4        180.000     10.460     2
    41    22    21    23     4        180.000     10.460     2
    36    17    13    16     4        180.000     10.460     2
    26     5     4     6     4        180.000     10.460     2
    35    15    14    16     4        180.000     10.460     2
    42    23    19    22     4        180.000     10.460     2
    27     7     6     8     4        180.000     10.460     2
    28     8     4     7     4        180.000     10.460     2
    34    14    13    15     4        180.000     10.460     2
    19     1     2    12     4        180.000     10.460     2
    13    11    10    12     4        180.000     10.460     2

[ dihedrals ]
; PROPER DIHEDRAL ANGLES
;  ai    aj    ak    al funct            c0            c1            c2            c3            c4            c5
   11    12     1     2        3      30.334    0.000   -30.334   -0.000   -0.000    0.000
   11    10     3     2        3      30.334    0.000   -30.334   -0.000   -0.000    0.000
   11    10     3     4        3      30.334    0.000   -30.334   -0.000   -0.000    0.000
   10     3     2     1        3      30.334    0.000   -30.334   -0.000   -0.000    0.000
   12    11    10     3        3      30.334    0.000   -30.334   -0.000   -0.000    0.000
   10    11    12     1        3      30.334    0.000   -30.334   -0.000   -0.000    0.000
   12     1     2     3        3      30.334    0.000   -30.334   -0.000   -0.000    0.000
   10     3     4     5        3      30.334    0.000   -30.334   -0.000   -0.000    0.000
   10     3     4     8        3       9.079    0.000    -9.079   -0.000   -0.000    0.000
   22    23    19     1        3      20.920    0.000   -20.920   -0.000   -0.000    0.000
   22    23    19    20        3      20.920    0.000   -20.920   -0.000   -0.000    0.000
   22    21    20    19        3       8.786    0.000    -8.786   -0.000   -0.000    0.000
   17    16    15    14        3      20.920    0.000   -20.920   -0.000   -0.000    0.000
    5     4     3     2        3      30.334    0.000   -30.334   -0.000   -0.000    0.000
   17    13    11    12        3      30.334    0.000   -30.334   -0.000   -0.000    0.000
   17    13    11    10        3      30.334    0.000   -30.334   -0.000   -0.000    0.000
   17    13    14    15        3      20.920    0.000   -20.920   -0.000   -0.000    0.000
   24    21    22    23        3       0.000    0.000     0.000   -0.000   -0.000    0.000
   24    21    20    19        3       8.786    0.000    -8.786   -0.000   -0.000    0.000
    9     6     5     4        3      41.840    0.000   -41.840   -0.000   -0.000    0.000
   18    16    17    13        3      41.840    0.000   -41.840   -0.000   -0.000    0.000
```

18	16	15	14	3	20.920	0.000	-20.920	-0.000	-0.000	0.000
9	6	7	8	3	20.920	0.000	-20.920	-0.000	-0.000	0.000
23	22	21	20	3	0.000	0.000	0.000	-0.000	-0.000	0.000
8	7	6	5	3	20.920	0.000	-20.920	-0.000	-0.000	0.000
7	8	4	3	3	20.920	0.000	-20.920	-0.000	-0.000	0.000
15	14	13	11	3	20.920	0.000	-20.920	-0.000	-0.000	0.000
7	8	4	5	3	20.920	0.000	-20.920	-0.000	-0.000	0.000
23	19	1	12	3	9.079	0.000	-9.079	-0.000	-0.000	0.000
23	19	1	2	3	9.079	0.000	-9.079	-0.000	-0.000	0.000
15	16	17	13	3	41.840	0.000	-41.840	-0.000	-0.000	0.000
7	6	5	4	3	41.840	0.000	-41.840	-0.000	-0.000	0.000
23	19	20	21	3	30.334	0.000	-30.334	-0.000	-0.000	0.000
14	13	11	12	3	9.079	0.000	-9.079	-0.000	-0.000	0.000
8	4	3	2	3	9.079	0.000	-9.079	-0.000	-0.000	0.000
14	13	11	10	3	9.079	0.000	-9.079	-0.000	-0.000	0.000
8	4	5	6	3	41.840	0.000	-41.840	-0.000	-0.000	0.000
20	19	1	12	3	30.334	0.000	-30.334	-0.000	-0.000	0.000
20	19	1	2	3	30.334	0.000	-30.334	-0.000	-0.000	0.000
25	2	3	10	3	30.334	0.000	-30.334	-0.000	-0.000	0.000
33	12	1	2	3	30.334	0.000	-30.334	-0.000	-0.000	0.000
33	12	11	10	3	30.334	0.000	-30.334	-0.000	-0.000	0.000
32	10	3	2	3	30.334	0.000	-30.334	-0.000	-0.000	0.000
25	2	1	12	3	30.334	0.000	-30.334	-0.000	-0.000	0.000
32	10	11	12	3	30.334	0.000	-30.334	-0.000	-0.000	0.000
25	2	1	19	3	30.334	0.000	-30.334	-0.000	-0.000	0.000
33	12	1	19	3	30.334	0.000	-30.334	-0.000	-0.000	0.000
33	12	11	13	3	30.334	0.000	-30.334	-0.000	-0.000	0.000
32	10	3	4	3	30.334	0.000	-30.334	-0.000	-0.000	0.000
32	10	11	13	3	30.334	0.000	-30.334	-0.000	-0.000	0.000
25	2	3	4	3	30.334	0.000	-30.334	-0.000	-0.000	0.000
41	22	23	19	3	30.334	0.000	-30.334	-0.000	-0.000	0.000
41	22	21	24	3	0.632	1.895	0.000	-2.527	-0.000	0.000
41	22	21	20	3	0.967	2.900	0.000	-3.866	-0.000	0.000
36	17	16	18	3	41.840	0.000	-41.840	-0.000	-0.000	0.000
26	5	6	9	3	41.840	0.000	-41.840	-0.000	-0.000	0.000
36	17	16	15	3	41.840	0.000	-41.840	-0.000	-0.000	0.000
26	5	6	7	3	41.840	0.000	-41.840	-0.000	-0.000	0.000
26	5	4	3	3	41.840	0.000	-41.840	-0.000	-0.000	0.000
36	17	13	11	3	41.840	0.000	-41.840	-0.000	-0.000	0.000
36	17	13	14	3	41.840	0.000	-41.840	-0.000	-0.000	0.000
26	5	4	8	3	41.840	0.000	-41.840	-0.000	-0.000	0.000
42	23	22	41	3	30.334	0.000	-30.334	-0.000	-0.000	0.000
42	23	22	21	3	44.978	0.000	-44.978	-0.000	-0.000	0.000
28	8	7	27	3	44.978	0.000	-44.978	-0.000	-0.000	0.000
35	15	14	34	3	44.978	0.000	-44.978	-0.000	-0.000	0.000
28	8	7	6	3	44.978	0.000	-44.978	-0.000	-0.000	0.000
34	14	15	16	3	44.978	0.000	-44.978	-0.000	-0.000	0.000
27	7	8	4	3	44.978	0.000	-44.978	-0.000	-0.000	0.000
35	15	14	13	3	44.978	0.000	-44.978	-0.000	-0.000	0.000
42	23	19	1	3	20.920	0.000	-20.920	-0.000	-0.000	0.000
35	15	16	17	3	20.920	0.000	-20.920	-0.000	-0.000	0.000
27	7	6	5	3	20.920	0.000	-20.920	-0.000	-0.000	0.000
27	7	6	9	3	20.920	0.000	-20.920	-0.000	-0.000	0.000
35	15	16	18	3	20.920	0.000	-20.920	-0.000	-0.000	0.000
42	23	19	20	3	20.920	0.000	-20.920	-0.000	-0.000	0.000
34	14	13	11	3	20.920	0.000	-20.920	-0.000	-0.000	0.000
28	8	4	3	3	20.920	0.000	-20.920	-0.000	-0.000	0.000
28	8	4	5	3	20.920	0.000	-20.920	-0.000	-0.000	0.000
34	14	13	17	3	20.920	0.000	-20.920	-0.000	-0.000	0.000
44	24	21	22	3	0.967	2.900	0.000	-3.866	-0.000	0.000
43	24	21	22	3	0.967	2.900	0.000	-3.866	-0.000	0.000
45	24	21	22	3	0.967	2.900	0.000	-3.866	-0.000	0.000
44	24	21	20	3	0.967	2.900	0.000	-3.866	-0.000	0.000
45	24	21	20	3	0.967	2.900	0.000	-3.866	-0.000	0.000
43	24	21	20	3	0.967	2.900	0.000	-3.866	-0.000	0.000
38	18	16	17	3	0.000	0.000	0.000	-0.000	-0.000	0.000
29	9	6	5	3	0.000	0.000	0.000	-0.000	-0.000	0.000
30	9	6	5	3	0.000	0.000	0.000	-0.000	-0.000	0.000
37	18	16	17	3	0.000	0.000	0.000	-0.000	-0.000	0.000
31	9	6	5	3	0.000	0.000	0.000	-0.000	-0.000	0.000
39	18	16	17	3	0.000	0.000	0.000	-0.000	-0.000	0.000
38	18	16	15	3	0.000	0.000	0.000	-0.000	-0.000	0.000
31	9	6	7	3	0.000	0.000	0.000	-0.000	-0.000	0.000
30	9	6	7	3	0.000	0.000	0.000	-0.000	-0.000	0.000
39	18	16	15	3	0.000	0.000	0.000	-0.000	-0.000	0.000
29	9	6	7	3	0.000	0.000	0.000	-0.000	-0.000	0.000
37	18	16	15	3	0.000	0.000	0.000	-0.000	-0.000	0.000

```
   40   20   21   22        3        0.000   0.000   0.000  -0.000  -0.000   0.000
   40   20   21   24        3        0.632   1.895   0.000  -2.527  -0.000   0.000
   40   20   19    1        3        0.000   0.000   0.000  -0.000  -0.000   0.000
   40   20   19   23        3        0.000   0.000   0.000  -0.000  -0.000   0.000
   21   22   23   19        3       44.978   0.000  -44.978  -0.000  -0.000   0.000
   21   20   19    1        3       30.334   0.000  -30.334  -0.000  -0.000   0.000
   19    1    2    3        3       30.334   0.000  -30.334  -0.000  -0.000   0.000
   19    1   12   11        3       30.334   0.000  -30.334  -0.000  -0.000   0.000
   16   17   13   11        3       41.840   0.000  -41.840  -0.000  -0.000   0.000
    6    5    4    3        3       41.840   0.000  -41.840  -0.000  -0.000   0.000
   16   17   13   14        3       41.840   0.000  -41.840  -0.000  -0.000   0.000
   16   15   14   13        3       44.978   0.000  -44.978  -0.000  -0.000   0.000
    6    7    8    4        3       44.978   0.000  -44.978  -0.000  -0.000   0.000
   13   11   10    3        3       30.334   0.000  -30.334  -0.000  -0.000   0.000
   13   11   12    1        3       30.334   0.000  -30.334  -0.000  -0.000   0.000
    4    3    2    1        3       30.334   0.000  -30.334  -0.000  -0.000   0.000

[ pairs ]
    1    4    1
    2    5    1
    3    6    1
    3    7    1
    2    8    1
    1   10    1
    4    9    1
    2   11    1
    1   13    1
    5   10    1
    4   11    1
    3   12    1
    3   13    1
    8    9    1
    8   10    1
    3   19    1
    2   20    1
    1   21    1
    1   22    1
   10   14    1
    2   23    1
   12   14    1
   11   15    1
   11   16    1
   10   17    1
   12   17    1
    4   25    1
    3   26    1
   11   19    1
   13   18    1
    4   27    1
    3   28    1
   14   18    1
   12   20    1
    5   27    1
    7   26    1
    5   28    1
    8   26    1
    6   28    1
    5   29    1
    2   32    1
   12   23    1
   10   25    1
    9   26    1
    5   30    1
    2   33    1
    9   27    1
    7   29    1
    5   31    1
    4   32    1
   12   25    1
    7   30    1
    7   31    1
    1   40    1
   19   24    1
   10   33    1
    1   42    1
   19   25    1
   12   32    1
```

```
   13    32    1
   11    34    1
   13    33    1
   23    24    1
   11    36    1
   13    35    1
   16    34    1
   14    36    1
   17    34    1
   15    36    1
   19    33    1
   17    35    1
   15    37    1
   18    35    1
   15    38    1
   18    36    1
   17    37    1
   15    39    1
   27    28    1
   17    38    1
   17    39    1
   19    41    1
   20    41    1
   22    40    1
   20    42    1
   23    40    1
   21    42    1
   20    43    1
   24    40    1
   20    44    1
   24    41    1
   22    43    1
   20    45    1
   22    44    1
   22    45    1
   34    35    1
   41    42    1
```

Non-bonded parameters

```
[ atomtypes ]
  opls_1026  H1026     1.0080     0.000    A    2.42000E-01   1.25520E-01
  opls_1005  N1005    14.0070     0.000    A    3.25000E-01   7.11280E-01
  opls_1010  C1010    12.0110     0.000    A    3.55000E-01   2.92880E-01
  opls_1043  H1043     1.0080     0.000    A    2.50000E-01   1.25520E-01
  opls_1036  H1036     1.0080     0.000    A    2.50000E-01   1.25520E-01
  opls_1033  H1033     1.0080     0.000    A    2.42000E-01   1.25520E-01
  opls_1028  H1028     1.0080     0.000    A    2.50000E-01   1.25520E-01
  opls_1014  C1014    12.0110     0.000    A    3.55000E-01   2.92880E-01
  opls_1003  N1003    14.0070     0.000    A    3.25000E-01   7.11280E-01
  opls_1041  H1041     1.0080     0.000    A    2.42000E-01   1.25520E-01
  opls_1023  C1023    12.0110     0.000    A    3.50000E-01   2.76144E-01
  opls_1038  H1038     1.0080     0.000    A    2.50000E-01   1.25520E-01
  opls_1006  C1006    12.0110     0.000    A    3.55000E-01   2.92880E-01
  opls_1044  H1044     1.0080     0.000    A    2.50000E-01   1.25520E-01
  opls_1030  H1030     1.0080     0.000    A    2.50000E-01   1.25520E-01
  opls_1001  C1001    12.0110     0.000    A    3.55000E-01   2.92880E-01
  opls_1040  H1040     1.0080     0.000    A    2.42000E-01   1.25520E-01
  opls_1029  H1029     1.0080     0.000    A    2.50000E-01   1.25520E-01
  opls_1042  H1042     1.0080     0.000    A    2.50000E-01   1.25520E-01
  opls_1016  C1016    12.0110     0.000    A    3.55000E-01   2.92880E-01
  opls_1009  C1009    12.0110     0.000    A    3.55000E-01   2.92880E-01
  opls_1037  H1037     1.0080     0.000    A    2.50000E-01   1.25520E-01
  opls_1013  C1013    12.0110     0.000    A    3.55000E-01   2.92880E-01
  opls_1004  C1004    12.0110     0.000    A    3.55000E-01   2.92880E-01
  opls_1019  C1019    12.0110     0.000    A    3.45000E-01   3.47272E-01
  opls_1031  H1031     1.0080     0.000    A    2.42000E-01   1.25520E-01
  opls_1011  C1011    12.0110     0.000    A    3.55000E-01   2.92880E-01
  opls_1015  N1015    14.0070     0.000    A    3.25000E-01   7.11280E-01
  opls_1027  H1027     1.0080     0.000    A    2.42000E-01   1.25520E-01
  opls_1021  C1021    12.0110     0.000    A    3.55000E-01   3.17984E-01
  opls_1024  H1024     1.0080     0.000    A    2.42000E-01   1.25520E-01
  opls_1002  C1002    12.0110     0.000    A    3.55000E-01   2.92880E-01
  opls_1035  H1035     1.0080     0.000    A    2.42000E-01   1.25520E-01
  opls_1000  C1000    12.0110     0.000    A    3.55000E-01   2.92880E-01
```

```
opls_1020  N1020    14.0070     0.000    A    3.25000E-01   7.11280E-01
opls_1018  N1018    14.0070     0.000    A    3.25000E-01   7.11280E-01
opls_1039  H1039     1.0080     0.000    A    2.50000E-01   1.25520E-01
opls_1017  C1017    12.0110     0.000    A    3.50000E-01   2.76144E-01
opls_1034  H1034     1.0080     0.000    A    2.42000E-01   1.25520E-01
opls_1007  C1007    12.0110     0.000    A    3.55000E-01   2.92880E-01
opls_1008  C1008    12.0110     0.000    A    3.50000E-01   2.76144E-01
opls_1025  H1025     1.0080     0.000    A    2.42000E-01   1.25520E-01
opls_1022  C1022    12.0110     0.000    A    3.55000E-01   2.92880E-01
opls_1032  H1032     1.0080     0.000    A    2.42000E-01   1.25520E-01
opls_1012  N1012    14.0070     0.000    A    3.25000E-01   7.11280E-01
```

Topology file for cation C3 $[Bzmim_4]^{4+}$

Bonded parameters

```
[ moleculetype ]
; Name               nrexcl
C3                   3
[ atoms ]
;   nr       type  resnr residue  atom   cgnr     charge       mass
     1   opls_1000      1     C3   C000      1   0.05968     12.0110
     2   opls_1001      1     C3   H001      1   0.19524      1.0080
     3   opls_1002      1     C3   C002      1   0.09712     12.0110
     4   opls_1003      1     C3   H003      1   0.22064      1.0080
     5   opls_1004      1     C3   N004      1   -0.24339    14.0070
     6   opls_1005      1     C3   C005      1   -0.07824    12.0110
     7   opls_1006      1     C3   H006      1   0.17297      1.0080
     8   opls_1007      1     C3   H007      1   0.18433      1.0080
     9   opls_1008      1     C3   H008      1   0.18128      1.0080
    10   opls_1009      1     C3   C009      1   0.25249     12.0110
    11   opls_1010      1     C3   H00A      1   0.21383      1.0080
    12   opls_1011      1     C3   N00B      1   -0.26764    14.0070
    13   opls_1012      1     C3   C00C      1   0.14993     12.0110
    14   opls_1013      1     C3   C00D      1   -0.05157    12.0110
    15   opls_1014      1     C3   H00E      1   0.17544      1.0080
    16   opls_1015      1     C3   C00F      1   0.15124     12.0110
    17   opls_1016      1     C3   N00G      1   -0.26608    14.0070
    18   opls_1017      1     C3   C00H      1   0.25380     12.0110
    19   opls_1018      1     C3   H00I      1   0.21573      1.0080
    20   opls_1019      1     C3   N00J      1   -0.24269    14.0070
    21   opls_1020      1     C3   C00K      1   -0.07755    12.0110
    22   opls_1021      1     C3   H00M      1   0.17422      1.0080
    23   opls_1022      1     C3   H00N      1   0.18152      1.0080
    24   opls_1023      1     C3   H00O      1   0.18459      1.0080
    25   opls_1024      1     C3   C00P      1   0.09585     12.0110
    26   opls_1025      1     C3   H00Q      1   0.21988      1.0080
    27   opls_1026      1     C3   C00R      1   0.05750     12.0110
    28   opls_1027      1     C3   H00S      1   0.18986      1.0080
    29   opls_1028      1     C3   C00T      1   0.14994     12.0110
    30   opls_1029      1     C3   N00U      1   -0.26764    14.0070
    31   opls_1030      1     C3   C00V      1   0.25248     12.0110
    32   opls_1031      1     C3   H00W      1   0.21381      1.0080
    33   opls_1032      1     C3   N00X      2   -0.24339    14.0070
    34   opls_1033      1     C3   C00Y      2   -0.07824    12.0110
    35   opls_1034      1     C3   H00Z      2   0.17297      1.0080
    36   opls_1035      1     C3   H010      2   0.18432      1.0080
    37   opls_1036      1     C3   H011      2   0.18129      1.0080
    38   opls_1037      1     C3   C012      2   0.09713     12.0110
    39   opls_1038      1     C3   H013      2   0.22064      1.0080
    40   opls_1039      1     C3   C014      2   0.05969     12.0110
    41   opls_1040      1     C3   H015      2   0.19524      1.0080
    42   opls_1041      1     C3   C016      2   -0.05158    12.0110
    43   opls_1042      1     C3   H017      2   0.17543      1.0080
    44   opls_1043      1     C3   C018      2   0.15126     12.0110
    45   opls_1044      1     C3   N019      2   -0.26607    14.0070
    46   opls_1045      1     C3   C01A      2   0.25382     12.0110
    47   opls_1046      1     C3   H01B      2   0.21573      1.0080
    48   opls_1047      1     C3   N01C      2   -0.24268    14.0070
    49   opls_1048      1     C3   C01D      2   -0.07754    12.0110
    50   opls_1049      1     C3   H01E      2   0.17422      1.0080
    51   opls_1050      1     C3   H01F      2   0.18152      1.0080
    52   opls_1051      1     C3   H01G      2   0.18459      1.0080
    53   opls_1052      1     C3   C01H      2   0.09585     12.0110
    54   opls_1053      1     C3   H01I      2   0.21988      1.0080
    55   opls_1054      1     C3   C01J      2   0.05749     12.0110
    56   opls_1055      1     C3   H01K      2   0.18984      1.0080
 [ bonds ]
    2     1     1      0.1080 307105.600
    3     1     1      0.1375 428441.600
    4     3     1      0.1080 307105.600
    5     3     1      0.1381 357313.600
    6     5     1      0.1475 282001.600
    7     6     1      0.1090 284512.000
    8     6     1      0.1090 284512.000
    9     6     1      0.1090 284512.000
   10     5     1      0.1343 399153.600
   11    10     1      0.1080 307105.600
```

```
    12     1     1      0.1381 357313.600
    13    12     1      0.1440 322168.000
    14    13     1      0.1400 392459.200
    15    14     1      0.1080 307105.600
    16    14     1      0.1400 392459.200
    17    16     1      0.1440 322168.000
    18    17     1      0.1343 399153.600
    19    18     1      0.1080 307105.600
    20    18     1      0.1343 399153.600
    21    20     1      0.1475 282001.600
    22    21     1      0.1090 284512.000
    23    21     1      0.1090 284512.000
    24    21     1      0.1090 284512.000
    25    20     1      0.1381 357313.600
    26    25     1      0.1080 307105.600
    27    17     1      0.1381 357313.600
    28    27     1      0.1080 307105.600
    29    16     1      0.1400 392459.200
    30    29     1      0.1450 334720.000
    31    30     1      0.1450 334720.000
    32    31     1      0.1080 307105.600
    33    31     1      0.1365 374886.400
    34    33     1      0.1475 282001.600
    35    34     1      0.1090 284512.000
    36    34     1      0.1090 284512.000
    37    34     1      0.1090 284512.000
    38    33     1      0.1381 357313.600
    39    38     1      0.1080 307105.600
    40    30     1      0.1450 334720.000
    41    40     1      0.1080 307105.600
    42    29     1      0.1400 392459.200
    43    42     1      0.1080 307105.600
    44    13     1      0.1400 392459.200
    45    44     1      0.1450 334720.000
    46    45     1      0.1450 334720.000
    47    46     1      0.1080 307105.600
    48    46     1      0.1365 374886.400
    49    48     1      0.1475 282001.600
    50    49     1      0.1090 284512.000
    51    49     1      0.1090 284512.000
    52    49     1      0.1090 284512.000
    53    48     1      0.1381 357313.600
    54    53     1      0.1080 307105.600
    55    45     1      0.1450 334720.000
    56    55     1      0.1080 307105.600
    12    10     1      0.1343 399153.600
    27    25     1      0.1375 428441.600
    40    38     1      0.1367 456892.800
    44    42     1      0.1400 392459.200
    55    53     1      0.1367 456892.800

[ angles ]
;  ai    aj    ak funct            c0            c1            c2            c3
     2     1     3     1    130.700    292.880
     1     3     4     1    130.700    292.880
     1     3     5     1    120.000    585.760
     3     5     6     1    112.400    527.184
     5     6     7     1    109.500    292.880
     5     6     8     1    109.500    292.880
     5     6     9     1    109.500    292.880
     3     5    10     1    109.800    585.760
     5    10    11     1    120.000    292.880
     2     1    12     1    121.600    292.880
     1    12    13     1    125.200    585.760
    12    13    14     1    108.700    585.760
    13    14    15     1    120.000    292.880
    13    14    16     1    120.000    527.184
    14    16    17     1    108.700    585.760
    16    17    18     1    125.200    585.760
    17    18    19     1    120.000    292.880
    17    18    20     1    120.000    585.760
    18    20    21     1    112.400    527.184
    20    21    22     1    109.500    292.880
    20    21    23     1    109.500    292.880
    20    21    24     1    109.500    292.880
    18    20    25     1    109.800    585.760
    20    25    26     1    121.600    292.880
```

16	17	27	1	125.200	585.760
17	27	28	1	121.600	292.880
14	16	29	1	120.000	527.184
16	29	30	1	120.000	585.760
29	30	31	1	109.500	334.720
30	31	32	1	118.760	505.678
30	31	33	1	120.000	585.760
31	33	34	1	112.400	527.184
33	34	35	1	109.500	292.880
33	34	36	1	109.500	292.880
33	34	37	1	109.500	292.880
31	33	38	1	125.200	585.760
33	38	39	1	121.600	292.880
29	30	40	1	109.500	334.720
30	40	41	1	118.760	505.678
16	29	42	1	120.000	527.184
29	42	43	1	120.000	292.880
12	13	44	1	108.700	585.760
13	44	45	1	120.000	585.760
44	45	46	1	109.500	334.720
45	46	47	1	118.760	505.678
45	46	48	1	120.000	585.760
46	48	49	1	112.400	527.184
48	49	50	1	109.500	292.880
48	49	51	1	109.500	292.880
48	49	52	1	109.500	292.880
46	48	53	1	125.200	585.760
48	53	54	1	121.600	292.880
44	45	55	1	109.500	334.720
45	55	56	1	118.760	505.678
10	12	13	1	125.200	585.760
42	44	45	1	120.000	585.760
11	10	12	1	120.000	292.880
36	34	37	1	107.800	276.144
54	53	55	1	130.700	292.880
38	40	41	1	126.900	292.880
1	12	10	1	109.800	585.760
51	49	52	1	107.800	276.144
5	10	12	1	120.000	585.760
15	14	16	1	120.000	292.880
22	21	23	1	107.800	276.144
6	5	10	1	112.400	527.184
32	31	33	1	120.000	292.880
46	45	55	1	112.400	527.184
26	25	27	1	130.700	292.880
4	3	5	1	121.600	292.880
33	38	40	1	121.600	585.760
29	42	44	1	120.000	527.184
30	29	42	1	120.000	585.760
49	48	53	1	112.400	527.184
3	1	12	1	120.000	585.760
35	34	36	1	107.800	276.144
50	49	52	1	107.800	276.144
39	38	40	1	130.700	292.880
22	21	24	1	107.800	276.144
34	33	38	1	112.400	527.184
25	27	28	1	130.700	292.880
31	30	40	1	112.400	527.184
43	42	44	1	120.000	292.880
23	21	24	1	107.800	276.144
53	55	56	1	126.900	292.880
19	18	20	1	120.000	292.880
8	6	9	1	107.800	276.144
50	49	51	1	107.800	276.144
17	27	25	1	120.000	585.760
13	44	42	1	120.000	527.184
35	34	37	1	107.800	276.144
7	6	9	1	107.800	276.144
30	40	38	1	119.700	711.280
45	55	53	1	119.700	711.280
47	46	48	1	120.000	292.880
18	17	27	1	109.800	585.760
48	53	55	1	121.600	585.760
7	6	8	1	107.800	276.144
17	16	29	1	108.700	585.760
21	20	25	1	112.400	527.184
20	25	27	1	120.000	585.760

```
   14    13    44     1    120.000    527.184

[ dihedrals ]
; IMPROPER DIHEDRAL ANGLES
;  ai    aj    ak    al funct            c0           c1            c2            c3            c4            c5
    16    14    13    15    4        180.000     10.460     2
    29    16    14    17    4        180.000     10.460     2
    44    13    12    14    4        180.000     10.460     2
    42    29    16    30    4        180.000     10.460     2
    40    38    33    39    4        180.000     10.460     2
    43    42    44    29    4        180.000     10.460     2
    56    55    45    53    4        180.000     10.460     2
    41    40    30    38    4        180.000     10.460     2
    11    10    12     5    4        180.000     10.460     2
    26    25    27    20    4        180.000     10.460     2
    28    27    17    25    4        180.000     10.460     2
    45    44    13    42    4        180.000     10.460     2
    48    46    45    47    4        180.000     10.460     2
    33    31    30    32    4        180.000     10.460     2
    20    18    17    19    4        180.000     10.460     2
     5     3     1     4    4        180.000     10.460     2
    48    53    54    55    4        180.000     10.460     2
    12     1     2     3    4        180.000     10.460     2

[ dihedrals ]
; PROPER DIHEDRAL ANGLES
;  ai    aj    ak    al funct            c0           c1            c2            c3            c4            c5
   16   14   13   12        3      30.334   0.000  -30.334  -0.000  -0.000   0.000
   13   12   10   11        3      41.840   0.000  -41.840  -0.000  -0.000   0.000
   13   12   10    5        3      41.840   0.000  -41.840  -0.000  -0.000   0.000
   13   12    1    3        3      20.920   0.000  -20.920  -0.000  -0.000   0.000
   13   12    1    2        3      20.920   0.000  -20.920  -0.000  -0.000   0.000
   44   13   14   16        3      30.334   0.000  -30.334  -0.000  -0.000   0.000
   29   16   14   13        3      30.334   0.000  -30.334  -0.000  -0.000   0.000
   29   16   14   15        3      30.334   0.000  -30.334  -0.000  -0.000   0.000
   44   13   14   15        3      30.334   0.000  -30.334  -0.000  -0.000   0.000
   14   13   12   10        3      30.334   0.000  -30.334  -0.000  -0.000   0.000
   44   13   12   10        3      30.334   0.000  -30.334  -0.000  -0.000   0.000
   29   16   17   18        3      30.334   0.000  -30.334  -0.000  -0.000   0.000
   14   13   12    1        3       9.079   0.000   -9.079  -0.000  -0.000   0.000
   29   16   17   27        3       9.079   0.000   -9.079  -0.000  -0.000   0.000
   44   13   12    1        3       9.079   0.000   -9.079  -0.000  -0.000   0.000
   42   44   13   14        3      30.334   0.000  -30.334  -0.000  -0.000   0.000
   42   29   16   14        3      30.334   0.000  -30.334  -0.000  -0.000   0.000
   42   29   16   17        3      30.334   0.000  -30.334  -0.000  -0.000   0.000
   42   44   13   12        3      30.334   0.000  -30.334  -0.000  -0.000   0.000
   29   42   44   13        3      30.334   0.000  -30.334  -0.000  -0.000   0.000
   44   42   29   16        3      30.334   0.000  -30.334  -0.000  -0.000   0.000
   44   42   29   30        3      30.334   0.000  -30.334  -0.000  -0.000   0.000
   42   29   30   40        3       0.000   0.000    0.000  -0.000  -0.000   0.000
   42   29   30   31        3       0.000   0.000    0.000  -0.000  -0.000   0.000
   40   38   33   31        3      20.920   0.000  -20.920  -0.000  -0.000   0.000
   55   53   48   46        3      20.920   0.000  -20.920  -0.000  -0.000   0.000
   55   53   48   49        3      20.920   0.000  -20.920  -0.000  -0.000   0.000
   40   38   33   34        3      20.920   0.000  -20.920  -0.000  -0.000   0.000
   46   45   44   13        3       0.000   0.000    0.000  -0.000  -0.000   0.000
   55   45   44   13        3       0.000   0.000    0.000  -0.000  -0.000   0.000
   40   30   29   16        3       0.000   0.000    0.000  -0.000  -0.000   0.000
   31   30   29   16        3       0.000   0.000    0.000  -0.000  -0.000   0.000
   46   45   44   42        3       0.000   0.000    0.000  -0.000  -0.000   0.000
   55   45   44   42        3       0.000   0.000    0.000  -0.000  -0.000   0.000
   55   45   46   47        3       0.967   2.900    0.000  -3.866  -0.000   0.000
   40   30   31   32        3       0.967   2.900    0.000  -3.866  -0.000   0.000
   40   30   31   33        3       8.786   0.000   -8.786  -0.000  -0.000   0.000
   55   45   46   48        3       8.786   0.000   -8.786  -0.000  -0.000   0.000
   10    5    6    9        3       0.000   0.000    0.000  -0.000  -0.000   0.000
   10    5    6    8        3       0.000   0.000    0.000  -0.000  -0.000   0.000
   10    5    6    7        3       0.000   0.000    0.000  -0.000  -0.000   0.000
   10    5    3    1        3      20.920   0.000  -20.920  -0.000  -0.000   0.000
   10    5    3    4        3      20.920   0.000  -20.920  -0.000  -0.000   0.000
   18   17   16   14        3      30.334   0.000  -30.334  -0.000  -0.000   0.000
   10   12    1    3        3      20.920   0.000  -20.920  -0.000  -0.000   0.000
   10   12    1    2        3      20.920   0.000  -20.920  -0.000  -0.000   0.000
   49   48   46   47        3       1.590   4.770    0.000  -6.360  -0.000   0.000
   34   33   31   32        3       1.590   4.770    0.000  -6.360  -0.000   0.000
   49   48   46   45        3      33.204   0.000  -33.204  -0.000  -0.000   0.000
   34   33   31   30        3      33.204   0.000  -33.204  -0.000  -0.000   0.000
```

21	20	18	19	3	41.840	0.000	-41.840	-0.000	-0.000	0.000
21	20	18	17	3	41.840	0.000	-41.840	-0.000	-0.000	0.000
6	5	3	1	3	20.920	0.000	-20.920	-0.000	-0.000	0.000
6	5	3	4	3	20.920	0.000	-20.920	-0.000	-0.000	0.000
53	55	45	44	3	0.000	0.000	0.000	-0.000	-0.000	0.000
38	40	30	29	3	0.000	0.000	0.000	-0.000	-0.000	0.000
53	55	45	46	3	0.000	0.000	0.000	-0.000	-0.000	0.000
38	40	30	31	3	0.000	0.000	0.000	-0.000	-0.000	0.000
27	25	20	18	3	20.920	0.000	-20.920	-0.000	-0.000	0.000
27	25	20	21	3	20.920	0.000	-20.920	-0.000	-0.000	0.000
25	27	17	16	3	20.920	0.000	-20.920	-0.000	-0.000	0.000
25	27	17	18	3	20.920	0.000	-20.920	-0.000	-0.000	0.000
38	33	31	32	3	30.334	0.000	-30.334	-0.000	-0.000	0.000
53	48	46	47	3	30.334	0.000	-30.334	-0.000	-0.000	0.000
38	33	31	30	3	30.334	0.000	-30.334	-0.000	-0.000	0.000
53	48	46	45	3	30.334	0.000	-30.334	-0.000	-0.000	0.000
25	20	18	19	3	41.840	0.000	-41.840	-0.000	-0.000	0.000
25	20	18	17	3	41.840	0.000	-41.840	-0.000	-0.000	0.000
38	33	34	37	3	0.000	0.000	0.000	-0.000	-0.000	0.000
25	20	21	22	3	0.000	0.000	0.000	-0.000	-0.000	0.000
25	20	21	24	3	0.000	0.000	0.000	-0.000	-0.000	0.000
53	48	49	51	3	0.000	0.000	0.000	-0.000	-0.000	0.000
53	48	49	52	3	0.000	0.000	0.000	-0.000	-0.000	0.000
38	33	34	35	3	0.000	0.000	0.000	-0.000	-0.000	0.000
53	48	49	50	3	0.000	0.000	0.000	-0.000	-0.000	0.000
38	33	34	36	3	0.000	0.000	0.000	-0.000	-0.000	0.000
25	20	21	23	3	0.000	0.000	0.000	-0.000	-0.000	0.000
27	17	16	14	3	9.079	0.000	-9.079	-0.000	-0.000	0.000
27	17	18	19	3	41.840	0.000	-41.840	-0.000	-0.000	0.000
27	17	18	20	3	41.840	0.000	-41.840	-0.000	-0.000	0.000
15	14	13	12	3	30.334	0.000	-30.334	-0.000	-0.000	0.000
43	42	29	16	3	30.334	0.000	-30.334	-0.000	-0.000	0.000
43	42	44	13	3	30.334	0.000	-30.334	-0.000	-0.000	0.000
43	42	29	30	3	30.334	0.000	-30.334	-0.000	-0.000	0.000
56	55	53	54	3	30.334	0.000	-30.334	-0.000	-0.000	0.000
41	40	38	39	3	30.334	0.000	-30.334	-0.000	-0.000	0.000
41	40	38	33	3	30.334	0.000	-30.334	-0.000	-0.000	0.000
56	55	53	48	3	30.334	0.000	-30.334	-0.000	-0.000	0.000
32	31	30	29	3	0.967	2.900	0.000	-3.866	-0.000	0.000
47	46	45	44	3	0.967	2.900	0.000	-3.866	-0.000	0.000
56	55	45	44	3	0.967	2.900	0.000	-3.866	-0.000	0.000
41	40	30	29	3	0.967	2.900	0.000	-3.866	-0.000	0.000
56	55	45	46	3	0.967	2.900	0.000	-3.866	-0.000	0.000
41	40	30	31	3	0.967	2.900	0.000	-3.866	-0.000	0.000
11	10	5	6	3	41.840	0.000	-41.840	-0.000	-0.000	0.000
11	10	5	3	3	41.840	0.000	-41.840	-0.000	-0.000	0.000
19	18	17	16	3	41.840	0.000	-41.840	-0.000	-0.000	0.000
11	10	12	1	3	41.840	0.000	-41.840	-0.000	-0.000	0.000
39	38	40	30	3	44.978	0.000	-44.978	-0.000	-0.000	0.000
54	53	55	45	3	44.978	0.000	-44.978	-0.000	-0.000	0.000
28	27	25	26	3	44.978	0.000	-44.978	-0.000	-0.000	0.000
4	3	1	2	3	44.978	0.000	-44.978	-0.000	-0.000	0.000
28	27	25	20	3	44.978	0.000	-44.978	-0.000	-0.000	0.000
26	25	27	17	3	44.978	0.000	-44.978	-0.000	-0.000	0.000
54	53	48	46	3	20.920	0.000	-20.920	-0.000	-0.000	0.000
39	38	33	31	3	20.920	0.000	-20.920	-0.000	-0.000	0.000
26	25	20	18	3	20.920	0.000	-20.920	-0.000	-0.000	0.000
26	25	20	21	3	20.920	0.000	-20.920	-0.000	-0.000	0.000
54	53	48	49	3	20.920	0.000	-20.920	-0.000	-0.000	0.000
39	38	33	34	3	20.920	0.000	-20.920	-0.000	-0.000	0.000
28	27	17	16	3	20.920	0.000	-20.920	-0.000	-0.000	0.000
28	27	17	18	3	20.920	0.000	-20.920	-0.000	-0.000	0.000
35	34	33	31	3	0.000	0.000	0.000	-0.000	-0.000	0.000
37	34	33	31	3	0.000	0.000	0.000	-0.000	-0.000	0.000
36	34	33	31	3	0.000	0.000	0.000	-0.000	-0.000	0.000
50	49	48	46	3	0.000	0.000	0.000	-0.000	-0.000	0.000
52	49	48	46	3	0.000	0.000	0.000	-0.000	-0.000	0.000
51	49	48	46	3	0.000	0.000	0.000	-0.000	-0.000	0.000
22	21	20	18	3	0.000	0.000	0.000	-0.000	-0.000	0.000
23	21	20	18	3	0.000	0.000	0.000	-0.000	-0.000	0.000
24	21	20	18	3	0.000	0.000	0.000	-0.000	-0.000	0.000
8	6	5	3	3	0.000	0.000	0.000	-0.000	-0.000	0.000
9	6	5	3	3	0.000	0.000	0.000	-0.000	-0.000	0.000
7	6	5	3	3	0.000	0.000	0.000	-0.000	-0.000	0.000
45	44	13	14	3	30.334	0.000	-30.334	-0.000	-0.000	0.000
30	29	16	14	3	30.334	0.000	-30.334	-0.000	-0.000	0.000
45	44	13	12	3	30.334	0.000	-30.334	-0.000	-0.000	0.000

```
   30   29   16   17        3      30.334   0.000  -30.334  -0.000  -0.000   0.000
   45   44   42   29        3      30.334   0.000  -30.334  -0.000  -0.000   0.000
   45   44   42   43        3      30.334   0.000  -30.334  -0.000  -0.000   0.000
   48   46   45   44        3       8.786   0.000  -8.786  -0.000  -0.000   0.000
   33   31   30   29        3       8.786   0.000  -8.786  -0.000  -0.000   0.000
   20   18   17   16        3      41.840   0.000  -41.840  -0.000  -0.000   0.000
    5   10   12    1        3      41.840   0.000  -41.840  -0.000  -0.000   0.000
   48   53   55   45        3      44.978   0.000  -44.978  -0.000  -0.000   0.000
   33   38   40   30        3      44.978   0.000  -44.978  -0.000  -0.000   0.000
    5    3    1    2        3      44.978   0.000  -44.978  -0.000  -0.000   0.000
   20   25   27   17        3      44.978   0.000  -44.978  -0.000  -0.000   0.000
   17   16   14   13        3      30.334   0.000  -30.334  -0.000  -0.000   0.000
   17   16   14   15        3      30.334   0.000  -30.334  -0.000  -0.000   0.000
   12   10    5    6        3      41.840   0.000  -41.840  -0.000  -0.000   0.000
   12   10    5    3        3      41.840   0.000  -41.840  -0.000  -0.000   0.000
   12    1    3    4        3      44.978   0.000  -44.978  -0.000  -0.000   0.000
   12    1    3    5        3      44.978   0.000  -44.978  -0.000  -0.000   0.000

[ pairs ]
    2     4    1
    2     5    1
    1     6    1
    4     6    1
    3     7    1
    3     8    1
    3     9    1
    2    10    1
    1    11    1
    4    10    1
    3    11    1
    2    13    1
    1    14    1
    4    12    1
    3    13    1
    7    10    1
    6    11    1
    8    10    1
    6    12    1
    5    13    1
    9    10    1
   11    13    1
   10    14    1
   12    15    1
   12    16    1
   13    17    1
   15    17    1
   14    18    1
   16    19    1
   16    20    1
   17    21    1
   19    21    1
   18    22    1
   18    23    1
   16    25    1
   14    27    1
   18    24    1
   13    29    1
   17    26    1
   19    25    1
   18    26    1
   16    28    1
   15    29    1
   14    30    1
    1    44    1
   19    27    1
   18    28    1
   22    25    1
   21    26    1
   18    29    1
   17    30    1
   16    31    1
   23    25    1
   21    27    1
   20    28    1
   24    25    1
   26    28    1
   12    42    1
```

```
   10    44    1
   27    29    1
   16    40    1
   14    42    1
   13    43    1
   12    45    1
   17    42    1
   16    43    1
   15    44    1
   14    45    1
   13    46    1
   16    44    1
   29    32    1
   29    33    1
   30    34    1
   32    34    1
   31    35    1
   31    36    1
   29    38    1
   31    37    1
   13    55    1
   30    39    1
   32    38    1
   31    39    1
   29    41    1
   32    40    1
   31    41    1
   35    38    1
   34    39    1
   31    42    1
   30    43    1
   36    38    1
   34    40    1
   33    41    1
   30    44    1
   29    45    1
   37    38    1
   39    41    1
   40    42    1
   43    45    1
   42    46    1
   44    47    1
   44    48    1
   45    49    1
   47    49    1
   46    50    1
   46    51    1
   44    53    1
   42    55    1
   46    52    1
   45    54    1
   47    53    1
   46    54    1
   44    56    1
   47    55    1
   46    56    1
   50    53    1
   49    54    1
   51    53    1
   49    55    1
   48    56    1
   52    53    1
   54    56    1
```

Non-bonded parameters

```
[ atomtypes ]
  opls_1038  H1038     1.0080     0.000    A    2.42000E-01   1.25520E-01
  opls_1016  N1016    14.0070     0.000    A    3.25000E-01   7.11280E-01
  opls_1018  H1018     1.0080     0.000    A    2.42000E-01   1.25520E-01
  opls_1052  C1052    12.0110     0.000    A    3.55000E-01   2.92880E-01
  opls_1017  C1017    12.0110     0.000    A    3.55000E-01   2.92880E-01
  opls_1055  H1055     1.0080     0.000    A    2.42000E-01   1.25520E-01
  opls_1050  H1050     1.0080     0.000    A    2.50000E-01   1.25520E-01
  opls_1046  H1046     1.0080     0.000    A    2.42000E-01   1.25520E-01
  opls_1036  H1036     1.0080     0.000    A    2.50000E-01   1.25520E-01
  opls_1043  C1043    12.0110     0.000    A    3.55000E-01   2.92880E-01
```

opls_1035	H1035	1.0080	0.000	A	2.50000E-01	1.25520E-01
opls_1034	H1034	1.0080	0.000	A	2.50000E-01	1.25520E-01
opls_1026	C1026	12.0110	0.000	A	3.55000E-01	2.92880E-01
opls_1019	N1019	14.0070	0.000	A	3.25000E-01	7.11280E-01
opls_1051	H1051	1.0080	0.000	A	2.50000E-01	1.25520E-01
opls_1031	H1031	1.0080	0.000	A	2.42000E-01	1.25520E-01
opls_1037	C1037	12.0110	0.000	A	3.55000E-01	2.92880E-01
opls_1024	C1024	12.0110	0.000	A	3.55000E-01	2.92880E-01
opls_1047	N1047	14.0070	0.000	A	3.25000E-01	7.11280E-01
opls_1008	H1008	1.0080	0.000	A	2.50000E-01	1.25520E-01
opls_1004	N1004	14.0070	0.000	A	3.25000E-01	7.11280E-01
opls_1007	H1007	1.0080	0.000	A	2.50000E-01	1.25520E-01
opls_1040	H1040	1.0080	0.000	A	2.42000E-01	1.25520E-01
opls_1021	H1021	1.0080	0.000	A	2.50000E-01	1.25520E-01
opls_1048	C1048	12.0110	0.000	A	3.50000E-01	2.76144E-01
opls_1006	H1006	1.0080	0.000	A	2.50000E-01	1.25520E-01
opls_1053	H1053	1.0080	0.000	A	2.42000E-01	1.25520E-01
opls_1012	C1012	12.0110	0.000	A	3.55000E-01	2.92880E-01
opls_1013	C1013	12.0110	0.000	A	3.55000E-01	2.92880E-01
opls_1029	N1029	14.0070	0.000	A	3.25000E-01	7.11280E-01
opls_1041	C1041	12.0110	0.000	A	3.55000E-01	2.92880E-01
opls_1033	C1033	12.0110	0.000	A	3.50000E-01	2.76144E-01
opls_1039	C1039	12.0110	0.000	A	3.55000E-01	3.17984E-01
opls_1003	H1003	1.0080	0.000	A	2.42000E-01	1.25520E-01
opls_1054	C1054	12.0110	0.000	A	3.55000E-01	3.17984E-01
opls_1010	H1010	1.0080	0.000	A	2.42000E-01	1.25520E-01
opls_1023	H1023	1.0080	0.000	A	2.50000E-01	1.25520E-01
opls_1002	C1002	12.0110	0.000	A	3.55000E-01	2.92880E-01
opls_1030	C1030	12.0110	0.000	A	3.55000E-01	3.17984E-01
opls_1027	H1027	1.0080	0.000	A	2.42000E-01	1.25520E-01
opls_1042	H1042	1.0080	0.000	A	2.42000E-01	1.25520E-01
opls_1015	C1015	12.0110	0.000	A	3.55000E-01	2.92880E-01
opls_1020	C1020	12.0110	0.000	A	3.50000E-01	2.76144E-01
opls_1032	N1032	14.0070	0.000	A	3.25000E-01	7.11280E-01
opls_1000	C1000	12.0110	0.000	A	3.55000E-01	2.92880E-01
opls_1009	C1009	12.0110	0.000	A	3.55000E-01	2.92880E-01
opls_1005	C1005	12.0110	0.000	A	3.50000E-01	2.76144E-01
opls_1045	C1045	12.0110	0.000	A	3.55000E-01	3.17984E-01
opls_1025	H1025	1.0080	0.000	A	2.42000E-01	1.25520E-01
opls_1001	H1001	1.0080	0.000	A	2.42000E-01	1.25520E-01
opls_1049	H1049	1.0080	0.000	A	2.50000E-01	1.25520E-01
opls_1011	N1011	14.0070	0.000	A	3.25000E-01	7.11280E-01
opls_1028	C1028	12.0110	0.000	A	3.55000E-01	2.92880E-01
opls_1022	H1022	1.0080	0.000	A	2.50000E-01	1.25520E-01
opls_1014	H1014	1.0080	0.000	A	2.42000E-01	1.25520E-01
opls_1044	N1044	14.0070	0.000	A	3.25000E-01	7.11280E-01

Topology file for [BMIM]$^+$ (C4)

Bonded parameters

```
[  moleculetype  ]
;    name    nrexcl
C4    3

[  atoms  ]
;  nr    type resnr residu atom  cgnr   charge    mass
1     opls_801    1    C4    N02    1    0.176     14.007
2     opls_802    1    C4    N00    2    0.176     14.007
3     opls_803    1    C4    C01    3    -0.072    12.011
4     opls_804    1    C4    H07    3    0.168     1.008
5     opls_805    1    C4    C04    4    -0.192    12.011
6     opls_806    1    C4    H09    4    0.216     1.008
7     opls_807    1    C4    C03    5    -0.192    12.011
8     opls_808    1    C4    H08    5    0.216     1.008
9     opls_810    1    C4    C05    6    -0.28     12.011
10    opls_811    1    C4    H0B    6    0.144     1.008
11    opls_812    1    C4    H0C    6    0.144     1.008
12    opls_813    1    C4    H0D    6    0.144     1.008
13    opls_814    1    C4    C06    7    -0.136    12.011
14    opls_815    1    C4    H0E    7    0.144     1.008
15    opls_816    1    C4    H0F    7    0.144     1.008
16    opls_817    1    C4    C0G    8    -0.096    12.011
17    opls_818    1    C4    H0H    8    0.048     1.008
18    opls_819    1    C4    H0I    8    0.048     1.008
19    opls_820    1    C4    C0J    9    -0.096    12.011
20    opls_821    1    C4    H0K    9    0.048     1.008
21    opls_822    1    C4    H0M    9    0.048     1.008
22    opls_823    1    C4    C0N    10    -0.192   12.011
23    opls_824    1    C4    H0O    10    0.064    1.008
24    opls_825    1    C4    H0P    10    0.064    1.008
25    opls_826    1    C4    H0Q    10    0.064    1.008

[  bonds  ]
;   ai    aj funct   c0(nm)    c1(kJ mol-1 nm-2) ro(Ang.)  kr(kcal mol-1 Ang.-2)
1     3     1    0.1315    399153.6    ;    1.315    477    NA-CR
1     5     1    0.1378    357313.6    ;    1.378    427    NA-CW
1     13    1    0.1476    282001.6    ;    1.476    337    NA-CA
2     3     1    0.1315    399153.6    ;    1.315    477    NA-CR
2     7     1    0.1378    357313.6    ;    1.378    427    NA-CW
2     9     1    0.1465    282001.6    ;    1.465    337    NA-CM
3     4     1    0.1069    307105.6    ;    1.069    367    CR-HR
5     6     1    0.1068    307105.6    ;    1.068    367    CW-HW
5     7     1    0.1336    435136.0    ;    1.336    520    CW-CW
7     8     1    0.1068    307105.6    ;    1.068    367    CW-HW
9     10    1    0.1080    284512.0    ;    1.08     340    CM-HM
9     11    1    0.1080    284512.0    ;    1.08     340    CM-HM
9     12    1    0.1080    284512.0    ;    1.08     340    CM-HM
13    14    1    0.1080    284512.0    ;    1.08     340    CA-HA
13    15    1    0.1080    284512.0    ;    1.08     340    CA-HA
13    16    1    0.1526    224262.4    ;    1.526    268    CA-CS
16    17    1    0.1087    284512.0    ;    1.087    340    CS-HS
16    18    1    0.1087    284512.0    ;    1.087    340    CS-HS
16    19    1    0.1531    224262.4    ;    1.531    268    CS-CS
19    20    1    0.1087    284512.0    ;    1.087    340    CS-HS
19    21    1    0.1087    284512.0    ;    1.087    340    CS-HS
19    22    1    0.1528    224262.4    ;    1.528    268    CS-CT
22    23    1    0.1084    284512.0    ;    1.084    340    CT-HT
22    24    1    0.1084    284512.0    ;    1.084    340    CT-HT
22    25    1    0.1084    284512.0    ;    1.084    340    CT-HT

[  angles  ]
;   ai    aj    ak funct c0(deg)  c1(kJ mol-1 rad-2) c0(deg) c1(kcal mol-1 rad-2)
1     3     2     1    109.80    585.76    ;    109.8    70        NA-CR-NA
1     3     4     1    125.10    292.88    ;    125.1    35        NA-CR-HR
1     5     6     1    122.00    292.88    ;    122      35        NA-CW-HW
1     5     7     1    107.10    585.76    ;    107.1    70        NA-CW-CW
1     13    14    1    107.50    313.80    ;    107.5    37.5      NA-CA-HA
1     13    15    1    107.50    313.80    ;    107.5    37.5      NA-CA-HA
1     13    16    1    113.00    488.27    ;    113      58.35     NA-CA-CS
2     3     4     1    125.10    292.88    ;    125.1    35        NA-CR-HR
2     7     5     1    107.10    585.76    ;    107.1    70        NA-CW-CW
2     7     8     1    122.00    292.88    ;    122      35        NA-CW-HW
```

```
2     9     10    1    109.20    313.80    ;    109.2    37.5       NA-CM-HM
2     9     11    1    109.20    313.80    ;    109.2    37.5       NA-CM-HM
2     9     12    1    109.20    313.80    ;    109.2    37.5       NA-CM-HM
5     1     3     1    107.90    585.76    ;    107.9    70         CW-NA-CR
5     7     8     1    130.90    292.88    ;    130.9    35         CW-CW-HW
7     2     3     1    107.90    585.76    ;    107.9    70         CW-NA-CR
7     5     6     1    130.90    292.88    ;    130.9    35         CW-CW-HW
9     2     3     1    126.40    585.76    ;    126.4    70         CM-NA-CR
9     2     7     1    125.60    585.76    ;    125.6    70         CM-NA-CW
11    9     10    1    109.80    276.14    ;    109.8    33         HM-CM-HM
12    9     10    1    109.80    276.14    ;    109.8    33         HM-CM-HM
12    9     11    1    109.80    276.14    ;    109.8    33         HM-CM-HM
13    1     3     1    126.80    585.76    ;    126.8    70         CA-NA-CR
13    1     5     1    125.30    585.76    ;    125.3    70         CA-NA-CW
13    16    17    1    108.60    313.80    ;    108.6    37.5       CA-CS-HS
13    16    18    1    108.60    313.80    ;    108.6    37.5       CA-CS-HS
13    16    19    1    113.30    488.27    ;    113.3    58.35      CA-CS-CS
14    13    15    1    108.90    276.14    ;    108.9    33         HA-CA-HA
14    13    16    1    111.10    313.80    ;    111.1    37.5       HA-CA-CS
15    13    16    1    111.10    313.80    ;    111.1    37.5       HA-CA-CS
16    19    20    1    109.60    313.80    ;    109.6    37.5       CS-CS-HS
16    19    21    1    109.60    313.80    ;    109.6    37.5       CS-CS-HS
16    19    22    1    112.30    488.27    ;    112.3    58.35      CS-CS-CT
17    16    18    1    106.70    276.14    ;    106.7    33         HS-CS-HS
19    16    17    1    109.60    313.80    ;    109.6    37.5       CS-CS-HS
19    16    18    1    109.60    313.80    ;    109.6    37.5       CS-CS-HS
19    22    23    1    111.10    313.80    ;    111.1    37.5       CS-CT-HT
19    22    24    1    111.10    313.80    ;    111.1    37.5       CS-CT-HT
19    22    25    1    111.10    313.80    ;    111.1    37.5       CS-CT-HT
21    19    20    1    106.70    276.14    ;    106.7    33         HS-CS-HS
22    19    20    1    109.70    313.80    ;    109.7    37.5       CT-CS-HS
22    19    21    1    109.70    313.80    ;    109.7    37.5       CT-CS-HS
24    22    23    1    107.90    276.14    ;    107.9    33         HT-CT-HT
25    22    23    1    107.90    276.14    ;    107.9    33         HT-CT-HT
25    22    24    1    107.90    276.14    ;    107.9    33         HT-CT-HT

[  dihedrals  ]
;   ai    aj    ak    al funct    c0        c1       c2      c3(kJ/mol)      v1    v2       v3     v4 (kcal/mol)
1     5     7     2     5    0.000    44.980   0.000    0.000    ;    0    10.75     0     0     NA-CW-CW-NA
1     5     7     8     5    0.000    44.980   0.000    0.000    ;    0    10.75     0     0     NA-CW-CW-HW
1     13    16    17    5    0.000    0.000    0.000    0.000    ;    0     0        0     0     NA-CA-CS-HS
1     13    16    18    5    0.000    0.000    0.000    0.000    ;    0     0        0     0     NA-CA-CS-HS
1     13    16    19    5   -3.297    3.347    1.674    0.000    ;  -0.788 0.8     0.4    0     NA-CA-CS-CS
3     1     5     6     5    0.000    12.552   0.000    0.000    ;    0     3        0     0     CR-NA-CW-HW
3     1     5     7     5    0.000    12.552   0.000    0.000    ;    0     3        0     0     CR-NA-CW-CW
3     1     13    14    5    0.000    0.000    0.000    0.000    ;    0     0        0     0     CR-NA-CA-HA
3     1     13    15    5    0.000    0.000    0.000    0.000    ;    0     0        0     0     CR-NA-CA-HA
3     1     13    16    5   -0.665    0.397   -0.042    0.000    ;  -0.159 0.095 -0.01   0     CR-NA-CA-CS
3     2     7     5     5    0.000    12.552   0.000    0.000    ;    0     3        0     0     CR-NA-CW-CW
3     2     7     8     5    0.000    12.552   0.000    0.000    ;    0     3        0     0     CR-NA-CW-HW
3     2     9     10    5    0.000    0.000    0.000    0.000    ;    0     0        0     0     CR-NA-CM-HM
3     2     9     11    5    0.000    0.000    0.000    0.000    ;    0     0        0     0     CR-NA-CM-HM
3     2     9     12    5    0.000    0.000    0.000    0.000    ;    0     0        0     0     CR-NA-CM-HM
5     1     3     2     5    0.000    19.460   0.000    0.000    ;    0    4.651     0     0     CW-NA-CR-NA
5     1     3     4     5    0.000    19.460   0.000    0.000    ;    0    4.651     0     0     CW-NA-CR-HR
5     1     13    14    5  -11.297   -23.640   1.485    0.000    ;  -2.7   -5.65   0.355   0     CW-NA-CA-HA
5     1     13    15    5  -11.297   -23.640   1.485    0.000    ;  -2.7   -5.65   0.355   0     CW-NA-CA-HA
5     1     13    16    5  -8.828    -20.920   1.443    0.000    ;  -2.11  -5      0.345   0     CW-NA-CA-CS
6     5     7     2     5    0.000     44.978   0.000    0.000    ;    0     10.75     0     0     HW-CW-CW-NA
6     5     7     8     5    0.000     44.978   0.000    0.000    ;    0     10.75     0     0     HW-CW-CW-HW
7     2     3     1     5    0.000    19.460   0.000    0.000    ;    0    4.651     0     0     CW-NA-CR-NA
7     2     3     4     5    0.000    19.460   0.000    0.000    ;    0    4.651     0     0     CW-NA-CR-HR
7     2     9     10    5    0.000    0.000    0.519    0.000    ;    0     0      0.124   0     CW-NA-CM-HM
7     2     9     11    5    0.000    0.000    0.519    0.000    ;    0     0      0.124   0     CW-NA-CM-HM
7     2     9     12    5    0.000    0.000    0.519    0.000    ;    0     0      0.124   0     CW-NA-CM-HM
9     2     3     1     5    0.000    19.460   0.000    0.000    ;    0    4.651     0     0     CM-NA-CR-NA
9     2     3     4     5    0.000    19.460   0.000    0.000    ;    0    4.651     0     0     CM-NA-CR-HR
9     2     7     5     5    0.000    12.552   0.000    0.000    ;    0     3        0     0     CM-NA-CW-CW
9     2     7     8     5    0.000    12.552   0.000    0.000    ;    0     3        0     0     CM-NA-CW-HW
13    1     3     2     5    0.000    19.460   0.000    0.000    ;    0    4.651     0     0     CA-NA-CR-NA
13    1     3     4     5    0.000    19.460   0.000    0.000    ;    0    4.651     0     0     CA-NA-CR-HR
13    1     5     6     5    0.000    12.552   0.000    0.000    ;    0     3        0     0     CA-NA-CW-HW
13    1     5     7     5    0.000    12.552   0.000    0.000    ;    0     3        0     0     CA-NA-CW-CW
13    16    19    20    5    0.000    0.000    1.531    0.000    ;    0     0      0.366   0     CA-CS-CS-HS
13    16    19    21    5    0.000    0.000    1.531    0.000    ;    0     0      0.366   0     CA-CS-CS-HS
13    16    19    22    5    5.439   -0.209    0.837    0.000    ;   1.3  -0.05     0.2    0     CA-CS-CS-CT
14    13    16    17    5    0.000   -0.628    2.167    0.000    ;    0   -0.15   0.518   0     HA-CA-CS-HS
```

```
14    13    16    18    5    0.000   -0.628    2.167    0.000    ;    0   -0.15  0.518   0    HA-CA-CS-HS
14    13    16    19    5    0.000    0.000    1.531    0.000    ;    0    0     0.366   0    HA-CA-CS-CS
15    13    16    17    5    0.000   -0.628    2.167    0.000    ;    0   -0.15  0.518   0    HA-CA-CS-HS
15    13    16    18    5    0.000   -0.628    2.167    0.000    ;    0   -0.15  0.518   0    HA-CA-CS-HS
15    13    16    19    5    0.000    0.000    1.531    0.000    ;    0    0     0.366   0    HA-CA-CS-CS
16    19    22    23    5    0.000    0.000    1.531    0.000    ;    0    0     0.366   0    CS-CS-CT-HT
16    19    22    24    5    0.000    0.000    1.531    0.000    ;    0    0     0.366   0    CS-CS-CT-HT
16    19    22    25    5    0.000    0.000    1.531    0.000    ;    0    0     0.366   0    CS-CS-CT-HT
17    16    19    20    5    0.000    0.000    1.331    0.000    ;    0    0     0.318   0    HS-CS-CS-HS
17    16    19    21    5    0.000    0.000    1.331    0.000    ;    0    0     0.318   0    HS-CS-CS-HS
17    16    19    22    5    0.000    0.000    1.531    0.000    ;    0    0     0.366   0    HS-CS-CS-CT
18    16    19    20    5    0.000    0.000    1.331    0.000    ;    0    0     0.318   0    HS-CS-CS-HS
18    16    19    21    5    0.000    0.000    1.331    0.000    ;    0    0     0.318   0    HS-CS-CS-HS
18    16    19    22    5    0.000    0.000    1.531    0.000    ;    0    0     0.366   0    HS-CS-CS-CT
20    19    22    23    5    0.000    0.000    1.331    0.000    ;    0    0     0.318   0    HS-CS-CT-HT
20    19    22    24    5    0.000    0.000    1.331    0.000    ;    0    0     0.318   0    HS-CS-CT-HT
20    19    22    25    5    0.000    0.000    1.331    0.000    ;    0    0     0.318   0    HS-CS-CT-HT
21    19    22    23    5    0.000    0.000    1.331    0.000    ;    0    0     0.318   0    HS-CS-CT-HT
21    19    22    24    5    0.000    0.000    1.331    0.000    ;    0    0     0.318   0    HS-CS-CT-HT
21    19    22    25    5    0.000    0.000    1.331    0.000    ;    0    0     0.318   0    HS-CS-CT-HT
9     2     3     7     5    0.000    8.368    0.000    0.000    ;    0    2       0     0    CM-NA-CR-CW  improper
13    1     3     5     5    0.000    8.368    0.000    0.000    ;    0    2       0     0    CA-NA-CR-CW  improper
6     5     1     7     5    0.000    9.205    0.000    0.000    ;    0    2.2     0     0    HW-CW-NA-CW  improper
8     7     2     5     5    0.000    9.205    0.000    0.000    ;    0    2.2     0     0    HW-CW-NA-CW  improper
4     3     2     1     5    0.000    9.205    0.000    0.000    ;    0    2.2     0     0    HR-CR-NA-NA  improper
```

Nonbonded parameters

```
[  atomtypes  ]
opls_803    C01       12.011    0.000   A    0.355    0.292880    ;    3.55    0.07
opls_801    N02       14.007    0.000    A    0.325    0.711280    ;    3.25    0.17
opls_802    N00       14.007    0.000    A    0.325    0.711280    ;    3.25    0.17
opls_805    C04       12.011    0.000    A    0.355    0.292880    ;    3.55    0.07
opls_807    C03       12.011    0.000    A    0.355    0.292880    ;    3.55    0.07
opls_804    H07       1.008     0.000    A    0.242    0.125520    ;    2.42    0.03
opls_806    H09       1.008     0.000    A    0.242    0.125520    ;    2.42    0.03
opls_808    H08       1.008     0.000    A    0.242    0.125520    ;    2.42    0.03
opls_810    C05       12.011    0.000    A    0.350    0.276144    ;    3.5     0.066
opls_811    H0B       1.008     0.000    A    0.250    0.125520    ;    2.5     0.03
opls_812    H0C       1.008     0.000    A    0.250    0.125520    ;    2.5     0.03
opls_813    H0D       1.008     0.000    A    0.250    0.125520    ;    2.5     0.03
opls_814    C06       12.011    0.000    A    0.350    0.276144    ;    3.5     0.066
opls_815    H0E       1.008     0.000    A    0.250    0.125520    ;    2.5     0.03
opls_816    H0F       1.008     0.000    A    0.250    0.125520    ;    2.5     0.03
opls_817    C0G       12.011    0.000    A    0.350    0.276144    ;    3.5     0.066
opls_820    C0J       12.011    0.000    A    0.350    0.276144    ;    3.5     0.066
opls_818    H0H       1.008     0.000    A    0.250    0.125520    ;    2.5     0.03
opls_819    H0I       1.008     0.000    A    0.250    0.125520    ;    2.5     0.03
opls_821    H0K       1.008     0.000    A    0.250    0.125520    ;    2.5     0.03
opls_822    H0M       1.008     0.000    A    0.250    0.125520    ;    2.5     0.03
opls_823    C0N       12.011    0.000    A    0.350    0.276144    ;    3.5     0.066
opls_824    H0O       1.008     0.000    A    0.250    0.125520    ;    2.5     0.03
opls_825    H0P       1.008     0.000    A    0.250    0.125520    ;    2.5     0.03
opls_826    H0Q       1.008     0.000    A    0.250    0.125520    ;    2.5     0.03
```

Topology file for [EMIM]$^+$ (C5)

Bonded parameters

```
[  moleculetype  ]
;    name    nrexcl
C5    3

[  atoms  ]
;   nr   type resnr residu atom  cgnr   charge     mass
1     epls_801    1    C5    C01    1    -0.072    12.011
2     epls_802    1    C5    C04    2    -0.192    12.011
3     epls_803    1    C5    C03    3    -0.192    12.011
4     epls_804    1    C5    H07    1    0.168     1.008
5     epls_805    1    C5    H09    2    0.216     1.008
6     epls_806    1    C5    H08    3    0.216     1.008
7     epls_807    1    C5    C05    4    -0.280    12.011
8     epls_808    1    C5    H0B    4    0.144     1.011
9     epls_809    1    C5    H0C    4    0.144     1.011
10    epls_810    1    C5    H0D    4    0.144     1.011
11    epls_811    1    C5    N00    5    0.176     14.007
12    epls_812    1    C5    C06    6    -0.136    12.011
13    epls_813    1    C5    H0F    6    0.144     1.011
14    epls_814    1    C5    C0N    7    -0.192    12.011
15    epls_815    1    C5    H0O    7    0.064     1.011
16    epls_816    1    C5    H0P    7    0.064     1.011
17    epls_817    1    C5    H0Q    7    0.064     1.011
18    epls_818    1    C5    N02    8    0.176     14.007
19    epls_819    1    C5    H0E    6    0.144     1.011

[  bonds  ]
;   ai    aj  funct  c0(nm)  c1(kJ mol-1 nm-2)  ro(Ang.)  kr(kcal mol-1 Ang.-2)
1     11    1    0.1315    399153.6    ;    1.315    477        CR-NA
1     18    1    0.1315    399153.6    ;    1.315    477        CR-NA
7     8     1    0.1080    284512.0    ;    1.08     340        CM-HM
7     9     1    0.1080    284512.0    ;    1.08     340        CM-HM
7     10    1    0.1080    284512.0    ;    1.08     340        CM-HM
7     11    1    0.1465    282001.6    ;    1.465    337        CM-NA
1     4     1    0.1069    307105.6    ;    1.069    367        CR-HR
2     18    1    0.1378    357313.6    ;    1.378    427        CW-NA
3     11    1    0.1378    357313.6    ;    1.378    427        CW-NA
2     3     1    0.1336    435136.0    ;    1.336    520        CW-CW
2     5     1    0.1068    307105.6    ;    1.068    367        CW-HW
3     6     1    0.1068    307105.6    ;    1.068    367        CW-HW
18    12    1    0.1476    282001.6    ;    1.476    337        NA-CA
12    13    1    0.1080    284512.0    ;    1.08     340        CA-HA
12    19    1    0.1080    284512.0    ;    1.08     340        CA-HA
12    14    1    0.1521    224262.4    ;    1.521    268        CA-CT
14    15    1    0.1084    284512.0    ;    1.084    340        CT-HT
14    16    1    0.1084    284512.0    ;    1.084    340        CT-HT
14    17    1    0.1084    284512.0    ;    1.084    340        CT-HT

[  angles  ]
;   ai    aj    ak  funct  c0(deg) c1(kJ mol-1 rad-2) c0(deg) c1(kcal mol-1 rad-2)
8     7     9     1    109.8    276.14    ;    109.8    33    HM-CM-HM
8     7     10    1    109.8    276.14    ;    109.8    33    HM-CM-HM
9     7     10    1    109.8    276.14    ;    109.8    33    HM-CM-HM
8     7     11    1    109.2    313.80    ;    109.2    37.5  HM-CM-NA
9     7     11    1    109.2    313.80    ;    109.2    37.5  HM-CM-NA
10    7     11    1    109.2    313.80    ;    109.2    37.5  HM-CM-NA
7     11    1     1    126.4    585.76    ;    126.4    70    CM-NA-CR
7     11    3     1    125.6    585.76    ;    125.6    70    CM-NA-CW
11    1     4     1    125.1    292.88    ;    125.1    35    NA-CR-HR
18    1     4     1    125.1    292.88    ;    125.1    35    NA-CR-HR
11    1     18    1    109.8    585.76    ;    109.8    70    NA-CR-NA
1     11    3     1    107.9    585.76    ;    107.9    70    CR-NA-CW
1     18    2     1    107.9    585.76    ;    107.9    70    CR-NA-CW
11    3     2     1    107.1    585.76    ;    107.1    70    NA-CW-CW
18    2     3     1    107.1    585.76    ;    107.1    70    NA-CW-CW
11    3     6     1    122.0    292.88    ;    122      35    NA-CW-HW
18    2     5     1    122.0    292.88    ;    122      35    NA-CW-HW
6     3     2     1    130.9    292.88    ;    130.9    35    HW-CW-CW
5     2     3     1    130.9    292.88    ;    130.9    35    HW-CW-CW
2     18    12    1    125.3    585.76    ;    125.3    70    CW-NA-CA
1     18    12    1    126.8    585.76    ;    126.8    70    CR-NA-CA
18    12    13    1    107.5    313.80    ;    107.5    37.5  NA-CA-HA
```

```
18    12    19    1    107.5    313.80    ;    107.5    37.5  NA-CA-HA
19    12    14    1    111.2    313.80    ;    111.2    37.5  HA-CA-CT
13    12    14    1    111.2    313.80    ;    111.2    37.5  HA-CA-CT
13    12    19    1    108.9    276.14    ;    108.9    33    HA-CA-HA
12    14    15    1    110.7    313.80    ;    110.7    37.5  CA-CT-HT
12    14    16    1    110.7    313.80    ;    110.7    37.5  CA-CT-HT
12    14    17    1    110.7    313.80    ;    110.7    37.5  CA-CT-HT
15    14    16    1    107.9    276.14    ;    107.9    33    HT-CT-HT
15    14    17    1    107.9    276.14    ;    107.9    33    HT-CT-HT
16    14    17    1    107.9    276.14    ;    107.9    33    HT-CT-HT
18    12    14    1    112.6    488.27    ;    112.6    58.35 NA-CA-CT

[  dihedrals  ]
;   ai    aj    ak    al funct     c0      c1       c2    c3(kJ/mol)  ;    V1       V2       V3       V4  (kcal/mol)
8     7     11    1     5    0.000    0.000     0.000    0.000    ;    0        0        0        0    HM-CM-NA-CR
9     7     11    1     5    0.000    0.000     0.000    0.000    ;    0        0        0        0    HM-CM-NA-CR
10    7     11    1     5    0.000    0.000     0.000    0.000    ;    0        0        0        0    HM-CM-NA-CR
8     7     11    3     5    0.000    0.000     0.519    0.000    ;    0        0       0.124     0    HM-CM-NA-CW
9     7     11    3     5    0.000    0.000     0.519    0.000    ;    0        0       0.124     0    HM-CM-NA-CW
10    7     11    3     5    0.000    0.000     0.519    0.000    ;    0        0       0.124     0    HM-CM-NA-CW
7     11    1     4     5    0.000    19.460    0.000    0.000    ;    0       4.651     0        0    CM-NA-CR-HR
7     11    1     18    5    0.000    19.460    0.000    0.000    ;    0       4.651     0        0    CM-NA-CR-NA
7     11    3     2     5    0.000    12.552    0.000    0.000    ;    0        3        0        0    CM-NA-CW-CW
7     11    3     6     5    0.000    12.552    0.000    0.000    ;    0        3        0        0    CM-NA-CW-HW
11    1     18    12    5    0.000    19.460    0.000    0.000    ;    0       4.651     0        0    NA-CR-NA-CA
11    3     2     5     5    0.000    44.978    0.000    0.000    ;    0      10.75      0        0    NA-CW-CW-HW
18    2     3     6     5    0.000    44.978    0.000    0.000    ;    0      10.75      0        0    NA-CW-CW-HW
11    3     2     18    5    0.000    44.978    0.000    0.000    ;    0      10.75      0        0    NA-CW-CW-NA
4     1     11    3     5    0.000    19.460    0.000    0.000    ;    0       4.651     0        0    HR-CR-NA-CW
4     1     18    2     5    0.000    19.460    0.000    0.000    ;    0       4.651     0        0    HR-CR-NA-CW
1     11    3     6     5    0.000    12.552    0.000    0.000    ;    0        3        0        0    CR-NA-CW-HW
1     18    2     5     5    0.000    12.552    0.000    0.000    ;    0        3        0        0    CR-NA-CW-HW
1     11    3     2     5    0.000    12.552    0.000    0.000    ;    0        3        0        0    CR-NA-CW-CW
1     18    2     3     5    0.000    12.552    0.000    0.000    ;    0        3        0        0    CR-NA-CW-CW
4     1     18    12    5    0.000    19.460    0.000    0.000    ;    0       4.651     0        0    HR-CR-NA-CA
5     2     18    12    5    0.000    12.552    0.000    0.000    ;    0        3        0        0    HW-CW-NA-CA
3     2     18    12    5    0.000    12.552    0.000    0.000    ;    0        3        0        0    CW-CW-NA-CA
1     18    12    13    5    0.000    0.000     0.000    0.000    ;    0        0        0        0    CR-NA-CA-HA
1     18    12    19    5    0.000    0.000     0.000    0.000    ;    0        0        0        0    CR-NA-CA-HA
13    12    14    15    5    0.000    0.000     1.331    0.000    ;    0        0       0.318     0    HA-CA-CT-HT
13    12    14    16    5    0.000    0.000     1.331    0.000    ;    0        0       0.318     0    HA-CA-CT-HT
13    12    14    17    5    0.000    0.000     1.331    0.000    ;    0        0       0.318     0    HA-CA-CT-HT
19    12    14    15    5    0.000    0.000     1.331    0.000    ;    0        0       0.318     0    HA-CA-CT-HT
19    12    14    16    5    0.000    0.000     1.331    0.000    ;    0        0       0.318     0    HA-CA-CT-HT
19    12    14    17    5    0.000    0.000     1.331    0.000    ;    0        0       0.318     0    HA-CA-CT-HT
5     2     3     6     5    0.000    44.978    0.000    0.000    ;    0      10.75      0        0    HW-CW-CW-HW
3     11    1     18    5    0.000    19.460    0.000    0.000    ;    0       4.651     0        0    CW-NA-CR-NA
2     18    1     11    5    0.000    19.460    0.000    0.000    ;    0       4.651     0        0    CW-NA-CR-NA
1     18    12    14    5  -8.368    -1.151    -6.904    0.000    ;   -2      -0.275   -1.65     0    CR-NA-CA-CT
2     18    12    13    5  -11.297    23.640    1.485    0.000    ;   -2.7     5.65     0.355     0    CW-NA-CA-HA
2     18    12    14    5  -18.221   -19.142   -5.753    0.000    ;   -4.355  -4.575   -1.375     0    CW-NA-CA-CT
2     18    12    19    5  -11.297   23.640    1.485    0.000    ;   -2.7     5.65     0.355     0    CW-NA-CA-HA
18    12    14    15    5    0.000    0.000     0.000    0.000    ;    0        0        0        0    NA-CA-CT-HT
18    12    14    16    5    0.000    0.000     0.000    0.000    ;    0        0        0        0    NA-CA-CT-HT
18    12    14    17    5    0.000    0.000     0.000    0.000    ;    0        0        0        0    NA-CA-CT-HT
7     11    1     3     5    0.000    8.368     0.000    0.000    ;    0        2        0        0    CM-NA-CR-CW
improper
12    18    1     2     5    0.000    8.368     0.000    0.000    ;    0        2        0        0    CA-NA-CR-CW
improper
5     2     18    3     5    0.000    9.205     0.000    0.000    ;    0       2.20      0        0    HW-CW-NA-CW
improper
6     3     11    2     5    0.000    9.205     0.000    0.000    ;    0       2.20      0        0    HW-CW-NA-CW
improper
4     1     11    18    5    0.000    9.205     0.000    0.000    ;    0       2.20      0        0    HR-CR-NA-NA
improper
```

Nonbonded parameters

```
[  atomtypes  ]
;  type    mass     charge  ptype sigma(nm) epsilon(kJ/mol) sigma(Ang.) epsilon (kcal/mol)
epls_801    C01              12.011    0.000    A    0.355    0.292880    ;    3.55    0.07
epls_811    N00              14.007    0.000    A    0.325    0.711280    ;    3.25    0.17
epls_818    N02              14.007    0.000    A    0.325    0.711280    ;    3.25    0.17
epls_802    C04              12.011    0.000    A    0.355    0.292880    ;    3.55    0.07
epls_803    C03              12.011    0.000    A    0.355    0.292880    ;    3.55    0.07
epls_804    H07              1.008     0.000    A    0.242    0.125520    ;    2.42    0.03
epls_805    H09              1.008     0.000    A    0.242    0.125520    ;    2.42    0.03
```

```
epls_806    H08             1.008     0.000    A    0.242    0.125520    ;    2.42    0.03
epls_807    C05             12.011    0.000    A    0.350    0.276144    ;    3.5     0.066
epls_808    H0B             1.008     0.000    A    0.250    0.125520    ;    2.5     0.03
epls_809    H0C             1.008     0.000    A    0.250    0.125520    ;    2.5     0.03
epls_810    H0D             1.008     0.000    A    0.250    0.125520    ;    2.5     0.03
epls_812    C06             12.011    0.000    A    0.350    0.276144    ;    3.5     0.066
epls_813    H0F             1.008     0.000    A    0.250    0.125520    ;    2.5     0.03
epls_819    H0E             1.008     0.000    A    0.250    0.125520    ;    2.5     0.03
epls_814    C0N             12.011    0.000    A    0.350    0.276144    ;    3.5     0.066
epls_815    H0O             1.008     0.000    A    0.250    0.125520    ;    2.5     0.03
epls_816    H0P             1.008     0.000    A    0.250    0.125520    ;    2.5     0.03
epls_817    H0Q             1.008     0.000    A    0.250    0.125520    ;    2.5     0.03
```

Topology file for [HMIM]$^+$ (C6)

Bonded parameters

```
[  moleculetype  ]
;    name    nrexcl
C6    3

[  atoms  ]
;   nr  type  resnr residu atom  cgnr    charge    mass
1     lpls_801    1    C6    N02    1     0.176    14.007
2     lpls_802    1    C6    N00    2     0.176    14.007
3     lpls_803    1    C6    C01    3    -0.072    12.011
4     lpls_804    1    C6    H07    3     0.168    1.008
5     lpls_805    1    C6    C04    4    -0.192    12.011
6     lpls_806    1    C6    H09    4     0.216    1.008
7     lpls_807    1    C6    C03    5    -0.192    12.011
8     lpls_808    1    C6    H08    5     0.216    1.008
9     lpls_809    1    C6    C05    6     -0.28    12.011
10    lpls_810    1    C6    H0B    6     0.144    1.008
11    lpls_811    1    C6    H0C    6     0.144    1.008
12    lpls_812    1    C6    H0D    6     0.144    1.008
13    lpls_813    1    C6    C06    7    -0.130    12.011
14    lpls_814    1    C6    H0E    7     0.144    1.008
15    lpls_815    1    C6    H0F    7     0.144    1.008
16    lpls_816    1    C6    C0G    8    -0.096    12.011
17    lpls_817    1    C6    H0H    8     0.048    1.008
18    lpls_818    1    C6    H0I    8     0.048    1.008
19    lpls_819    1    C6    C0J    9    -0.096    12.011
20    lpls_820    1    C6    H0K    9     0.048    1.008
21    lpls_821    1    C6    H0M    9     0.048    1.008
22    lpls_822    1    C6    C0N    10   -0.096    12.011
23    lpls_823    1    C6    H0O    10    0.048    1.008
24    lpls_824    1    C6    H0P    10    0.048    1.008
25    lpls_825    1    C6    C0Q    11   -0.096    12.011
26    lpls_826    1    C6    H0R    11    0.048    1.008
27    lpls_827    1    C6    H0S    11    0.048    1.008
28    lpls_828    1    C6    C0Z    14   -0.192    12.011
29    lpls_829    1    C6    H00    14    0.064    1.008
30    lpls_830    1    C6    H01    14    0.064    1.008
31    lpls_831    1    C6    H02    14    0.064    1.008

[  bonds  ]
;   ai    aj  funct  c0 (nm) c1(kJ mol-1 nm-2) ro(Ang.)  kr(kcal mol-1 Ang.-2)
3     1     1    0.1315    399153.6    ;    1.315    477    CR-NA
3     2     1    0.1315    299153.6    ;    1.315    297.5  CR-NA
9     10    1    0.1080    284512.0    ;    1.08     280    HM-CM
9     11    1    0.1080    284512.0    ;    1.08     280    HM-CM
9     12    1    0.1080    284512.0    ;    1.08     280    HM-CM
2     9     1    0.1465    282001.6    ;    1.465    331    NA-CM
3     4     1    0.1069    307105.6    ;    1.069    307    CR-HR
7     2     1    0.1318    297313.6    ;    1.318    427    CW-NA
5     1     1    0.1318    297313.6    ;    1.318    427    CW-NA
7     5     1    0.1330    429130.0    ;    1.330    520    CW-CW
7     8     1    0.1068    307105.6    ;    1.068    307    CW-HW
5     6     1    0.1068    307105.6    ;    1.068    307    CW-HW
1     13    1    0.1476    282001.6    ;    1.476    331    NA-CA
13    14    1    0.1080    284512.0    ;    1.08     280    CA-HA
13    15    1    0.1080    284512.0    ;    1.08     280    CA-HA
13    16    1    0.1526    224262.4    ;    1.526    268    CA-HA
16    17    1    0.1087    284512.0    ;    1.087    280    CS-HS
16    18    1    0.1087    284512.0    ;    1.087    280    CS-HS
16    19    1    0.1531    224262.4    ;    1.531    268    CS-CS
19    20    1    0.1087    284512.0    ;    1.087    280    CS-HS
19    21    1    0.1087    284512.0    ;    1.087    280    CS-HS
19    22    1    0.1531    224262.4    ;    1.531    268    CS-CS
22    23    1    0.1087    284512.0    ;    1.087    280    CS-HS
22    24    1    0.1087    284512.0    ;    1.087    280    CS-HS
22    25    1    0.1531    224262.4    ;    1.531    268    CS-CS
25    26    1    0.1087    284512.0    ;    1.087    280    CS-HS
25    27    1    0.1087    284512.0    ;    1.087    280    CS-HS
25    28    1    0.1087    284512.0    ;    1.087    280    CS-HS
28    29    1    0.1084    284512.0    ;    1.084    280    CT-HT
28    30    1    0.1084    284512.0    ;    1.084    280    CT-HT
28    31    1    0.1084    284512.0    ;    1.084    280    CT-HT
```

```
[  angles  ]
;   ai    aj    ak  funct  c0(deg) c1(kJ mol-1 rad-2) c0(deg) c1(kcal mol-1 rad-2)
10    9     11    1    109.8    276.144    ;    109.8    33      HM-CM-HM
10    9     12    1    109.8    276.144    ;    109.8    33      HM-CM-HM
11    9     12    1    109.8    276.144    ;    109.8    33      HM-CM-HM
10    9     2     1    109.2    313.800    ;    109.2    31.5    HM-CM-NA
11    9     2     1    109.2    313.800    ;    109.2    31.5    HM-CM-NA
12    9     2     1    109.2    313.800    ;    109.2    31.5    HM-CM-NA
9     2     3     1    126.4    585.760    ;    126.4    70      CM-NA-CR
9     2     7     1    125.6    585.760    ;    125.6    70      CM-NA-CW
2     3     4     1    125.1    292.880    ;    125.1    29      NA-CR-HR
1     3     4     1    125.1    292.880    ;    125.1    29      NA-CR-HR
2     3     1     1    109.8    585.760    ;    109.8    70      NA-CR-NA
3     2     7     1    107.9    585.760    ;    107.9    70      CR-NA-CW
3     1     5     1    107.9    585.760    ;    107.9    70      CR-NA-CW
2     7     5     1    107.1    585.760    ;    107.1    70      NA-CW-CW
1     5     7     1    107.1    585.760    ;    107.1    70      NA-CW-CW
2     7     8     1    122.0    292.880    ;    122      29      NA-CW-HW
1     5     6     1    122.0    292.880    ;    122      29      NA-CW-HW
6     5     7     1    130.9    292.880    ;    130.9    29      HW-CW-CW
8     7     5     1    130.9    292.880    ;    130.9    29      HW-CW-CW
5     1     13    1    125.3    585.760    ;    125.3    70      CW-NA-CA
3     1     13    1    126.8    585.760    ;    126.8    70      CR-NA-CA
1     13    14    1    107.5    313.800    ;    107.5    31.5    NA-CA-HA
1     13    15    1    107.5    313.800    ;    107.5    31.5    NA-CA-HA
1     13    16    1    113.0    488.273    ;    113     58.29    NA-CA-CS
14    13    16    1    111.1    313.800    ;    111.1    31.5    HA-CA-CS
15    13    16    1    111.1    313.800    ;    111.1    31.5    HA-CA-CS
14    13    15    1    108.9    276.144    ;    108.9    33      HA-CA-HA
13    16    17    1    108.6    313.800    ;    108.6    31.5    CA-CS-HS
13    16    18    1    108.6    313.800    ;    108.6    31.5    CA-CS-HS
13    16    19    1    113.3    488.273    ;    113.3   58.29    CA-CS-CS
32    31    28    1    109.7    313.800    ;    109.7    31.5    HS-CS-CT
33    31    28    1    109.7    313.800    ;    109.7    31.5    HS-CS-CT
17    16    19    1    109.6    313.800    ;    109.6    31.5    HS-CS-CS
18    16    19    1    109.6    313.800    ;    109.6    31.5    HS-CS-CS
20    19    16    1    109.6    313.800    ;    109.6    31.5    HS-CS-CS
21    19    16    1    109.6    313.800    ;    109.6    31.5    HS-CS-CS
20    19    22    1    109.6    313.800    ;    109.6    31.5    HS-CS-CS
21    19    22    1    109.6    313.800    ;    109.6    31.5    HS-CS-CS
23    22    19    1    109.6    313.800    ;    109.6    31.5    HS-CS-CS
24    22    19    1    109.6    313.800    ;    109.6    31.5    HS-CS-CS
23    22    25    1    109.6    313.800    ;    109.6    31.5    HS-CS-CS
24    22    25    1    109.6    313.800    ;    109.6    31.5    HS-CS-CS
26    25    22    1    109.6    313.800    ;    109.6    31.5    HS-CS-CS
27    25    22    1    109.6    313.800    ;    109.6    31.5    HS-CS-CS
26    25    28    1    109.6    313.800    ;    109.6    31.5    HS-CS-CS
27    25    28    1    109.6    313.800    ;    109.6    31.5    HS-CS-CS
29    28    25    1    109.6    313.800    ;    109.6    31.5    HS-CS-CS
30    28    25    1    109.6    313.800    ;    109.6    31.5    HS-CS-CS
29    28    31    1    109.6    313.800    ;    109.6    31.5    HS-CS-CS
30    28    31    1    109.6    313.800    ;    109.6    31.5    HS-CS-CS
32    31    28    1    109.6    313.800    ;    109.6    31.5    HS-CS-CS
33    31    28    1    109.6    313.800    ;    109.6    31.5    HS-CS-CS
17    16    18    1    106.7    276.144    ;    106.7    33      HS-CS-HS
20    19    21    1    106.7    276.144    ;    106.7    33      HS-CS-HS
23    22    24    1    106.7    276.144    ;    106.7    33      HS-CS-HS
26    25    27    1    106.7    276.144    ;    106.7    33      HS-CS-HS
29    28    30    1    106.7    276.144    ;    106.7    33      HS-CS-HS
32    31    33    1    106.7    276.144    ;    106.7    33      HS-CS-HS
28    31    28    1    112.3    488.273    ;    112.3   58.29    CS-CS-CT
16    19    22    1    112.3    488.273    ;    112.3   58.29    CS-CS-CS
19    22    25    1    112.3    488.273    ;    112.3   58.29    CS-CS-CS
25    28    29    1    111.1    313.800    ;    111.1    31.5    CS-CT-HT
25    28    30    1    111.1    313.800    ;    111.1    31.5    CS-CT-HT
25    28    31    1    111.1    313.800    ;    111.1    31.5    CS-CT-HT
29    28    30    1    107.9    276.144    ;    107.9    33      HT-CT-HT
29    28    31    1    107.9    276.144    ;    107.9    33      HT-CT-HT
30    28    31    1    107.9    276.144    ;    107.9    33     HT-CT-HT

[  dihedrals  ]
;   ai    aj    ak    al funct    c0       c1       c2     c3(kJ/mol);    V1    V2    V3       V4  (kcal/mol)
10    9     2     3     5    0.000    0.000    0.000    0.000    ;    0     0     0        0    HM-CM-NA-CR
11    9     2     3     5    0.000    0.000    0.000    0.000    ;    0     0     0        0    HM-CM-NA-CR
12    9     2     3     5    0.000    0.000    0.000    0.000    ;    0     0     0        0    HM-CM-NA-CR
10    9     2     7     5    0.000    0.000    0.519    0.000    ;    0     0    0.124     0    HM-CM-NA-CW
11    9     2     7     5    0.000    0.000    0.519    0.000    ;    0     0    0.124     0    HM-CM-NA-CW
```

```
12    9     2     7     5    0.000    0.000    0.519    0.000    ;    0     0    0.124    0    HM-CM-NA-CW
9     2     3     4     5    0.000   19.460    0.000    0.000    ;    0    4.651  0        0    CM-NA-CR-HR
9     2     3     1     5    0.000   19.460    0.000    0.000    ;    0    4.651  0        0    CM-NA-CR-NA
9     2     7     5     5    0.000   12.552    0.000    0.000    ;    0     3     0        0    CM-NA-CW-CW
9     2     7     8     5    0.000   12.552    0.000    0.000    ;    0     3     0        0    CM-NA-CW-HW
2     3     1     13    5    0.000   19.460    0.000    0.000    ;    0    4.651  0        0    NA-CR-NA-CA
2     7     5     6     5    0.000   44.978    0.000    0.000    ;    0    10.75  0        0    NA-CW-CW-HW
1     5     7     8     5    0.000   44.978    0.000    0.000    ;    0    10.75  0        0    NA-CW-CW-HW
2     7     5     1     5    0.000   44.978    0.000    0.000    ;    0    10.75  0        0    NA-CW-CW-NA
4     3     2     7     5    0.000   19.460    0.000    0.000    ;    0    4.651  0        0    HR-CR-NA-CW
4     3     1     5     5    0.000   19.460    0.000    0.000    ;    0    4.651  0        0    HR-CR-NA-CW
3     2     7     8     5    0.000   12.552    0.000    0.000    ;    0     3     0        0    CR-NA-CW-HW
3     1     5     6     5    0.000   12.552    0.000    0.000    ;    0     3     0        0    CR-NA-CW-HW
3     1     5     7     5    0.000   12.552    0.000    0.000    ;    0     3     0        0    CR-NA-CW-CW
3     2     7     5     5    0.000   12.552    0.000    0.000    ;    0     3     0        0    CR-NA-CW-CW
4     3     1     13    5    0.000   19.460    0.000    0.000    ;    0    4.651  0        0    HR-CR-NA-CA
6     5     1     13    5    0.000   12.552    0.000    0.000    ;    0     3     0        0    HW-CW-NA-CA
7     5     1     13    5    0.000   12.552    0.000    0.000    ;    0     3     0        0    CW-CW-NA-CA
3     1     13    14    5    0.000    0.000    0.000    0.000    ;    0     0     0        0    CR-NA-CA-HA
3     1     13    15    5    0.000    0.000    0.000    0.000    ;    0     0     0        0    CR-NA-CA-HA
13    16    19    20    5    0.000    0.000    1.531    0.000    ;    0     0    0.306    0    CA-CS-CS-HS
13    16    19    21    5    0.000    0.000    1.531    0.000    ;    0     0    0.306    0    CA-CS-CS-HS
17    16    19    20    5    0.000    0.000    1.331    0.000    ;    0     0    0.318    0    HS-CS-CS-HS
17    16    19    21    5    0.000    0.000    1.331    0.000    ;    0     0    0.318    0    HS-CS-CS-HS
18    16    19    20    5    0.000    0.000    1.331    0.000    ;    0     0    0.318    0    HS-CS-CS-HS
18    16    19    21    5    0.000    0.000    1.331    0.000    ;    0     0    0.318    0    HS-CS-CS-HS
20    19    22    23    5    0.000    0.000    1.331    0.000    ;    0     0    0.318    0    HS-CS-CS-HS
20    19    22    24    5    0.000    0.000    1.331    0.000    ;    0     0    0.318    0    HS-CS-CS-HS
21    19    22    23    5    0.000    0.000    1.331    0.000    ;    0     0    0.318    0    HS-CS-CS-HS
21    19    22    24    5    0.000    0.000    1.331    0.000    ;    0     0    0.318    0    HS-CS-CS-HS
23    22    25    27    5    0.000    0.000    1.331    0.000    ;    0     0    0.318    0    HS-CS-CS-HS
23    22    25    26    5    0.000    0.000    1.331    0.000    ;    0     0    0.318    0    HS-CS-CS-HS
24    22    25    27    5    0.000    0.000    1.331    0.000    ;    0     0    0.318    0    HS-CS-CS-HS
24    22    25    26    5    0.000    0.000    1.331    0.000    ;    0     0    0.318    0    HS-CS-CS-HS
32    31    28    29    5    0.000    0.000    1.331    0.000    ;    0     0    0.318    0    HS-CS-CT-HT
32    31    28    30    5    0.000    0.000    1.331    0.000    ;    0     0    0.318    0    HS-CS-CT-HT
32    31    28    31    5    0.000    0.000    1.331    0.000    ;    0     0    0.318    0    HS-CS-CT-HT
33    31    28    29    5    0.000    0.000    1.331    0.000    ;    0     0    0.318    0    HS-CS-CT-HT
33    31    28    30    5    0.000    0.000    1.331    0.000    ;    0     0    0.318    0    HS-CS-CT-HT
33    31    28    31    5    0.000    0.000    1.331    0.000    ;    0     0    0.318    0    HS-CS-CT-HT
13    16    19    22    5    5.439   -0.209    0.831    0.000    ;   1.30  -0.05  0.20     0    CA-CS-CS-CS
16    19    22    25    5    5.439   -0.209    0.831    0.000    ;   1.30  -0.05  0.20     0    CA-CS-CS-CS
19    22    25    26    5    0.000    0.000    1.531    0.000    ;    0     0    0.306    0    CS-CS-CS-HS
19    22    25    27    5    0.000    0.000    1.531    0.000    ;    0     0    0.306    0    CS-CS-CS-HS
16    19    22    23    5    0.000    0.000    1.531    0.000    ;    0     0    0.306    0    CS-CS-CS-HS
16    19    22    24    5    0.000    0.000    1.531    0.000    ;    0     0    0.306    0    CS-CS-CS-HS
22    19    16    17    5    0.000    0.000    1.531    0.000    ;    0     0    0.306    0    CS-CS-CS-HS
22    19    16    18    5    0.000    0.000    1.531    0.000    ;    0     0    0.306    0    CS-CS-CS-HS
25    22    19    20    5    0.000    0.000    1.531    0.000    ;    0     0    0.306    0    CS-CS-CS-HS
25    22    19    21    5    0.000    0.000    1.531    0.000    ;    0     0    0.306    0    CS-CS-CS-HS
8     7     5     6     5    0.000    44.978   0.000    0.000    ;    0    10.75  0        0    HW-CW-CW-HW
5     1     13    14    5   -11.297  -23.640   1.485    0.000    ;  -2.70  -5.65 0.295    0    CW-NA-CA-HA
5     1     13    15    5   -11.297  -23.640   1.485    0.000    ;  -2.70  -5.65 0.295    0    CW-NA-CA-HA
5     1     13    16    5   -8.828   -20.920   1.443    0.000    ;  -2.11  -5    0.285    0    CW-NA-CA-CS
3     1     13    16    5   -0.665    0.397   -0.042    0.000    ;  -0.159 0.095 -0.010    0    CR-NA-CA-CS
1     13    16    19    5   -3.297    3.287    1.674    0.000    ;  -0.788  0.8  0.400    0    NA-CA-CS-CS
14    13    16    17    5    0.000   -0.628    2.167    0.000    ;    0    -0.15 0.518    0    HA-CA-CS-HS
14    13    16    18    5    0.000   -0.628    2.167    0.000    ;    0    -0.15 0.518    0    HA-CA-CS-HS
15    13    16    17    5    0.000   -0.628    2.167    0.000    ;    0    -0.15 0.518    0    HA-CA-CS-HS
15    13    16    18    5    0.000   -0.628    2.167    0.000    ;    0    -0.15 0.518    0    HA-CA-CS-HS
1     13    16    17    5    0.000    0.000    0.000    0.000    ;    0    0      0       0    NA-CA-CS-HS
1     13    16    18    5    0.000    0.000    0.000    0.000    ;    0    0      0       0    NA-CA-CS-HS
14    13    16    19    5    0.000    0.000    1.531    0.000    ;    0    0     0.306    0    HA-CA-CS-CS
15    13    16    19    5    0.000    0.000    1.531    0.000    ;    0    0     0.306    0    HS-CA-CS-CS
7     2     3     1     5    0.000    19.46    0.000    0.000    ;    0    4.651  0        0    CW-NA-CR-NA
5     1     3     2     5    0.000    19.46    0.000    0.000    ;    0    4.651  0        0    CW-NA-CR-NA
6     5     1     7     5    0.000    9.205    0.000    0.000    ;    0    2.2    0        0    HW-CW-NA-CW
improper
8     7     2     5     5    0.000    9.205    0.000    0.000    ;    0    2.2    0        0    HW-CW-NA-CW
improper
4     3     2     1     5    0.000    9.205    0.000    0.000    ;    0    2.2    0        0    HR-CR-NA-NA
improper
9     2     3     7     5    0.000    8.308    0.000    0.000    ;    0    2      0        0    CM-NA-CR-CW
improper
13    1     3     5     5    0.000    8.308    0.000    0.000    ;    0    2      0        0    CA-NA-CR-CW
improper
```

Nonbonded parameters

```
[  atomtypes  ]
;  type    mass     charge  ptype sigma(nm) epsilon(kJ/mol) sigma(Ang.) epsilon(kcal/mol)
lpls_803    C01          12.011    0.000    A    0.355    0.292880    ;    3.55    0.07
lpls_801    N02          14.007    0.000    A    0.325    0.711280    ;    3.25    0.17
lpls_802    N00          14.007    0.000    A    0.325    0.711280    ;    3.25    0.17
lpls_805    C04          12.011    0.000    A    0.355    0.292880    ;    3.55    0.07
lpls_807    C03          12.011    0.000    A    0.355    0.292880    ;    3.55    0.07
lpls_804    H07          1.008     0.000    A    0.242    0.125520    ;    2.42    0.03
lpls_806    H09          1.008     0.000    A    0.242    0.125520    ;    2.42    0.03
lpls_808    H08          1.008     0.000    A    0.242    0.125520    ;    2.42    0.03
lpls_809    C05          12.011    0.000    A    0.350    0.276144    ;    3.5     0.066
lpls_810    H0B          1.008     0.000    A    0.250    0.125520    ;    2.5     0.03
lpls_811    H0C          1.008     0.000    A    0.250    0.125520    ;    2.5     0.03
lpls_812    H0D          1.008     0.000    A    0.250    0.125520    ;    2.5     0.03
lpls_813    C06          12.011    0.000    A    0.350    0.276144    ;    3.5     0.066
lpls_814    H0E          1.008     0.000    A    0.250    0.125520    ;    2.5     0.03
lpls_815    H0F          1.008     0.000    A    0.250    0.125520    ;    2.5     0.03
lpls_816       C0G   12.011    0.000    A    0.350    0.276144    ;    3.5     0.066
lpls_819       C0J    12.011    0.000    A    0.350    0.276144    ;    3.5     0.066
lpls_822       C0N    12.011    0.000    A    0.350    0.276144    ;    3.5     0.066
lpls_825       C0Q    12.011    0.000    A    0.350    0.276144    ;    3.5     0.066
lpls_817       H0H    1.008     0.000    A    0.250    0.125520    ;    2.5     0.03
lpls_818       H0I    1.008     0.000    A    0.250    0.125520    ;    2.5     0.03
lpls_820       H0K    1.008     0.000    A    0.250    0.125520    ;    2.5     0.03
lpls_821       H0M    1.008     0.000    A    0.250    0.125520    ;    2.5     0.03
lpls_823       H0O    1.008     0.000    A    0.250    0.125520    ;    2.5     0.03
lpls_824       H0P    1.008     0.000    A    0.250    0.125520    ;    2.5     0.03
lpls_826       H0R    1.008     0.000    A    0.250    0.125520    ;    2.5     0.03
lpls_827       H0S    1.008     0.000    A    0.250    0.125520    ;    2.5     0.03
lpls_828       C0Z    12.011    0.000    A    0.350    0.276144    ;    3.5     0.066
lpls_829       H00    1.008     0.000    A    0.250    0.125520    ;    2.5     0.03
lpls_830       H01    1.008     0.000    A    0.250    0.125520    ;    2.5     0.03
lpls_831       H02    1.008     0.000    A    0.250    0.125520    ;    2.5     0.03
```

Topology file for anion A1 $[NapO_2]^{2-}$

Bonded parameters

```
[ moleculetype ]
; Name               nrexcl
A1                   3
[ atoms ]
;   nr       type  resnr residue  atom   cgnr     charge       mass
     1   opls_800      1    A1   C00      1    -0.12975    12.0110
     2   opls_801      1    A1   C01      1    -0.02062    12.0110
     3   opls_802      1    A1   C02      1    -0.00224    12.0110
     4   opls_803      1    A1   C03      1    -0.00224    12.0110
     5   opls_804      1    A1   C04      1    -0.11404    12.0110
     6   opls_805      1    A1   C05      1    -0.14015    12.0110
     7   opls_806      1    A1   H06      1    0.10900      1.0080
     8   opls_807      1    A1   H07      1    0.09975      1.0080
     9   opls_808      1    A1   C08      1    -0.11404    12.0110
    10   opls_809      1    A1   C09      1    -0.02062    12.0110
    11   opls_810      1    A1   H0A      1    0.10900      1.0080
    12   opls_811      1    A1   H0B      1    0.08535      1.0080
    13   opls_812      1    A1   C0C      1    -0.12975    12.0110
    14   opls_813      1    A1   C0D      1    -0.14015    12.0110
    15   opls_814      1    A1   H0E      1    0.09975      1.0080
    16   opls_815      1    A1   H0F      1    0.08535      1.0080
    17   opls_816      1    A1   S0G      1    0.57241     32.0600
    18   opls_817      1    A1   O0H      1    -0.55407    15.9990
    19   opls_818      1    A1   O0I      1    -0.55156    15.9990
    20   opls_819      1    A1   O0J      1    -0.55407    15.9990
    21   opls_820      1    A1   S0K      1    0.57241     32.0600
    22   opls_821      1    A1   O0M      1    -0.55407    15.9990
    23   opls_822      1    A1   O0N      1    -0.55407    15.9990
    24   opls_823      1    A1   O0O      1    -0.55156    15.9990
[ bonds ]
    2     1     1      0.1400 392459.200
    3     2     1      0.1404 392459.200
    4     3     1      0.1370 435136.000
    5     4     1      0.1404 392459.200
    6     1     1      0.1400 392459.200
    7     9     1      0.1080 307105.600
    8     1     1      0.1080 307105.600
    9     3     1      0.1404 392459.200
   10     4     1      0.1404 392459.200
   11     5     1      0.1080 307105.600
   12     6     1      0.1080 307105.600
   13    10     1      0.1400 392459.200
   14     9     1      0.1400 392459.200
   15    13     1      0.1080 307105.600
   16    14     1      0.1080 307105.600
   17    10     1      0.1770 284512.000
   18    17     1      0.1440 585760.000
   19    17     1      0.1440 585760.000
   20    17     1      0.1440 585760.000
   21     2     1      0.1770 284512.000
   22    21     1      0.1440 585760.000
   23    21     1      0.1440 585760.000
   24    21     1      0.1440 585760.000
    6     5     1      0.1400 392459.200
   14    13     1      0.1400 392459.200

[ angles ]
;  ai    aj    ak funct            c0            c1            c2            c3
    1     2     3     1    120.000    527.184
    2     3     4     1    117.300    711.280
    3     4     5     1    117.300    711.280
    2     1     6     1    120.000    527.184
    3     9     7     1    120.000    292.880
    2     1     8     1    120.000    292.880
    2     3     9     1    134.900    711.280
    3     4    10     1    117.300    711.280
    4     5    11     1    120.000    292.880
    1     6    12     1    120.000    292.880
    4    10    13     1    120.000    527.184
    3     9    14     1    120.000    527.184
   10    13    15     1    120.000    292.880
    9    14    16     1    120.000    292.880
```

```
   4    10    17     1    119.400    711.280
  10    17    18     1    107.200    619.232
  10    17    19     1    107.200    619.232
  10    17    20     1    107.200    619.232
   1     2    21     1    119.400    711.280
   2    21    22     1    107.200    619.232
   2    21    23     1    107.200    619.232
   2    21    24     1    107.200    619.232
  22    21    23     1    119.000    870.272
  18    17    20     1    119.000    870.272
   6     5    11     1    120.000    292.880
   7     9    14     1    120.000    292.880
   3     2    21     1    119.400    711.280
   4     5     6     1    120.000    527.184
  13    14    16     1    120.000    292.880
  14    13    15     1    120.000    292.880
   5     6    12     1    120.000    292.880
   4     3     9     1    117.300    711.280
   6     1     8     1    120.000    292.880
   9    14    13     1    120.000    527.184
  18    17    19     1    119.000    870.272
  23    21    24     1    119.000    870.272
  10    13    14     1    120.000    527.184
   1     6     5     1    120.000    527.184
   5     4    10     1    134.900    711.280
  19    17    20     1    119.000    870.272
  22    21    24     1    119.000    870.272
  13    10    17     1    119.400    711.280

[ dihedrals ]
; IMPROPER DIHEDRAL ANGLES
;  ai    aj    ak    al funct            c0           c1            c2            c3            c4            c5
    14     9     3     7    4        180.000     10.460     2
     9     3     2     4    4        180.000     10.460     2
    10     4     3     5    4        180.000     10.460     2
     8     1     2     6    4        180.000     10.460     2
    12     6     1     5    4        180.000     10.460     2
    16    14     9    13    4        180.000     10.460     2
    15    13    10    14    4        180.000     10.460     2
    11     5     4     6    4        180.000     10.460     2
    21     2     1     3    4        180.000     10.460     2
    17    10     4    13    4        180.000     10.460     2

[ dihedrals ]
; PROPER DIHEDRAL ANGLES
;  ai    aj    ak    al funct            c0           c1            c2            c3            c4            c5
   10   13   14    9        3      30.334   0.000  -30.334  -0.000  -0.000   0.000
    5    6    1    2        3      30.334   0.000  -30.334  -0.000  -0.000   0.000
    6    1    2    3        3      30.334   0.000  -30.334  -0.000  -0.000   0.000
   14   13   10    4        3      30.334   0.000  -30.334  -0.000  -0.000   0.000
   13   14    9    3        3      30.334   0.000  -30.334  -0.000  -0.000   0.000
   13   14    9    7        3      30.334   0.000  -30.334  -0.000  -0.000   0.000
   13   10    4    5        3      29.288   0.000  -29.288  -0.000  -0.000   0.000
   14    9    3    2        3      29.288   0.000  -29.288  -0.000  -0.000   0.000
   13   10    4    3        3      29.288   0.000  -29.288  -0.000  -0.000   0.000
    6    5    4    3        3      29.288   0.000  -29.288  -0.000  -0.000   0.000
   14    9    3    4        3      29.288   0.000  -29.288  -0.000  -0.000   0.000
    9    3    2    1        3      29.288   0.000  -29.288  -0.000  -0.000   0.000
   10    4    5    6        3      29.288   0.000  -29.288  -0.000  -0.000   0.000
   10    4    3    9        3      30.334   0.000  -30.334  -0.000  -0.000   0.000
   10    4    3    2        3      30.334   0.000  -30.334  -0.000  -0.000   0.000
    5    4    3    2        3      30.334   0.000  -30.334  -0.000  -0.000   0.000
    9    3    4    5        3      30.334   0.000  -30.334  -0.000  -0.000   0.000
    4    5    6    1        3      30.334   0.000  -30.334  -0.000  -0.000   0.000
    4    3    2    1        3      29.288   0.000  -29.288  -0.000  -0.000   0.000
   12    6    1    2        3      30.334   0.000  -30.334  -0.000  -0.000   0.000
    8    1    6    5        3      30.334   0.000  -30.334  -0.000  -0.000   0.000
   16   14   13   10        3      30.334   0.000  -30.334  -0.000  -0.000   0.000
   11    5    6    1        3      30.334   0.000  -30.334  -0.000  -0.000   0.000
   15   13   14    9        3      30.334   0.000  -30.334  -0.000  -0.000   0.000
   15   13   10    4        3      30.334   0.000  -30.334  -0.000  -0.000   0.000
   16   14    9    3        3      30.334   0.000  -30.334  -0.000  -0.000   0.000
    8    1    2    3        3      30.334   0.000  -30.334  -0.000  -0.000   0.000
   12    6    5    4        3      30.334   0.000  -30.334  -0.000  -0.000   0.000
   16   14   13   15        3      30.334   0.000  -30.334  -0.000  -0.000   0.000
   16   14    9    7        3      30.334   0.000  -30.334  -0.000  -0.000   0.000
   12    6    5   11        3      30.334   0.000  -30.334  -0.000  -0.000   0.000
```

```
   12    6    1    8        3      30.334   0.000  -30.334  -0.000  -0.000   0.000
   11    5    4   10        3      30.334   0.000  -30.334  -0.000  -0.000   0.000
    7    9    3    2        3      30.334   0.000  -30.334  -0.000  -0.000   0.000
    7    9    3    4        3      30.334   0.000  -30.334  -0.000  -0.000   0.000
   11    5    4    3        3      30.334   0.000  -30.334  -0.000  -0.000   0.000
   24   21    2    1        3       0.000   0.000    0.000  -0.000  -0.000   0.000
   23   21    2    1        3       0.000   0.000    0.000  -0.000  -0.000   0.000
   18   17   10   13        3       0.000   0.000    0.000  -0.000  -0.000   0.000
   20   17   10   13        3       0.000   0.000    0.000  -0.000  -0.000   0.000
   22   21    2    1        3       0.000   0.000    0.000  -0.000  -0.000   0.000
   19   17   10   13        3       0.000   0.000    0.000  -0.000  -0.000   0.000
   18   17   10    4        3       0.000   0.000    0.000  -0.000  -0.000   0.000
   20   17   10    4        3       0.000   0.000    0.000  -0.000  -0.000   0.000
   24   21    2    3        3       0.000   0.000    0.000  -0.000  -0.000   0.000
   22   21    2    3        3       0.000   0.000    0.000  -0.000  -0.000   0.000
   19   17   10    4        3       0.000   0.000    0.000  -0.000  -0.000   0.000
   23   21    2    3        3       0.000   0.000    0.000  -0.000  -0.000   0.000
   21    2    1    6        3      30.334   0.000  -30.334  -0.000  -0.000   0.000
   17   10   13   14        3      30.334   0.000  -30.334  -0.000  -0.000   0.000
   17   10   13   15        3      30.334   0.000  -30.334  -0.000  -0.000   0.000
   21    2    1    8        3      30.334   0.000  -30.334  -0.000  -0.000   0.000
   21    2    3    9        3      30.334   0.000  -30.334  -0.000  -0.000   0.000
   17   10    4    5        3      30.334   0.000  -30.334  -0.000  -0.000   0.000
   21    2    3    4        3      29.288   0.000  -29.288  -0.000  -0.000   0.000
   17   10    4    3        3      29.288   0.000  -29.288  -0.000  -0.000   0.000

[ pairs ]
     1     4    1
     2     5    1
     3     6    1
     2     7    1
     1     9    1
     4     7    1
     3     8    1
     2    10    1
     1    11    1
     5     8    1
     5     9    1
     3    11    1
     2    12    1
     6    10    1
     4    12    1
     3    13    1
     2    14    1
     5    13    1
     4    14    1
     9    10    1
     4    15    1
     3    16    1
     8    12    1
     7    13    1
     3    17    1
    10    11    1
     5    17    1
     4    18    1
    11    12    1
     7    16    1
     4    19    1
     1    22    1
     9    15    1
     4    20    1
     1    23    1
     4    21    1
     3    22    1
     1    24    1
    10    16    1
     3    23    1
     6    21    1
     3    24    1
     8    21    1
     9    21    1
    15    16    1
    14    17    1
    13    18    1
    15    17    1
    13    19    1
    13    20    1
```

Non-bonded parameters

```
[ atomtypes ]
  opls_802  C802    12.0110     0.000    A    3.50000E-01   3.34720E-01
  opls_805  C805    12.0110     0.000    A    3.55000E-01   2.92880E-01
  opls_818  O818    15.9990     0.000    A    2.96000E-01   7.11280E-01
  opls_816  S816    32.0600     0.000    A    3.55000E-01   1.04600E+00
  opls_801  C801    12.0110     0.000    A    3.55000E-01   2.92880E-01
  opls_812  C812    12.0110     0.000    A    3.55000E-01   2.92880E-01
  opls_822  O822    15.9990     0.000    A    2.96000E-01   7.11280E-01
  opls_813  C813    12.0110     0.000    A    3.55000E-01   2.92880E-01
  opls_803  C803    12.0110     0.000    A    3.50000E-01   3.34720E-01
  opls_804  C804    12.0110     0.000    A    3.55000E-01   2.92880E-01
  opls_811  H811     1.0080     0.000    A    2.42000E-01   1.25520E-01
  opls_810  H810     1.0080     0.000    A    2.42000E-01   1.25520E-01
  opls_820  S820    32.0600     0.000    A    3.55000E-01   1.04600E+00
  opls_815  H815     1.0080     0.000    A    2.42000E-01   1.25520E-01
  opls_806  H806     1.0080     0.000    A    2.42000E-01   1.25520E-01
  opls_800  C800    12.0110     0.000    A    3.55000E-01   2.92880E-01
  opls_809  C809    12.0110     0.000    A    3.55000E-01   2.92880E-01
  opls_823  O823    15.9990     0.000    A    2.96000E-01   7.11280E-01
  opls_807  H807     1.0080     0.000    A    2.42000E-01   1.25520E-01
  opls_817  O817    15.9990     0.000    A    2.96000E-01   7.11280E-01
  opls_821  O821    15.9990     0.000    A    2.96000E-01   7.11280E-01
  opls_808  C808    12.0110     0.000    A    3.55000E-01   2.92880E-01
  opls_814  H814     1.0080     0.000    A    2.42000E-01   1.25520E-01
  opls_819  O819    15.9990     0.000    A    2.96000E-01   7.11280E-01
```

Topology file for anion A3 $[BzO_3]^{3-}$

Bonded parameters

```
[ moleculetype ]
; Name               nrexcl
A3                   3
[ atoms ]
;   nr       type  resnr residue  atom   cgnr     charge       mass
     1   opls_800      1     A3   O00      1   -0.58526    15.9990
     2   opls_801      1     A3   S01      1   0.56067     32.0600
     3   opls_802      1     A3   O02      1   -0.58524    15.9990
     4   opls_803      1     A3   O03      1   -0.57033    15.9990
     5   opls_804      1     A3   C04      1   -0.02657    12.0110
     6   opls_805      1     A3   C05      1   -0.10708    12.0110
     7   opls_806      1     A3   H06      1   0.11377      1.0080
     8   opls_807      1     A3   C07      1   -0.10707    12.0110
     9   opls_808      1     A3   H08      1   0.11378      1.0080
    10   opls_809      1     A3   C09      1   -0.02657    12.0110
    11   opls_810      1     A3   S0A      1   0.56067     32.0600
    12   opls_811      1     A3   O0B      1   -0.57034    15.9990
    13   opls_812      1     A3   O0C      1   -0.58526    15.9990
    14   opls_813      1     A3   O0D      1   -0.58522    15.9990
    15   opls_814      1     A3   C0E      1   -0.10708    12.0110
    16   opls_815      1     A3   H0F      1   0.11376      1.0080
    17   opls_816      1     A3   C0G      1   -0.02657    12.0110
    18   opls_817      1     A3   S0H      1   0.56070     32.0600
    19   opls_818      1     A3   O0I      1   -0.57034    15.9990
    20   opls_819      1     A3   O0J      1   -0.58513    15.9990
    21   opls_820      1     A3   O0K      1   -0.58531    15.9990
[ bonds ]
    2     1     1      0.1440 585760.000
    3     2     1      0.1440 585760.000
    4     2     1      0.1440 585760.000
    5     2     1      0.1770 284512.000
    6     5     1      0.1400 392459.200
    7     6     1      0.1080 307105.600
    8     5     1      0.1400 392459.200
    9     8     1      0.1080 307105.600
   10     8     1      0.1400 392459.200
   11    10     1      0.1770 284512.000
   12    11     1      0.1440 585760.000
   13    11     1      0.1440 585760.000
   14    11     1      0.1440 585760.000
   15    10     1      0.1400 392459.200
   16    15     1      0.1080 307105.600
   17     6     1      0.1400 392459.200
   18    17     1      0.1770 284512.000
   19    18     1      0.1440 585760.000
   20    18     1      0.1440 585760.000
   21    18     1      0.1670 376560.000
   17    15     1      0.1400 392459.200

[ angles ]
;  ai    aj    ak funct            c0            c1            c2            c3
    1     2     3     1    119.000    870.272
    1     2     4     1    119.000    870.272
    1     2     5     1    107.200    619.232
    2     5     6     1    119.400    711.280
    5     6     7     1    120.000    292.880
    2     5     8     1    119.400    711.280
    5     8     9     1    120.000    292.880
    5     8    10     1    120.000    527.184
    8    10    11     1    119.400    711.280
   10    11    12     1    107.200    619.232
   10    11    13     1    107.200    619.232
   10    11    14     1    107.200    619.232
    8    10    15     1    120.000    527.184
   10    15    16     1    120.000    292.880
    5     6    17     1    120.000    527.184
    6    17    18     1    119.400    711.280
```

```
   17    18    19     1    107.200    619.232
   17    18    20     1    107.200    619.232
   17    18    21     1     96.400    627.600
   20    18    21     1    108.700    619.232
    7     6    17     1    120.000    292.880
   11    10    15     1    119.400    711.280
   10    15    17     1    120.000    527.184
   15    17    18     1    119.400    711.280
    3     2     4     1    119.000    870.272
   12    11    14     1    119.000    870.272
    3     2     5     1    107.200    619.232
    4     2     5     1    107.200    619.232
   16    15    17     1    120.000    292.880
    6     5     8     1    120.000    527.184
    6    17    15     1    120.000    527.184
   19    18    20     1    119.000    870.272
   12    11    13     1    119.000    870.272
   13    11    14     1    119.000    870.272
   19    18    21     1    108.700    619.232
    9     8    10     1    120.000    292.880

[ dihedrals ]
; IMPROPER DIHEDRAL ANGLES
;  ai    aj    ak    al funct            c0            c1            c2            c3            c4            c5
    10     8     5     9    4        180.000     10.460     2
    17     6     5     7    4        180.000     10.460     2
    15    10     8    11    4        180.000     10.460     2
     8     5     2     6    4        180.000     10.460     2
    16    15    17    10    4        180.000     10.460     2
    18    17     6    15    4        180.000     10.460     2

[ dihedrals ]
; PROPER DIHEDRAL ANGLES
;  ai    aj    ak    al funct            c0            c1            c2            c3            c4            c5
   10    8    5    6        3      30.334   0.000  -30.334  -0.000  -0.000   0.000
   10   15   17    6        3      30.334   0.000  -30.334  -0.000  -0.000   0.000
   17   15   10    8        3      30.334   0.000  -30.334  -0.000  -0.000   0.000
   15   17    6    5        3      30.334   0.000  -30.334  -0.000  -0.000   0.000
   15   10    8    5        3      30.334   0.000  -30.334  -0.000  -0.000   0.000
   17    6    5    8        3      30.334   0.000  -30.334  -0.000  -0.000   0.000
   15   10    8    9        3      30.334   0.000  -30.334  -0.000  -0.000   0.000
    8    5    6    7        3      30.334   0.000  -30.334  -0.000  -0.000   0.000
   15   17    6    7        3      30.334   0.000  -30.334  -0.000  -0.000   0.000
   10    8    5    2        3      30.334   0.000  -30.334  -0.000  -0.000   0.000
   17   15   10   11        3      30.334   0.000  -30.334  -0.000  -0.000   0.000
   17    6    5    2        3      30.334   0.000  -30.334  -0.000  -0.000   0.000
    6    5    2    3        3       0.000   0.000   0.000  -0.000  -0.000   0.000
    8    5    2    1        3       0.000   0.000   0.000  -0.000  -0.000   0.000
   15   10   11   13        3       0.000   0.000   0.000  -0.000  -0.000   0.000
    8    5    2    3        3       0.000   0.000   0.000  -0.000  -0.000   0.000
    8    5    2    4        3       0.000   0.000   0.000  -0.000  -0.000   0.000
   15   10   11   12        3       0.000   0.000   0.000  -0.000  -0.000   0.000
    6    5    2    1        3       0.000   0.000   0.000  -0.000  -0.000   0.000
   15   10   11   14        3       0.000   0.000   0.000  -0.000  -0.000   0.000
    6    5    2    4        3       0.000   0.000   0.000  -0.000  -0.000   0.000
    9    8    5    6        3      30.334   0.000  -30.334  -0.000  -0.000   0.000
   16   15   10    8        3      30.334   0.000  -30.334  -0.000  -0.000   0.000
   16   15   17    6        3      30.334   0.000  -30.334  -0.000  -0.000   0.000
   16   15   10   11        3      30.334   0.000  -30.334  -0.000  -0.000   0.000
    9    8    5    2        3      30.334   0.000  -30.334  -0.000  -0.000   0.000
    7    6    5    2        3      30.334   0.000  -30.334  -0.000  -0.000   0.000
   21   18   17    6        3       0.006  -4.199   3.213   0.979  -0.000   0.000
   21   18   17   15        3       0.006  -4.199   3.213   0.979  -0.000   0.000
   19   18   17    6        3       0.000   0.000   0.000  -0.000  -0.000   0.000
   13   11   10    8        3       0.000   0.000   0.000  -0.000  -0.000   0.000
   19   18   17   15        3       0.000   0.000   0.000  -0.000  -0.000   0.000
   12   11   10    8        3       0.000   0.000   0.000  -0.000  -0.000   0.000
   14   11   10    8        3       0.000   0.000   0.000  -0.000  -0.000   0.000
   20   18   17   15        3       0.000   0.000   0.000  -0.000  -0.000   0.000
   20   18   17    6        3       0.000   0.000   0.000  -0.000  -0.000   0.000
   18   17   15   10        3      30.334   0.000  -30.334  -0.000  -0.000   0.000
   18   17    6    5        3      30.334   0.000  -30.334  -0.000  -0.000   0.000
```

```
   11   10    8    5        3      30.334   0.000  -30.334  -0.000  -0.000   0.000
   18   17    6    7        3      30.334   0.000  -30.334  -0.000  -0.000   0.000
   18   17   15   16        3      30.334   0.000  -30.334  -0.000  -0.000   0.000
   11   10    8    9        3      30.334   0.000  -30.334  -0.000  -0.000   0.000

[ pairs ]
     1     6    1
     3     6    1
     2     7    1
     1     8    1
     4     6    1
     3     8    1
     2     9    1
     4     8    1
     2    10    1
     7     8    1
     6     9    1
     6    10    1
     5    11    1
     2    17    1
     9    11    1
     8    12    1
     5    15    1
     8    13    1
     8    14    1
     7    15    1
     6    16    1
     5    18    1
     9    15    1
     8    16    1
     8    17    1
     7    18    1
     6    19    1
     6    20    1
    12    15    1
    11    16    1
     6    21    1
    13    15    1
    11    17    1
    10    18    1
    14    15    1
    16    18    1
    15    19    1
    15    20    1
    15    21    1
```

Nonbonded parameters

```
[ atomtypes ]
  opls_805  C805    12.0110     0.000    A    3.55000E-01   2.92880E-01
  opls_818  O818    15.9990     0.000    A    2.96000E-01   7.11280E-01
  opls_810  S810    32.0600     0.000    A    3.55000E-01   1.04600E+00
  opls_814  C814    12.0110     0.000    A    3.55000E-01   2.92880E-01
  opls_802  O802    15.9990     0.000    A    2.96000E-01   7.11280E-01
  opls_803  O803    15.9990     0.000    A    2.96000E-01   7.11280E-01
  opls_812  O812    15.9990     0.000    A    2.96000E-01   7.11280E-01
  opls_816  C816    12.0110     0.000    A    3.55000E-01   2.92880E-01
  opls_809  C809    12.0110     0.000    A    3.55000E-01   2.92880E-01
  opls_804  C804    12.0110     0.000    A    3.55000E-01   2.92880E-01
  opls_817  S817    32.0600     0.000    A    3.55000E-01   1.04600E+00
  opls_800  O800    15.9990     0.000    A    2.96000E-01   7.11280E-01
  opls_815  H815     1.0080     0.000    A    2.42000E-01   1.25520E-01
  opls_806  H806     1.0080     0.000    A    2.42000E-01   1.25520E-01
  opls_813  O813    15.9990     0.000    A    2.96000E-01   7.11280E-01
  opls_801  S801    32.0600     0.000    A    3.55000E-01   1.04600E+00
  opls_807  C807    12.0110     0.000    A    3.55000E-01   2.92880E-01
  opls_819  O819    15.9990     0.000    A    2.96000E-01   7.11280E-01
  opls_820  O820    15.9990     0.000    A    3.12000E-01   7.11280E-01
  opls_808  H808     1.0080     0.000    A    2.42000E-01   1.25520E-01
  opls_811  O811    15.9990     0.000    A    2.96000E-01   7.11280E-01
```

Topology file for $[BF_4]^-$ (A4)

Bonded parameters

```
[  moleculetype  ]
;    name    nrexcl
A4    3

[  atoms  ]
;   nr type resnr residu atom cgnr  charge    mass
1    bpls_800    1    A4    B    1     0.6620    10.811
2    bpls_801    1    A4    F    1    -0.3655    18.998
3    bpls_802    1    A4    F    1    -0.3655    18.998
4    bpls_803    1    A4    F    1    -0.3655    18.998
5    bpls_804    1    A4    F    1    -0.3655    18.998

[  bonds  ]
;   ai   aj funct  c0(nm)   c1(kJ mol-1 nm-2) ro(Ang.) kr(kcal mol-1 Ang.-2)
1    2    1    0.1394    323500    ;    1.394    386.59   B-F
1    3    1    0.1394    323500    ;    1.394    386.59   B-F
1    4    1    0.1394    323500    ;    1.394    386.59   B-F
1    5    1    0.1394    323500    ;    1.394    386.59   B-F

[  angles  ]
;   ai   aj   ak funct  c0(deg) c1(kJ mol-1 rad-2) c0(deg) c1(kcal mol-1 rad-2)
3    1    2    1    109.47    669.5    ;    109.47    80    F-B-F
4    1    2    1    109.47    669.5    ;    109.47    80    F-B-F
4    1    3    1    109.47    669.5    ;    109.47    80    F-B-F
5    1    2    1    109.47    669.5    ;    109.47    80    F-B-F
5    1    3    1    109.47    669.5    ;    109.47    80    F-B-F
5    1    4    1    109.47    669.5    ;    109.47    80    F-B-F
```

Nonbonded parameters

```
[  atomtypes  ]
bpls_800        B    10.811     0.000    A    0.35814    0.39748    ;    3.5814    0.095
bpls_801        F    18.998     0.000    A    0.31181    0.25104    ;    3.1181    0.06
bpls_802        F    18.998     0.000    A    0.31181    0.25104    ;    3.1181    0.06
bpls_803        F    18.998     0.000    A    0.31181    0.25104    ;    3.1181    0.06
bpls_804        F    18.998     0.000    A    0.31181    0.25104    ;    3.1181    0.06
```

Topology file for $[Tf_2N]^-$ (A5)

Bonded parameters

```
[  moleculetype  ]
;    name    nrexcl
A5    3

[  atoms  ]
;  nr    type  resnr residu  atom  cgnr    charge    mass
1     apls_801    1    A5    NBT    1    -0.528    14.000
2     apls_802    1    A5    SBT    2     0.816    32.066
3     apls_803    1    A5    SBT    3     0.816    32.066
4     apls_804    1    A5    OBT    3    -0.424    15.999
5     apls_805    1    A5    CBT    4     0.28     12.011
6     apls_806    1    A5    OBT    3    -0.424    15.999
7     apls_807    1    A5    OBT    2    -0.424    15.999
8     apls_808    1    A5    OBT    2    -0.424    15.999
9     apls_809    1    A5    F1     4    -0.128    18.998
10    apls_810    1    A5    F1     4    -0.128    18.998
11    apls_811    1    A5    F1     4    -0.128    18.998
12    apls_812    1    A5    CBT    5     0.28     12.011
13    apls_813    1    A5    F1     5    -0.128    18.998
14    apls_814    1    A5    F1     5    -0.128    18.998
15    apls_815    1    A5    F1     5    -0.128    18.998

[  bonds  ]
;   ai    aj funct   c0(nm)  c1(kJ mol-1 nm-2) ro(Ang.) kr(kcal mol-1 Ang.-2)
1    2    1    0.1570    313700    ;    1.57     374.88    N-S
1    3    1    0.1570    313700    ;    1.57     374.88    N-S
2    7    1    0.1437    533100    ;    1.437    637.07    S-O
2    8    1    0.1437    533100    ;    1.437    637.07    S-O
2    12   1    0.1818    195000    ;    1.818    233.03    S-C
3    4    1    0.1437    533100    ;    1.437    637.07    S-O
3    5    1    0.1818    195000    ;    1.818    233.03    S-C
3    6    1    0.1437    533100    ;    1.437    637.07    S-O
5    9    1    0.1323    369800    ;    1.323    441.92    C-F
5    10   1    0.1323    369800    ;    1.323    441.92    C-F
5    11   1    0.1323    369800    ;    1.323    441.92    C-F
12   13   1    0.1323    369800    ;    1.323    441.92    C-F
12   14   1    0.1323    369800    ;    1.323    441.92    C-F
12   15   1    0.1323    369800    ;    1.323    441.92    C-F

[  angles  ]
;   ai    aj    ak funct  c0(deg)  c1(kJ mol-1 rad-2) c0(deg) c1(kcal mol-1 rad-2)
1     2    7     1    113.6    789    ;    113.6    94.29    N-S-O
1     2    8     1    113.6    789    ;    113.6    94.29    N-S-O
1     2    12    1    103.5    764    ;    103.5    91.30    N-S-C
1     3    4     1    113.6    789    ;    113.6    94.29    N-S-O
1     3    5     1    103.5    764    ;    103.5    91.30    N-S-C
1     3    6     1    113.6    789    ;    113.6    94.29    N-S-O
2     12   13    1    111.7    694    ;    111.7    82.93    S-C-F
2     12   14    1    111.7    694    ;    111.7    82.93    S-C-F
2     12   15    1    111.7    694    ;    111.7    82.93    S-C-F
3     1    2     1    125.6    671    ;    125.6    80.19    S-N-S
3     5    9     1    111.7    694    ;    111.7    82.93    S-C-F
3     5    10    1    111.7    694    ;    111.7    82.93    S-C-F
3     5    11    1    111.7    694    ;    111.7    82.93    S-C-F
5     3    4     1    102.6    870    ;    102.6    103.97   C-S-O
6     3    4     1    118.5    969    ;    118.5    115.80   O-S-O
6     3    5     1    102.6    870    ;    102.6    103.97   O-S-C
8     2    7     1    118.5    969    ;    118.5    115.80   O-S-O
10    5    9     1    107.1    781    ;    107.1    93.33    F-C-F
11    5    9     1    107.1    781    ;    107.1    93.33    F-C-F
11    5    10    1    107.1    781    ;    107.1    93.33    F-C-F
12    2    7     1    102.6    870    ;    102.6    103.97   C-S-O
12    2    8     1    102.6    870    ;    102.6    103.97   C-S-O
14    12   13    1    107.1    781    ;    107.1    93.33    F-C-F
15    12   13    1    107.1    781    ;    107.1    93.33    F-C-F
15    12   14    1    107.1    781    ;    107.1    93.33    F-C-F

[  dihedrals  ]
;   ai   aj   ak    al  funct    c0       c1       c2   c3(kJ/mol) ;    V1    V2    V3    V4  (kcal/mol)
1    2    12    13    5    0.000    0.000    1.322    0.000    ;    0    0    0.316    0    N-S-C-F
1    2    12    14    5    0.000    0.000    1.322    0.000    ;    0    0    0.316    0    N-S-C-F
1    2    12    15    5    0.000    0.000    1.322    0.000    ;    0    0    0.316    0    N-S-C-F
```

```
1    3    5     9     5    0.000    0.000    1.322    0.000    ;    0    0    0.316    0    N-S-C-F
1    3    5     10    5    0.000    0.000    1.322    0.000    ;    0    0    0.316    0    N-S-C-F
1    3    5     11    5    0.000    0.000    1.322    0.000    ;    0    0    0.316    0    N-S-C-F
2    1    3     4     5    0.000    0.000   -0.015    0.000    ;    0    0   -0.004    0    S-N-S-O
2    1    3     5     5   32.773   -10.42   -3.195    0.000    ; 7.833 -2.49 -0.764    0    S-N-S-C
2    1    3     6     5    0.000    0.000   -0.015    0.000    ;    0    0   -0.004    0    S-N-S-O
3    1    2     7     5    0.000    0.000   -0.015    0.000    ;    0    0   -0.004    0    S-N-S-O
3    1    2     8     5    0.000    0.000   -0.015    0.000    ;    0    0   -0.004    0    S-N-S-O
3    1    2     12    5   32.773   -10.42   -3.195    0.000    ; 7.833 -2.49 -0.764    0    S-N-S-C
4    3    5     9     5    0.000    0.000    1.451    0.000    ;    0    0    0.347    0    O-S-C-F
4    3    5     10    5    0.000    0.000    1.451    0.000    ;    0    0    0.347    0    O-S-C-F
4    3    5     11    5    0.000    0.000    1.451    0.000    ;    0    0    0.347    0    O-S-C-F
6    3    5     9     5    0.000    0.000    1.451    0.000    ;    0    0    0.347    0    O-S-C-F
6    3    5     10    5    0.000    0.000    1.451    0.000    ;    0    0    0.347    0    O-S-C-F
6    3    5     11    5    0.000    0.000    1.451    0.000    ;    0    0    0.347    0    O-S-C-F
7    2    12    13    5    0.000    0.000    1.451    0.000    ;    0    0    0.347    0    O-S-C-F
7    2    12    14    5    0.000    0.000    1.451    0.000    ;    0    0    0.347    0    O-S-C-F
7    2    12    15    5    0.000    0.000    1.451    0.000    ;    0    0    0.347    0    O-S-C-F
8    2    12    13    5    0.000    0.000    1.451    0.000    ;    0    0    0.347    0    O-S-C-F
8    2    12    14    5    0.000    0.000    1.451    0.000    ;    0    0    0.347    0    O-S-C-F
8    2    12    15    5    0.000    0.000    1.451    0.000    ;    0    0    0.347    0    O-S-C-F
```

Nonbonded parameters

```
[  atomtypes  ]
;  type    mass      charge ptype  sigma(nm) epsilon(kJ/mol) sigma(Ang.) epsilon(kcal/mol)
apls_809       F1     18.998    0.000    A    0.295    0.22175    ;    2.95    0.053
apls_810       F1     18.998    0.000    A    0.295    0.22175    ;    2.95    0.053
apls_811       F1     18.998    0.000    A    0.295    0.22175    ;    2.95    0.053
apls_813       F1     18.998    0.000    A    0.295    0.22175    ;    2.95    0.053
apls_814       F1     18.998    0.000    A    0.295    0.22175    ;    2.95    0.053
apls_815       F1     18.998    0.000    A    0.295    0.22175    ;    2.95    0.053
apls_805       CBT    12.011    0.000     A   0.350    0.27614    ;    3.5     0.066
apls_812       CBT    12.011    0.000     A   0.350    0.27614    ;    3.5     0.066
apls_802       SBT    32.066    0.000    A    0.355    1.04600    ;    3.55    0.25
apls_803       SBT    32.066    0.000    A    0.355    1.04600    ;    3.55    0.25
apls_804       OBT    15.999    0.000    A    0.296    0.87864    ;    2.96    0.21
apls_806       OBT    15.999    0.000    A    0.296    0.87864    ;    2.96    0.21
apls_807       OBT    15.999    0.000    A    0.296    0.87864    ;    2.96    0.21
apls_808       OBT    15.999    0.000    A    0.296    0.87864    ;    2.96    0.21
apls_801       NBT    14.0      0.000    A    0.325    0.71128    ;    3.25    0.17
```

Topology file for $[PF_6]^-$ (A6)

Bonded parameters

```
[  moleculetype  ]
;    name    nrexcl
A6    3

[  atoms  ]
;   nr type resnr residu atom cgnr  charge     mass
1    hpls_801    1    A6    P    1     1.072    30.974
2    hpls_802    1    A6    F    1    -0.312    18.998
3    hpls_803    1    A6    F    1    -0.312    18.998
4    hpls_804    1    A6    F    1    -0.312    18.998
5    hpls_805    1    A6    F    1    -0.312    18.998
6    hpls_806    1    A6    F    1    -0.312    18.998
7    hpls_807    1    A6    F    1    -0.312    18.998

[  bonds  ]
;   ai   aj funct  c0(nm)   c1(kJ mol-1 nm-2) ro(Ang.) kr(kcal mol-1 Ang.-2)
1    2    1    0.1606    310000    ;    1.606    370.46    P-F
1    3    1    0.1606    310000    ;    1.606    370.46    P-F
1    4    1    0.1606    310000    ;    1.606    370.46    P-F
1    5    1    0.1606    310000    ;    1.606    370.46    P-F
1    6    1    0.1606    310000    ;    1.606    370.46    P-F
1    7    1    0.1606    310000    ;    1.606    370.46    P-F

[  angles  ]
;   ai   aj   ak funct c0(deg) c1(kJ mol-1 rad-2) c0(deg)  c1(kcal mol-1 rad-2)
2    1    3    1    90    1165    ;    90    139.22    F-P-F
2    1    4    1    90    1165    ;    90    139.22    F-P-F
2    1    6    1    90    1165    ;    90    139.22    F-P-F
2    1    7    1    90    1165    ;    90    139.22    F-P-F
3    1    4    1    90    1165    ;    90    139.22    F-P-F
3    1    5    1    90    1165    ;    90    139.22    F-P-F
3    1    7    1    90    1165    ;    90    139.22    F-P-F
4    1    5    1    90    1165    ;    90    139.22    F-P-F
4    1    6    1    90    1165    ;    90    139.22    F-P-F
5    1    6    1    90    1165    ;    90    139.22    F-P-F
5    1    7    1    90    1165    ;    90    139.22    F-P-F
6    1    7    1    90    1165    ;    90    139.22    F-P-F
```

Nonbonded parameters

```
[  atomtypes  ]
;  type   mass     charge  ptype sigma(nm)  epsilon(kJ/mol) sigma(Ang.) epsilon(kcal/mol)
hpls_801       P    30.974     0.000    A    0.37400    0.83700    ;    3.74      0.20
hpls_802       F    18.998     0.000    A    0.31181    0.25522    ;    3.1181    0.061
hpls_803       F    18.998     0.000    A    0.31181    0.25522    ;    3.1181    0.061
hpls_804       F    18.998     0.000    A    0.31181    0.25522    ;    3.1181    0.061
hpls_805       F    18.998     0.000    A    0.31181    0.25522    ;    3.1181    0.061
hpls_806       F    18.998     0.000    A    0.31181    0.25522    ;    3.1181    0.061
hpls_807       F    18.998     0.000    A    0.31181    0.25522    ;    3.1181    0.061
```

Topology file for CO_2

Bonded parameters

```
[ moleculetype ]
; name  nrexcl
   CO2   3

 [ atoms ]
;  nr    type   resnr   residu   atom   cgnr    charge      mass
    1     OZ     1       CO2      OZ     1  -0.35000  15.99940       ;   0.1861000
    2     CZ     1       CO2      CZ     1   0.70000  12.01100       ;   0.3722000
    3     OZ     1       CO2      OZ     1  -0.35000  15.99940       ;   0.0000000
; total molecule charge =   0.0000000

 [ bonds ]
;   ai  aj   funct      b0          kb
       1     2   1     0.11600      861899.816       ;    C-    O  TraPPE force field + Maginn and Wei Shi   ;
Modified by Osca almost equal to 2X  Wei Shi's FF
       2     3   1     0.11600      861899.816       ;    C-    O  TraPPE force field + Maginn and Wei Shi

[ angles ]
;   ai     aj    ak   funct   Thet0      kThet0     mutiplicity
     1     2     3     1     180.00     468.608      ;    C-    O   C   O TraPPE force field + Maginn and Wei Shi
; Modified by Osca almost equal to 2X  Wei Shi  FF
```

Nonbonded parameters

```
[ atomtypes ]
; name  bond_type    mass    charge   ptype          sigma [nm]     epsilon [kJ/mol]
CZ    CZ    6      12.01100     0.700       A    2.8000e-01  2.24500e-01       ; TraPPE force field
OZ    OZ    8      15.99940    -0.350       A    3.0500e-01  6.56800e-01       ; TraPPE force field
```

Topology file for CH_4

Bonded parameters

```
[ moleculetype ]
; name  nrexcl
   CH4   3

 [ atoms ]
;  nr    type   resnr   residue   atom   cgnr    charge      mass
    1     CM     1       CH4      CM    1    0.000   12.01100
    2     HM     1       CH4      HM    1    0.000    1.0080
    3     HM     1       CH4      HM    1    0.000    1.0080
    4     HM     1       CH4      HM    1    0.000    1.0080
    5     HM     1       CH4      HM    1    0.000    1.0080
; total molecule charge =   0.0000000

[ constraints ]
;   ai  aj   funct      b0
       1     2   1     0.11000
       1     3   1     0.11000
       1     4   1     0.11000
       1     5   1     0.11000

[ angles ]
;   ai     aj    ak    funct   Thet0   kThet0
     2     1     3     1     107.800   448.000
     2     1     4     1     107.800   448.000
     2     1     5     1     107.800   448.000
     3     1     4     1     107.800   448.000
     3     1     5     1     107.800   448.000
     4     1     5     1     107.800   448.000

[ exclusions ]
 1   2   3   4   5
 5   1   2   3   4
 4   5   1   2   3
 3   4   5   1   2
 2   3   4   5   1
```

Nonbonded parameters

```
[ atomtypes ]
; name  bond_type    mass    charge   ptype          sigma      epsilon
  CM    CM      12.01100    0.000       A     3.310000E-01  8.31E-05
  HM    HM       1.0080     0.000       A     3.310000E-01  1.27E-01
```

Topology file for C_2H_6

Bonded parameters

```
[ moleculetype ]
; Name               nrexcl
C2H6                 3
[ atoms ]
;   nr       type  resnr residue  atom   cgnr     charge       mass
     1   qpls_800      1    C2H6   C00      1    -0.2396    12.0110
     2   qpls_801      1    C2H6   C01      1    -0.2396    12.0110
     3   qpls_802      1    C2H6   H02      1     0.0799     1.0080
     4   qpls_803      1    C2H6   H03      1     0.0799     1.0080
     5   qpls_804      1    C2H6   H04      1     0.0799     1.0080
     6   qpls_805      1    C2H6   H05      1     0.0799     1.0080
     7   qpls_806      1    C2H6   H06      1     0.0799     1.0080
     8   qpls_807      1    C2H6   H07      1     0.0799     1.0080
[ bonds ]
    2     1     1      0.1529 224262.400
    3     1     1      0.1090 284512.000
    4     1     1      0.1090 284512.000
    5     1     1      0.1090 284512.000
    6     2     1      0.1090 284512.000
    7     2     1      0.1090 284512.000
    8     2     1      0.1090 284512.000

[ angles ]
;  ai    aj    ak funct            c0            c1            c2            c3
    2     1     3     1    110.700    313.800
    2     1     4     1    110.700    313.800
    2     1     5     1    110.700    313.800
    1     2     6     1    110.700    313.800
    1     2     7     1    110.700    313.800
    1     2     8     1    110.700    313.800
    3     1     4     1    107.800    276.144
    3     1     5     1    107.800    276.144
    6     2     7     1    107.800    276.144
    6     2     8     1    107.800    276.144
    7     2     8     1    107.800    276.144
    4     1     5     1    107.800    276.144

[ dihedrals ]
; IMPROPER DIHEDRAL ANGLES
;  ai    aj    ak    al funct            c0            c1            c2            c3            c4            c5

[ dihedrals ]
; PROPER DIHEDRAL ANGLES
;  ai    aj    ak    al funct            c0            c1            c2            c3            c4            c5
    6    2    1    3        3       0.628   1.883   0.000  -2.510  -0.000   0.000
    7    2    1    5        3       0.628   1.883   0.000  -2.510  -0.000   0.000
    6    2    1    5        3       0.628   1.883   0.000  -2.510  -0.000   0.000
    8    2    1    4        3       0.628   1.883   0.000  -2.510  -0.000   0.000
    8    2    1    3        3       0.628   1.883   0.000  -2.510  -0.000   0.000
    8    2    1    5        3       0.628   1.883   0.000  -2.510  -0.000   0.000
    7    2    1    3        3       0.628   1.883   0.000  -2.510  -0.000   0.000
    6    2    1    4        3       0.628   1.883   0.000  -2.510  -0.000   0.000
    7    2    1    4        3       0.628   1.883   0.000  -2.510  -0.000   0.000

[ pairs ]
     3     6    1
     4     6    1
     3     7    1
     5     6    1
     4     7    1
     3     8    1
     5     7    1
     4     8    1
     5     8    1
```

Nonbonded parameters

```
[ atomtypes ]
  qpls_803  H803     1.0080     0.000    A    2.50000E-01   1.25520E-01
  qpls_800  C800    12.0110     0.000    A    3.50000E-01   2.76144E-01
  qpls_801  C801    12.0110     0.000    A    3.50000E-01   2.76144E-01
  qpls_807  H807     1.0080     0.000    A    2.50000E-01   1.25520E-01
```

```
qpls_804  H804     1.0080     0.000    A    2.50000E-01   1.25520E-01
qpls_805  H805     1.0080     0.000    A    2.50000E-01   1.25520E-01
qpls_806  H806     1.0080     0.000    A    2.50000E-01   1.25520E-01
qpls_802  H802     1.0080     0.000    A    2.50000E-01   1.25520E-01
```

Topology file for C_3H_8

Bonded parameters

```
[ moleculetype ]
; Name               nrexcl
C3H8                 3
[ atoms ]
;   nr       type  resnr residue  atom   cgnr     charge       mass
     1   prls_800      1    C3H8   C00      1    -0.2381    12.0110
     2   prls_801      1    C3H8   C01      1      -0.18    12.0110
     3   prls_802      1    C3H8   C02      1    -0.2381    12.0110
     4   prls_803      1    C3H8   H03      1     0.0804     1.0080
     5   prls_804      1    C3H8   H04      1     0.0804     1.0080
     6   prls_805      1    C3H8   H05      1     0.0804     1.0080
     7   prls_806      1    C3H8   H06      1      0.087     1.0080
     8   prls_807      1    C3H8   H07      1      0.087     1.0080
     9   prls_808      1    C3H8   H08      1     0.0804     1.0080
    10   prls_809      1    C3H8   H09      1     0.0804     1.0080
    11   prls_810      1    C3H8   H0A      1     0.0804     1.0080
[ bonds ]
    2     1     1      0.1529 224262.400
    3     2     1      0.1529 224262.400
    4     1     1      0.1090 284512.000
    5     1     1      0.1090 284512.000
    6     1     1      0.1090 284512.000
    7     2     1      0.1090 284512.000
    8     2     1      0.1090 284512.000
    9     3     1      0.1090 284512.000
   10     3     1      0.1090 284512.000
   11     3     1      0.1090 284512.000

[ angles ]
;  ai    aj    ak funct            c0            c1            c2            c3
    1     2     3     1    112.700    488.273
    2     1     4     1    110.700    313.800
    2     1     5     1    110.700    313.800
    2     1     6     1    110.700    313.800
    1     2     7     1    110.700    313.800
    1     2     8     1    110.700    313.800
    2     3     9     1    110.700    313.800
    2     3    10     1    110.700    313.800
    2     3    11     1    110.700    313.800
    3     2     7     1    110.700    313.800
    4     1     5     1    107.800    276.144
    5     1     6     1    107.800    276.144
    9     3    10     1    107.800    276.144
   10     3    11     1    107.800    276.144
    9     3    11     1    107.800    276.144
    3     2     8     1    110.700    313.800
    4     1     6     1    107.800    276.144
    7     2     8     1    107.800    276.144

[ dihedrals ]
; IMPROPER DIHEDRAL ANGLES
;  ai    aj    ak    al funct            c0            c1            c2            c3            c4            c5

[ dihedrals ]
; PROPER DIHEDRAL ANGLES
;  ai    aj    ak    al funct            c0            c1            c2            c3            c4            c5
    4     1     2     3        3       0.628   1.883   0.000  -2.510  -0.000   0.000
    6     1     2     3        3       0.628   1.883   0.000  -2.510  -0.000   0.000
   11     3     2     1        3       0.628   1.883   0.000  -2.510  -0.000   0.000
    5     1     2     3        3       0.628   1.883   0.000  -2.510  -0.000   0.000
    9     3     2     1        3       0.628   1.883   0.000  -2.510  -0.000   0.000
   10     3     2     1        3       0.628   1.883   0.000  -2.510  -0.000   0.000
   11     3     2     8        3       0.628   1.883   0.000  -2.510  -0.000   0.000
    8     2     1     5        3       0.628   1.883   0.000  -2.510  -0.000   0.000
    8     2     1     4        3       0.628   1.883   0.000  -2.510  -0.000   0.000
    7     2     1     5        3       0.628   1.883   0.000  -2.510  -0.000   0.000
    9     3     2     7        3       0.628   1.883   0.000  -2.510  -0.000   0.000
   10     3     2     7        3       0.628   1.883   0.000  -2.510  -0.000   0.000
   10     3     2     8        3       0.628   1.883   0.000  -2.510  -0.000   0.000
    8     2     1     6        3       0.628   1.883   0.000  -2.510  -0.000   0.000
    7     2     1     6        3       0.628   1.883   0.000  -2.510  -0.000   0.000
   11     3     2     7        3       0.628   1.883   0.000  -2.510  -0.000   0.000
```

```
    9    3    2    8        3       0.628   1.883   0.000  -2.510  -0.000   0.000
    7    2    1    4        3       0.628   1.883   0.000  -2.510  -0.000   0.000

[ pairs ]
     3     4    1
     3     5    1
     3     6    1
     1     9    1
     4     7    1
     1    10    1
     5     7    1
     4     8    1
     1    11    1
     6     7    1
     5     8    1
     6     8    1
     7     9    1
     8     9    1
     7    10    1
     8    10    1
     7    11    1
     8    11    1
```

Nonbonded parameters

```
[ atomtypes ]
  prls_803  H803     1.0080     0.000    A    2.50000E-01   1.25520E-01
  prls_802  C802    12.0110     0.000    A    3.50000E-01   2.76144E-01
  prls_808  H808     1.0080     0.000    A    2.50000E-01   1.25520E-01
  prls_800  C800    12.0110     0.000    A    3.50000E-01   2.76144E-01
  prls_801  C801    12.0110     0.000    A    3.50000E-01   2.76144E-01
  prls_807  H807     1.0080     0.000    A    2.50000E-01   1.25520E-01
  prls_804  H804     1.0080     0.000    A    2.50000E-01   1.25520E-01
  prls_809  H809     1.0080     0.000    A    2.50000E-01   1.25520E-01
  prls_805  H805     1.0080     0.000    A    2.50000E-01   1.25520E-01
  prls_810  H810     1.0080     0.000    A    2.50000E-01   1.25520E-01
  prls_806  H806     1.0080     0.000    A    2.50000E-01   1.25520E-01
```

Topology file for C_3H_8O

Bonded parameters

```
[ moleculetype ]
; Name               nrexcl
C3OH                 3
[ atoms ]
;   nr       type  resnr residue  atom   cgnr     charge       mass
     1   pnls_800      1    C3OH   C00      1    -0.2359    12.0110
     2   pnls_801      1    C3OH   C01      1    -0.2259    12.0110
     3   pnls_802      1    C3OH   C02      1     0.1102    12.0110
     4   pnls_803      1    C3OH   O03      1    -0.6884    15.9990
     5   pnls_804      1    C3OH   H04      1     0.0842     1.0080
     6   pnls_805      1    C3OH   H05      1     0.0842     1.0080
     7   pnls_806      1    C3OH   H06      1     0.0842     1.0080
     8   pnls_807      1    C3OH   H07      1     0.0958     1.0080
     9   pnls_808      1    C3OH   H08      1     0.0958     1.0080
    10   pnls_809      1    C3OH   H09      1     0.0952     1.0080
    11   pnls_810      1    C3OH   H0A      1     0.0952     1.0080
    12   pnls_811      1    C3OH   H0B      1     0.4055     1.0080
[ bonds ]
    2     1     1      0.1529 224262.400
    3     2     1      0.1529 224262.400
    4     3     1      0.1410 267776.000
    5     1     1      0.1090 284512.000
    6     1     1      0.1090 284512.000
    7     1     1      0.1090 284512.000
    8     2     1      0.1090 284512.000
    9     2     1      0.1090 284512.000
   10     3     1      0.1090 284512.000
   11     3     1      0.1090 284512.000
   12     4     1      0.0945 462750.400

[ angles ]
;  ai    aj    ak funct            c0            c1            c2            c3
    1     2     3     1    112.700    488.273
    2     3     4     1    109.500    418.400
    2     1     5     1    110.700    313.800
    2     1     6     1    110.700    313.800
    2     1     7     1    110.700    313.800
    1     2     8     1    110.700    313.800
    1     2     9     1    110.700    313.800
    2     3    10     1    110.700    313.800
    2     3    11     1    110.700    313.800
    3     4    12     1    108.500    460.240
    6     1     7     1    107.800    276.144
    8     2     9     1    107.800    276.144
    4     3    11     1    109.500    292.880
    5     1     6     1    107.800    276.144
   10     3    11     1    107.800    276.144
    4     3    10     1    109.500    292.880
    3     2     8     1    110.700    313.800
    5     1     7     1    107.800    276.144
    3     2     9     1    110.700    313.800

[ dihedrals ]
; IMPROPER DIHEDRAL ANGLES
;  ai    aj    ak    al funct            c0            c1            c2            c3            c4            c5

[ dihedrals ]
; PROPER DIHEDRAL ANGLES
;  ai    aj    ak    al funct            c0            c1            c2            c3            c4            c5
    5     1     2     3        3       0.628   1.883   0.000  -2.510  -0.000   0.000
   10     3     2     1        3       0.628   1.883   0.000  -2.510  -0.000   0.000
   11     3     2     1        3       0.628   1.883   0.000  -2.510  -0.000   0.000
    7     1     2     3        3       0.628   1.883   0.000  -2.510  -0.000   0.000
    6     1     2     3        3       0.628   1.883   0.000  -2.510  -0.000   0.000
    8     2     1     5        3       0.628   1.883   0.000  -2.510  -0.000   0.000
   11     3     2     9        3       0.628   1.883   0.000  -2.510  -0.000   0.000
    8     2     1     7        3       0.628   1.883   0.000  -2.510  -0.000   0.000
   10     3     2     8        3       0.628   1.883   0.000  -2.510  -0.000   0.000
   10     3     2     9        3       0.628   1.883   0.000  -2.510  -0.000   0.000
    9     2     1     6        3       0.628   1.883   0.000  -2.510  -0.000   0.000
    9     2     1     7        3       0.628   1.883   0.000  -2.510  -0.000   0.000
   11     3     2     8        3       0.628   1.883   0.000  -2.510  -0.000   0.000
```

```
     8     2     1     6         3        0.628   1.883   0.000  -2.510  -0.000   0.000
     9     2     1     5         3        0.628   1.883   0.000  -2.510  -0.000   0.000
     8     2     3     4         3        0.979   2.937   0.000  -3.916  -0.000   0.000
     9     2     3     4         3        0.979   2.937   0.000  -3.916  -0.000   0.000
    12     4     3     2         3       -0.444   3.833   0.728  -4.117  -0.000   0.000
    12     4     3    11         3        0.736   2.209   0.000  -2.946  -0.000   0.000
    12     4     3    10         3        0.736   2.209   0.000  -2.946  -0.000   0.000
     4     3     2     1         3       -3.247   3.247   0.000  -0.000  -0.000   0.000

[ pairs ]
     1     4     1
     3     5     1
     3     6     1
     3     7     1
     1    10     1
     4     8     1
     1    11     1
     5     8     1
     4     9     1
     6     8     1
     5     9     1
     2    12     1
     7     8     1
     6     9     1
     7     9     1
     8    10     1
     9    10     1
     8    11     1
     9    11     1
    10    12     1
    11    12     1
```

Nonbonded parameters

```
[ atomtypes ]
  pnls_810  H810     1.0080     0.000    A    2.50000E-01   1.25520E-01
  pnls_802  C802    12.0110     0.000    A    3.50000E-01   2.76144E-01
  pnls_808  H808     1.0080     0.000    A    2.50000E-01   1.25520E-01
  pnls_800  C800    12.0110     0.000    A    3.50000E-01   2.76144E-01
  pnls_801  C801    12.0110     0.000    A    3.50000E-01   2.76144E-01
  pnls_807  H807     1.0080     0.000    A    2.50000E-01   1.25520E-01
  pnls_804  H804     1.0080     0.000    A    2.50000E-01   1.25520E-01
  pnls_803  O803    15.9990     0.000    A    3.12000E-01   7.11280E-01
  pnls_809  H809     1.0080     0.000    A    2.50000E-01   1.25520E-01
  pnls_805  H805     1.0080     0.000    A    2.50000E-01   1.25520E-01
  pnls_806  H806     1.0080     0.000    A    2.50000E-01   1.25520E-01
  pnls_811  H811     1.0080     0.000    A    0.00000E+00   0.00000E+00
```

Topology file for N_2

Bonded parameters

```
[ moleculetype ]
; name  nrexcl
   N2   3

 [ atoms ]
;  nr    type   resnr   residu   atom   cgnr    charge      mass
    1     N     1       N2      N    1       -0.482   14.0067
    2     D     1       N2      D    1       0.964    0.0000
    3     N     1       N2      N    1       -0.482   14.0067
; total molecule charge =   0.0000000

[ constraints ]
;   ai  aj   funct      b0
       1     3   1     0.11000
       1     2   1     0.05500
       2     3   1     0.05500

[ angles ]
;   ai     aj    ak   funct   Thet0     kThet0
     1     2     3    1     180.00    500.000

[ virtual_sites2 ]
; Vsite from    to       funct   a
2          1       3     1       0.5
```

Nonbonded parameters

```
[ atomtypes ]
; name  bond_type    mass    charge   ptype          sigma      epsilon
N     ND        14.0067    -0.482       A    3.31000E-01  2.99E-01        ; TraPPE force field
D     DN        0.0000      0.964       D    0.00000000   0.00000000      ; TraPPE force field
```